Title
Structural and Biochemical Studies of Replicative Helicase Loading in Bacteria

Author
Hood, Iris Vanessa

Publication Date
2015

Peer reviewed|Thesis/dissertation

Structural and Biochemical Studies of Replicative Helicase Loading in Bacteria

By

Iris Vanessa Hood

A dissertation submitted in partial satisfaction of the

Requirements for the degree of

Doctor in Philosophy

in

Molecular and Cell Biology

in the

Graduate Division

of the

University of California, Berkeley

Committee in charge:

Professor James M. Berger, Chair

Professor Michael R. Botchan

Professor David E. Wemmer

Professor Andreas Martin

Spring 2015

Structural and Biochemical Studies of Replicative Helicase Loading in Bacteria

By

Iris Vanessa Hood

Abstract

Structural and Biochemical Studies of Replicative Helicase Loading in Bacteria

By

Iris Vanessa Hood

Doctor in Philosophy in Molecular and Cell Biology

University of California, Berkeley

Professor James M. Berger, Chair

The initiation of DNA replication represents a defining commitment to the proliferation of all cellular organisms. Dedicated ATP-dependent initiation factors specifically mark replication start sites or "replication origins" and, together with ATP-dependent helicase loaders, help coordinate productive assembly of the replisome. In many bacterial species, helicase loaders belonging to the DnaC/I family of proteins assist the bacterial initiator factor DnaA with loading and activation of DnaB-type replicative helicases. Despite advances in understanding some of the essential proteins and common principles underlying initiation strategies, major questions still persist in defining how initiation programs are executed at the molecular level.

The present dissertation presents a combination of structural and biochemical studies of the DnaC helicase loader and DnaA initiator from the Gram-negative bacterium *Escherichia coli (E. coli)* and the DnaI helicase loader from the Gram-positive bacterium *Staphylococcus aureus (S. aureus)*. For the *E. coli* work, I developed several fluorescence-based helicase assays to help define the particular contributions of both DnaA and DnaC in promoting loading of DnaB at a replication origin. Investigations of DnaA mutants in this helicase assay revealed the importance of the initiator's N-terminal helicase binding domain in recruiting DnaB to a nascent bubble or fork to facilitate helicase loading. Parallel studies of the *E. coli* DnaC demonstrated: (i) that the loader's N-terminal DnaB binding domain is sufficient for activation of *E. coli* DnaB's duplex DNA unwinding activity and (ii) that the AAA+-family ATP binding and hydrolysis domain of DnaC likely serves as a regulatory element that helps enhance the efficiency of helicase activation.

To better characterize the activity of a Gram-positive *S. aureus* DnaI helicase loader, I structurally and biochemically characterized the protein's ATPase domain and activity, and also investigated how a particular viral peptide inhibitor from phage 77, termed "ORF104", interferes with host DNA replication by blocking *Sa*DnaI activity. Comparative structural analyses, combined with biochemical studies of *Sa*DnaI revealed not only how the viral inhibitor 77ORF104 blocks loader function but also revealed insights into how bacterial helicase loaders may in general auto-regulate their function. A complimentary viral-host interaction study of another staph-specific viral peptide that also inhibits host DNA replication ("ORF078" from phage 71) has revealed another promising anti-bacterial strategy: preliminary binding studies indicate that this gene product binds primase through its helicase-binding domain.

Overall, the studies presented in this dissertation provide multiple new insights into fundamental mechanisms underlying the initiation of DNA replication. One is an enhanced understanding of the role that the *E. coli* DnaA initiator and DnaC loader serve in recruiting the DnaB helicase to a replication origin. The other describes a novel viral mechanism for inhibition of the *S. aureus* DnaI helicase loader that helps establish how a virus may exploit an existing auto-regulatory element of the bacterial helicase loader as part of a strategy to inhibit host DNA replication. These findings collectively not only answer long-standing questions in the field, but also open up new avenues for future inquiry.

Dedication

This dissertation is dedicated
to my parents and siblings

James W. Hood and Julie A. Bur

Searose, Bud, Sam, and Jasmine Hood

Table of Contents

Acknowledgements

I would like to thank my friends and family, especially my mother and father (Julie and James Hood), brothers and sisters (Searose, Jasmine, Sam and Bud Hood), aunt and uncle (Susan and James Brown), guardian parents (Lisa Kasle, Judy and Tommy Muthig), James K. Nuñez, Nicole Fay, Hanadie Yousef, Hector Garcia Martin, Nicola Popp, Jane Binakonsky, Bernadette Kreh, Zulima Martin, Roberto Rayo Quesada, and Ajlai Basu for their support and encouragement throughout several years of challenges, successes and failures that contributed to this work. All members of the Berger lab provided helpful comments and discussions, especially Valerie O'Shea, Ernesto Arias-Palomo, Alessandro Costa, Franziska Bleichert, Artem Lyubimov, Karl Duderstadt, Melissa Mott, Richard Rymer, Alexia Miller, Melania Strycharska, Glenn Hauk, Tim Wendorff, Seychelle Vos, Tim Blower, Matthew Hobson, Matthew Parker, Michael Lawson, Philip Kranzusch, Yolanda Eby and Monica Chandra. Franziska Bleichert and Tim Blower provided valuable assistance with data collection at the National Synchrotron Light Source (NSLS) Beamline X25 at Brookhaven National Lab. This work greatly benefitted from the advice and insight of Michael Botchan, David Wemmer and Andreas Martin. I would also like to thank all members of the Department of Biophysics and Biophysical Chemistry at The Johns Hopkins University School of Medicine, especially the Wolberger, Leahy, Amzel and Bosch labs. Most of all, I would like to thank my thesis advisor, James Berger, for his unwavering support and invaluable input throughout my graduate career. I am tremendously grateful to have received guidance from such an exceptional mentor, who stands in a league of his own. This work was supported by a Department of Energy Pre-doctoral Graduate Fellowship (DOE SCGF 2010-2013) awarded to IVH, and by the NIGMS (RO1-GM071747) to JMB.

Chapter 1: Introduction to DNA Replication

(Portions of Chapter 1 of this dissertation were first published as an annual review article: Costa, A.*, Hood, I.V.*, and Berger, J.M. (2013). Mechanisms for Initiating Cellular DNA Replication. Annu. Rev. Biochem. 82, 25-54.)

* These authors contributed equally to this work.

DNA replication has been studied extensively for over 60 years. Since Arthur Kornberg's seminal discovery of the proteins required to copy the genetic material in *E. coli* (Adler et al., 1958; Bessman et al., 1956; Kornberg and Baker, T. A., 1992; Kornberg, 1960, 1968), advances in our understanding of how DNA replication machineries are assembled and how polymerases within the replisome "holoenzyme" catalyze DNA synthesis have greatly expanded our knowledge about both the mechanisms and dynamics of DNA replication in cellular organisms as well as how viruses co-opt host machinery to replicate viral genomes (Kornberg and Baker, T. A., 1992; Kornberg, 1968; LeBowitz and McMacken, 1984a; van Oijen and Loparo, 2010; Yao and O'Donnell, 2009; Yardimci et al., 2010; Yeeles and Marians, 2013). In this chapter, I will provide a general overview of the key steps of DNA replication initiation, as well as a brief summation of the challenges organisms and viruses overcome during replication. A particular emphasis will be placed on how DNA replication is initiated in bacteria; however, shared functional mechanisms will be discussed as they pertain to various archaeal, eukaryotic or viral initiation systems.

DNA Replication Initiation Mechanisms

DNA replication is essential to the proliferation of all cellular organisms and viruses. The assembly of replication machineries, termed replisomes, is coordinated by dedicated initiation proteins, which ensure that DNA synthesis begins at the correct chromosomal locus in accordance with cell cycle cues (Johnson and O'Donnell, 2005; Kaguni, 2006; Stillman, 2005). Given the critical importance genomic stability serves in promoting cell viability and proliferation, the timely and accurate initiation of DNA replication constitutes one of several essential events necessary for the faithful production of cellular progeny; inappropriate replication onset is linked to changes in gene copy number, DNA damage, and genetic instability (Arias and Walter, 2007; Simmons et al., 2004; Sutera Jr. and Lovett, 2006).

Key Stages of DNA Replication Initiation

In 1963, based on observations in *E. coli*, François Jacob and Sydney Brenner proposed the replicon model postulating that regulation of DNA replication involves at least two essential elements: a specific *trans-acting* factor, known as the initiator, which specifically binds to a *cis-acting* DNA sequence on the chromosome, termed the replicator, (Jacob et al., 1963). The replicon model constituted the first attempt to explain how DNA replication is regulated in bacteria and was later extended to include phage replication, as well as the replication of prokaryotic and eukaryotic genomes in general.

Five decades later, although many of the key aspects of the replicon hypothesis still hold true, numerous discoveries in DNA replication initiation have expanded our appreciation for the diversity observed among various cellular and viral initiation programs. Despite having markedly distinct initiation strategies, all organisms appear dependent on dedicated initiator proteins. Initiators are either single proteins that form homo-oligomers, such as the *E. coli* DnaA, or higher-order complexes composed of multiple, distinct subunits, such as the eukaryotic initiator ORC (Origin Recognition Complex) (Bell and Stillman, 1992; Dueber et al., 2007; Duncker et al., 2009; Grainge et al., 2003). Initiators typically perform two major roles in initiation: (i) recognizing double-stranded origin sites (and in some instances remodeling the DNA to promote origin melting (Bramhill and Kornberg, 1988a), and (ii) recruiting and/or facilitating the loading of replicative helicases onto origin DNA (**Figure 1.1**) (Bowers et al., 2004; Davey et al., 2002; Diffley et al., 1994; Dueber et al., 2007; Fang et al., 1999; Funnell et al., 1987; Kornberg and Baker, T. A., 1992; Randell et al., 2006; Remus et al., 2009; Sekimizu et al., 1988a; Speck and Stillman, 2007; Speck et al., 2005).

The Topological Challenges of Initiation and DNA Replication

The double-helical nature of DNA presents many physical challenges during initiation and subsequent DNA replication. For example, because of its inter-wound nature, duplex DNA must be melted and separated to generate single DNA strands (ssDNA) that serve as loading platforms for deposition of two replicative helicases. DNA unwinding also allows replication factors to access the genetic information encoded within the single bases of the DNA. However, because DNA is a double helical polymer, replicative helicases generate topological deformations in DNA as they processively unwind the substrate, including DNA supercoils or DNA catenanes (Hardy et al., 2004; Wang, 2002; Zechiedrich and Cozzarelli, 1995). It is important for cells to remove these topological problems prior to chromosome segregation and division.

In *E. coli* and many other bacterial species, specialized enzymes called topoisomerases serve to manage supercoils generated during DNA replication initiation, fork progression, and replication termination (Wang, 1971). Topoisomerases regulate chromosomal entanglements through their ability to transiently cleave the phosphodiester backbone of DNA and catalyze passage of single- or double-strands of DNA through one another; removing DNA supercoils generated during initiation and fork progression (Hiasa and Marians, 1994; Kaguni and Kornberg, 1984; Wang, JC., and Liu LF., 1979; Wang, 1971, 2002; Zechiedrich and Cozzarelli, 1995). The opposing activities of topoisomerases, topo IA and gyrase, are responsible for alleviating local supercoiling stress generated during initiation at the replication origin (Hiasa and Marians, 1994; Kaguni and Kornberg, 1984). During replication fork progression, the type II topoisomerases DNA gyrase and/or topo IV resolve positive supercoils that arise as a result of duplex DNA unwinding by the replicative helicase (Hiasa and Marians, 1996; Khodursky et al., 2000; Wang et al., 2011; Zechiedrich and Cozzarelli, 1995). Following replication, newly synthesized daughter chromosomes must also be disentangled; in most bacteria, topo IV is responsible for this function (Ullsperger and Cozzarelli, 1996).

Common Themes and Differences among various DNA Replication Initiation Mechanisms

Although specific initiation factors can vary in both their specific activities and mechanisms, all appear to utilize multi-protein complexes to facilitate origin recognition, generate nascent replication bubbles, and promote replisome assembly (see reviews (Bell and Dutta, 2002; Bryant and Aves, 2011; Costa et al., 2013; Diffley and Stillman, 1990; Duderstadt and Berger, 2008; Dutta and Bell, 1997; Kawakami and Katayama, 2010; Kelman and Kelman, 2003; Mott and Berger, 2007; O'Donnell et al., 2013; O'Donnell, 2006; Ozaki and Katayama, 2009)). Striking similarities observed among initiation programs suggest that this cellular process dates back to the last universal cellular ancestor (Duderstadt and Berger, 2008, 2013; Kaguni, 2011; Stillman, 2005). In cellular organisms, some factors and their activities are conserved across all three domains of life (bacteria, archaea, and eukaryotes); for example, all proteins responsible for recognizing origins (called initiators) possess a set of evolutionarily related ATPase domains fused to a helix-turn-helix (HTH)-type DNA binding element (Cunningham and Berger, 2005; Erzberger et al., 2002, 2006; Fujikawa et al., 2003; Iyer et al., 2004; Neuwald et al., 1999; Roth and Messer, 1995). Moreover, some viral initiators also contain AAA+ modules tethered to one or more DNA-binding domains (Arthur et al., 1988; Enemark et al., 2002; Meinke et al., 2007; Wilson and Ludes-Meyers, 1991).

Beyond their shared reliance on dedicated initiator proteins, cellular organisms and viruses display diverse replication initiation mechanisms (Barry and Bell, 2006; Costa et al., 2013; Duderstadt and Berger, 2008; Dutta and Bell, 1997; LeBowitz and McMacken, 1984a; Mott and Berger, 2007; Weigel and Seitz, 2006). This divergence likely is the result of particular evolutionary pressures, which impose constraints that necessitate adaptation for survival within changing environments. For example, in most Gram-negative bacterial species origin melting, duplex unwinding, and replicative helicase loading are performed by three different proteins: DnaA, DnaB, and DnaC, respectively (**Table 1.1**) (Bramhill and Kornberg, 1988b; Chakraborty et al., 1982; Hsu et al., 1994; Kobori and Kornberg, 1982a, 1982b; Kornberg and Baker, T. A., 1992; LeBowitz and McMacken, 1986; Wahle et al., 1989a). For *E. coli*, initiation factors also sometimes have additional activities outside of initiation. For example, DnaA can act as a transcription factor (Atlung et al., 1985; Braun et al., 1985; Messer and Weigel, 1997), while DnaB serves an essential role in DNA replication re-start pathways (Heller and Marians, 2006).

Even among different bacterial species, differences in replication initiation factors are observed. For example, the archetypal low-G+C-content Gram-positive firmicutes utilize unique primosomal machinery, quite distinct from that seen in *E. coli.* Although they also require a DnaA initiator for origin recognition and melting, firmicutes such as *B. subtilis* and *S. aureus* require additional co-loading factors, called DnaB and DnaD, which in collaboration with the helicase loader DnaI facilitate loading of the replicative helicase (called DnaC) (**Table 1.1**) (Bruand and Ehrlich, 1995; Sakamoto et al., 1995; Smits et al., 2010, 2011; Soultanas, 2002; Tsai et al., 2009).

In other systems, such as papilloma and polyoma viruses, only a single protein is needed to serve both as an initiator for origin melting and as the helicase for duplex DNA unwinding (Hickman and Dyda, 2005). By contrast, viruses like bacteriophage λ (lambda) encode two proteins, "O" and "P," that initiate phage replication (**Table 1.1**) (Klinkert and Klein, 1978; LeBowitz and McMacken, 1984a, 1984b; S, 1975). For cellular organisms, other aspects of initiation – such as DNA-unwinding and strand-synthesis enzymes (e.g., helicases and primases) – are distinct between bacterial and archaeal/eukaryal lineages (Aravind et al., 1998; Iyer et al., 2004; Leipe et al., 2000). Overall, although common themes exist in how initiation is executed and controlled, the specific pathways and players that promote this process can vary dramatically among and within cellular organisms and viruses.

Bacterial DNA Replication Initiation

In bacteria, DNA replication initiation proceeds through at least four distinct stages (**Figure 1.1**), including: (i) recognition of a replication origin by initiation factors (Schaper and Messer, 1995; Skarstad et al., 1993; Speck and Messer, 2001; Speck et al., 1999; Weigel et al., 1997), (ii) origin remodeling/melting, which results in the formation of a replication bubble (Bramhill and Kornberg, 1988a; Duderstadt et al., 2010; Gille and Messer, 1991; Hwang et al., 1992; Krause et al., 1997; Speck and Messer, 2001), (iii) deposition of two copies of the replicative helicase onto the melted replication origin (Fang et al., 1999), and (iv) the recruitment of replisomal factors (e.g., primase, polymerases, clamp loaders), which lead to the formation of two bidirectional replication forks that move in opposite directions from the origin (Funnell et al., 1987; Hiasa and Marians, 1996; Sekimizu et al., 1988a).

Once assembled, the replisome, using the single-strands of the melted duplex DNA as a template, synthesizes two new daughter strands through a highly coordinated and tightly coupled synthesis of both the continuous leading-strand and the discontinuous lagging strand (Baker and Bell, 1998; Benkovic et al., 2001; Davey et al., 2002b). The final products of bacterial DNA replication are two interlinked daughter chromosomes, which must be disentangled by topoisomerases so that the individual chromosomes can be appropriately partitioned into their individual cells during cell division (Zechiedrich and Cozzarelli, 1995).

Replisome assembly in *E. coli*

All cellular replication machineries share specific enzymatic activities including: a replicative helicase to unwind duplex DNA, a primase which synthesizes short RNA primers to initiate DNA synthesis, and two DNA polymerases that perform leading and lagging strand synthesis (Johansson and Dixon, 2013; Johnson and O'Donnell, 2005; Kornberg and Baker, T. A., 1992). Much of what we know about fundamental mechanisms of DNA synthesis, replication initiation and replisome dynamics come from studies in the Gram-negative bacterium *Escherichia coli (E. coli)*, a long-standing model organism, as well as two of its bacteriophages, T4 and T7 (Benkovic et al., 2001; Bramhill and Kornberg, 1988a; Duderstadt et al., 2014; Fuller et al., 1983; Hamdan et al., 2009; Hardy et al., 2004; O'Donnell, 2006; van Oijen and Loparo, 2010; Romano et al., 1981; Sherratt, 2003).

Decades of research have characterized the individual roles of each of the proteins that are key to the formation of an active replisome. For example, once loaded, DnaB recruits the primase protein (DnaG), forming the "primosome" (Arai and Kornberg, 1979, 1981). The association between DnaB and DnaG allows for the coupling of helicase unwinding activity to the synthesis of RNA primers

(Bird et al., 2000; Chang and Marians, 2000; Schaeffer et al., 2005), which is required to initiate strand synthesis by DNA polymerases (MacNeill, 2001; Okazaki et al., 1968). The hexameric motor DnaB resides at the head of the bacterial replication fork. DnaB encircles ssDNA on the lagging strand and hydrolyzes ATP to move along ssDNA in the 5′-3′ direction (LeBowitz and McMacken, 1986), unwinding the parental duplex DNA to generate the ssDNA template used for DNA synthesis by DNA polymerase III (Galletto et al., 2004a, 2004b; LeBowitz and McMacken, 1986). DNA polymerase III constitutes the catalytic core of the replisome and is bound to both the processivity sliding clamp and clamp loader proteins, which together form a single complex (McHenry and Crow, 1979; Naktinis et al., 1995). Sliding clamps tether the polymerase to its substrate during DNA synthesis thereby ensuring high processivity of the moving replication fork. The polymerase "holoenzyme" stays bound to the replicative helicase DnaB and the clamp loader via the clamp loader's τ subunit (Gao, 2000). During fork progression, the clamp loader orchestrates opening, loading and removal of sliding clamps on duplex DNA (Bowman et al., 2005; Jeruzalmi et al., 2002; Kelch et al., 2011).

In addition to learning about each of the individual components which make up the replisome, structural and biochemical studies in *E. coli* and T7 phage systems have provided numerous insights into the mechanisms driving leading and lagging strand synthesis at the replication fork, as well as the accuracy, high processivity, and dynamics of fork progression (Ellison and Stillman, 2001; Georgescu et al., 2011; Johnson and O'Donnell, 2005; Kelman and O'Donnell, 1995; MacNeill, 2001; van Oijen and Loparo, 2010; Yeeles and Marians, 2013). For example, although it had long been accepted that *E. coli* replication forks contained only two DNA polymerases to coordinate DNA synthesis on the lagging and leading strands, recent biochemical, *in vivo* experiments, and single molecule studies support a new model for bacterial DNA replication whereby a third DNA polymerase travels with the moving replication fork (Georgescu et al., 2011; McInerney et al., 2007; Reyes-Lamothe et al., 2010).

AAA+ ATPases and DNA Replication Initiation

AAA+ ATPases (ATPases associated with diverse cellular activities) play an integral role in the initiation of DNA replication (Duderstadt and Berger, 2008, 2013; Erzberger and Berger, 2006; Iyer et al., 2004). The "active" state of these proteins typically involves oligomerization of the AAA+ module as either a homo- or hetero-oligomers in a head-to-tail orientation; this assembly pattern forms higher-order ring-shaped or spiral oligomeric assemblies that can undergo conformational rearrangements upon binding and hydrolysis of ATP between the interface of neighboring subunits. Although AAA+ ATPases vary extensively in cellular function, most share the ability to couple ATP hydrolysis to molecular remodeling of their target macromolecules (Hartman and Vale, 1999; Iyer et al., 2004; Neuwald et al., 1999; Ogura and Wilkinson, 2001). AAA+ ATPases are defined by a structurally conserved ATP binding fold that belongs to the much larger superfamily of "P-loop"-type nucleoside triphosphate (NTP)-binding proteins (Iyer et al., 2004). This fold is defined in part by two distinct motifs, known as the Walker A (WA) and Walker B (WB) motifs, which are critically important in both nucleotide binding and nucleotide hydrolysis (Walker et al., 1982).

In cellular organisms, as well as in viruses, it has been well established that AAA+ initiation factors utilize ATP binding to execute and regulate initiation programs (Bell and Stillman, 1992; Borowiec and Hurwitz, 1988; Bramhill and Kornberg, 1988; Funnell et al., 1987; Sanders and Stenlund, 1998). In bacteria, although it is clear that an ATP-bound state is required for initiator and helicase loader activation, ATP hydrolysis and the subsequent conversion to an ADP-bound state also serves an essential function during initiation. For example, the bacterial initiator DnaA is inactivated by ATP hydrolysis, thereby preventing unwanted re-initiation of DNA replication in bacteria (Kaguni, 2006; Su'etsugu et al., 2004). In eukaryotes, ATP hydrolysis also serves a critical role in a key step in DNA replication initiation, particularly in loading of the replicative helicase (Bowers et al., 2004; Randell et al., 2006). Some viral initiators, specifically those of the superfamily III helicase family, also utilize ATP turnover for hexamer formation and DNA unwinding activity (Abbate et al., 2004; Borowiec and Hurwitz, 1988; Dean et al., 1987; Enemark and Joshua-Tor, 2006; Gai et al., 2004; Hughes and Romanos, 1993; Mastrangelo et al., 1989; Ray et al., 1992; Sedman and Stenlund, 1998; Stahl et al., 1986; Yang et al., 1993).

Clamp loader and initiator/helicase-loader clades

Clamp loader AAA+ ATPases function as ATP-dependent molecular switches. These systems become activated and able to bind to their target (the sliding clamp) when also bound to ATP (Bowman et al., 2004; Jeruzalmi et al., 2001; Johnson et al., 2006; Naktinis et al., 1995; Seybert and Wigley, 2004). For their part, cellular initiators and helicase-loaders also behave like ATP-dependent molecular switches in which active and inactive states are defined by either their ATP-bound or ADP-bound status, respectively. The clamp loader's core ATP-binding fold is one of the simplest in the AAA+ superfamily. By comparison, cellular initiator and helicase-loaders are structurally distinguished by the insertion of an additional α-helix between helix α2 and sheet β2 of the core ASCE fold (additional strand catalytic 'E' (ASCE) P-loop NTPases) (**Figure 1.3A (inset)**) (Erzberger and Berger, 2006; Iyer et al., 2004). Structural studies have revealed that, like clamp loaders, initiator/helicase-loader assemblies favor higher-order formation of open rings, and in some cases, even spiral filaments (Bleichert et al., 2013; Bleichert et al., 2015; Clarey et al., 2006; Duderstadt et al., 2011; Erzberger et al., 2006; Mott et al., 2008; Speck et al., 2005). For both the bacterial helicase-loader DnaC and initiator DnaA, the extra α-helix serves to rotate adjacent AAA+ domain subunits out-of-plane with respect to one another, thereby disrupting formation of a closed-ring assembly, and alternatively giving rise to a right-handed open-ended helical arrangement.

The Initiation of Bacterial DNA Replication

In bacteria, replication of the chromosome begins with the sequence-specific recognition of a single origin of replication, termed *oriC* (origin of chromosome) (Chakraborty et al., 1982; Fuller et al., 1984; Matsui et al., 1985). Although bacterial origins, vary tremendously with respect to both sequence and organization, *oriC* serves as an assembly site for the DnaA protein, a replication initiator that promotes origin melting and the start of DNA replication. To date, various *in silico* methods have predicted the locations of bacterial origins of over 1500 different bacterial chromosomes (Gao et al., 2013; Mackiewicz et al., 2004).

A key hallmark of bacterial origins is the presence of two classes of sequence elements: an AT-rich DNA unwinding element, which undergoes DnaA-mediated duplex unwinding upon assembly of the DnaA-*oriC* initiation "open complex," and a distinct arrangement of sequence specific elements recognized by DnaA that serve as a framework for DnaA binding and cooperative self-assembly on the origin (Bramhill and Kornberg, 1988; Gille and Messer, 1991; Kowalski and Eddy, 1989) (**Figure 1.2A**). In *E. coli oriC* and many other bacterial origins, other sequence motifs present in the DNA serve as binding sites for specific architectural proteins (called nucleoid-associated proteins (NAPs)). The binding of NAPs to origins serves important roles in both positive and negative regulation of replication initiation, not only to prevent unwanted re-initiation events, but also to aid in orchestrating and coordinating chromosomal initiation in accordance with cell cycle status and environmental cues. This section will focus on the fundamental steps and protein factors involved in coordinating initiation. A particular emphasis will be placed on the details of *ori*C, DnaA function, and the loading of the replicative helicase in *E. coli*; however, other bacterial organisms will be discussed for comparison.

Bacterial Replication Origins

The *E. coli* replication origin, *oriC*

E. coli has long served as an excellent model system for studying DNA replication and bacterial initiation. The *E. coli* origin, *oriC,* is a ~260 base-pair (bp) region containing a complex array of conserved sequence motifs that are bound by the initiator DnaA. Although most of these conserved sites are recognized by the ATP-dependent initiator DnaA (Fuller et al., 1984; McGarry et al., 2004; Speck et al., 1999), others are recognized by regulatory factors that modulate initiator/origin interactions such as IHF, HU and Fis (Finkel and Johnson, 1992; Friedman, 1988; Hwang et al., 1992; Ryan et al., 2002, 2004; Schmid, 1990; Wold et al., 1996) (**Figure 1.2A**).

One prevalent conserved sequence element within *oriC* is a motif termed a "DnaA-box" (sites R1-R5) (**Figure 1.2A**) (Fuller et al., 1984; Matsui et al., 1985). DnaA-boxes are recognized by multimeric (ATP-bound) and monomeric (ADP-bound) forms of DnaA (ATP-DnaA and ADP-DnaA, respectively), with regions R1, R2, and R4 bound most tightly (Leonard and Grimwade, 2011; Margulies and Kaguni, 1996; Schaper and Messer, 1995; Sekimizu et al., 1987). "I-sites" and "τ-sites" constitute two other classes of DnaA-binding sites found in *oriC* that associate more weakly with the initiator and are preferentially recognized by ATP-bound DnaA (**Figure 1.2A**) (Kawakami et al., 2005; McGarry et al., 2004). The collection of DnaA-boxes, I-sites, and tau-sites (referred to as τ-sites) in *oriC* together form an "organizing center", which is essential for promoting the higher-order assembly of DnaA and origin activation. Interestingly, the spacing between high- and low affinity sites is critically important, as even two-base insertions can abrogate origin function (Rozgaja et al., 2011).

A region of DNA adjacent to the *oriC* organizing center contains several copies of a fourth type of DnaA-binding element termed an "ATP-DnaA box." This portion of the origin constitutes a "DNA unwinding element" (termed DUE) (Kowalski and Eddy, 1989) that serves as the site of replisome assembly. Three 13bp AT-rich repeats historically designated as "L", "M", and "R" reside within the DUE (**Figure 1.2A**) (Bramhill and Kornberg, 1988; Gille and Messer, 1991). Like I-sites and τ-sites, ATP-DnaA boxes are bound preferentially by ATP-DnaA (Speck and Messer, 2001; Speck et al., 1999), an event that requires the cooperative assembly of multiple protomers and depends on initiator binding to the adjacent R1 element (Speck and Messer, 2001). As with the organizing center, the spacing between the DUE and other DnaA-binding sites is critical for *oriC* function (Hsu et al., 1994).

Sequence organization of DnaA boxes

The direct, sequence-based readout of specific origin binding sites by DnaA appears preserved across bacteria (Fujikawa et al., 2003; Holz et al., 1992; Sutton and Kaguni, 1997b; Tsodikov and Biswas, 2011). However, the replication origins of different bacterial species all display a unique number and arrangement of the consensus DnaA box sequence and its variants (Mackiewicz et al., 2004) (**Figure 1.2A**). In addition, DnaA orthologs also appear to differ in their relative affinity for DnaA-box sequences (**Table 1.2**) (Zawilak-Pawlik et al., 2005). For example, *Mycobacterium tuberculosis* DnaA does not stably associate with a single DnaA-box; instead, binding requires that multiple repeats be present in target substrates (Zawilak et al., 2004). By contrast, *Helicobacter pylori* DnaA exhibits a high affinity for two DnaA boxes (Zawilak et al., 2003).

The preferential binding of DnaA to multiple sites has led to the suggestion that the cooperative binding of DnaA molecules may be important for the productive formation of DnaA-*oriC* initiation complexes, particularly in bacteria species containing highly extended origins. Studies of bacteria containing longer than average origins, such as Actinomycetes, *M. tuberculosis* and *S. coelicolor*, have shown that increasing the number of DnaA boxes appears to correlate with an increased reliance on cooperative interactions between multiple DnaA monomers for stable DnaA-box binding (Zawilak-Pawlik et al., 2005). This variation, coupled with the distinct arrangement of DnaA boxes among different *oriC*s, suggests that DnaA orthologs are fine-tuned to act only on their cognate origins (**Figure 1.2A**). Consistent with this notion, *E. coli* DnaA cannot initiate replication on *B. subtilis oriC*, or *vice versa* (Krause et al., 1997). Why origins are so diverse among bacteria is unclear, but could reflect a speciation mechanism for preventing the replication of foreign origins acquired through phage infection or DNA uptake.

Another common theme observed within bacterial origins, like the *oriCs* of *Caulobacter crescentus (C. crescentus)* and *E. coli*, is that the total number of low-affinity boxes frequently outnumbers the amount of high-affinity sites (Rozgaja et al., 2011). Interestingly, studies in *E. coli* have shown that the distribution and quantity of low- and high-affinity sites is not only vital for *oriC* function, but also crucial for maintaining appropriate initiation frequency (Grimwade et al., 2007; Leonard and Grimwade, 2011).

DnaA Initiator and Origin Processing

Domain organization of DnaA

To date, only a single highly conserved bacterial initiator, DnaA, has been found in all eubacteria. Indeed, the first temperature-sensitive mutants isolated in bacteria mapped to the *dnaA* gene (Kohiyama, 1968; Kohiyama et al., 1966). DnaA not only specifically recognizes bacterial replication origins, but also induces duplex DNA melting to promote replication onset (Bramhill and Kornberg, 1988; Fuller et al., 1984). Biochemical characterization of *E. coli* DnaA, the archetypal member of this family, has shown that the protein is composed of four distinct domains (Messer, 2002; Messer et al., 1999; Sutton and Kaguni, 1997a) (**Figure 1.3A**). The first (domain I) is a small, globular **K-H**omology (**KH**) type fold (Abe et al., 2007; Seitz et al., 2000; Sutton et al., 1998), which homo-dimerizes, binds the replicative DnaB helicase (Abe et al., 2007; Sutton and Kaguni, 1997a; Weigel et al., 1999) and associates with a diverse number of regulatory proteins such as DiaA, Hda and HU (for reviews, see (Kaguni, 2006; Ozaki and Katayama, 2009)). The second element (domain II) is a variable and likely flexible linker element of unclear function (Ozaki and Katayama, 2009).

Domain III consists of the AAA+ ATPase fold mentioned earlier (Erzberger and Berger, 2006; Iyer et al., 2004; Koonin, 1992; Neuwald et al., 1999), and can form large homo-oligomeric arrays (Erzberger and Berger, 2006; Felczak and Kaguni, 2004; Funnell et al., 1987; Messer et al., 1999; Scholefield et al., 2012), bind ssDNA (**Figure 1.3B**) (Duderstadt et al., 2011; Ozaki et al., 2008), and promote *oriC* melting (Duderstadt et al., 2010; Felczak and Kaguni, 2004; Ozaki et al., 2008). The fourth region (domain IV) comprises a C-terminal **H**elix-**T**urn-**H**elix (**HTH**) element (Erzberger et al., 2002; Roth and Messer, 1995) that recognizes specific sites within the *oriC* organizing center (Blaesing et al., 2000; Fujikawa et al., 2003; Sutton and Kaguni, 1997b).

Origin recognition and ssDNA and dsDNA binding by DnaA

In addition to defining how domain IV DnaA associates with dsDNA DnaA-boxes though its HTH element (Fujikawa et al., 2003), structural work has also revealed how the initiator binds to ssDNA (Duderstadt et al., 2011). Upon binding ATP, the AAA+ domains of DnaA form a contiguous helical assembly (Erzberger et al., 2006). Single-stranded DNA associates then exclusively with these self-assembled ATPase regions, in a manner whereby each protomer binds three nucleotides of an extended, single strand (Duderstadt et al., 2011). Nearly all of the DnaA-ssDNA interactions observed in the crystal structure involve engagements with the phosphodiester backbone; biochemical studies of ssDNA binding by *Aquifex aeolicus* DnaA have corroborated the lack of sequence-specificity observed in the ssDNA-bound-DnaA structure (Duderstadt et al., 2010).

ATP-dependent activation of DnaA

Prior to replication onset, high-affinity DnaA boxes in *oriC* are bound by domain IV of ATP-DnaA or ADP-DnaA (Cassler et al., 1995; Samitt et al., 1989). As initiation commences, additional copies of ATP-DnaA localize to *oriC* (Cassler et al., 1995), filling weaker DnaA-binding sites and co-associating into a large nucleoprotein complex that is thought to wrap the organizing center of the origin into a solenoidal array (Crooke et al., 1993; Funnell et al., 1987; Grimwade et al., 2007; McGarry et al., 2004; Rozgaja et al., 2011) (see *E. coli oriC* in **Figure 1.2A**). Although domains I and IV also participate in assembly (Duderstadt et al., 2010; Felczak and Kaguni, 2004; Felczak et al., 2005), domain III is the primary mediator of DnaA oligomerization (Duderstadt et al., 2011; Erzberger et al., 2006; Felczak and Kaguni, 2004; Kawakami et al., 2005). The helical oligomer formed by DnaA reconstitutes a hydrolysis-competent ATPase site through joint action of several signature amino-acid motifs (Erzberger et al., 2006; Scholefield et al.,

2012), including the Walker A, Walker B, Sensor I, and Sensor II elements from one DnaA subunit, and a *trans*-acting "arginine finger" from a partner protomer (reviewed in (Ozaki and Katayama, 2009)). Upon assembly, the DnaA helix appears to wrap duplex DNA around itself, stabilizing one or more positive DNA supercoils. This activity has been suggested to induce torsional strain into origin that may assist with DUE unwinding (Erzberger et al., 2006; Zorman et al., 2012) (**Figure 1.3C**).

Mechanism of DnaA-mediated origin unwinding

The complex formed between DnaA and the organizing-center of *oriC* serves as an essential prerequisite to DUE melting (Bramhill and Kornberg, 1988; Gille and Messer, 1991; Speck and Messer, 2001). A negatively-supercoiled bacterial chromosome is required for DnaA-mediated opening (Bramhill and Kornberg, 1988), consistent with the idea that bubble formation might be aided by torsional strain (Erzberger et al., 2006). However, ATP-DnaA also associates directly with the DUE (Ozaki et al., 2008; Speck and Messer, 2001), and can actively melt short DNA duplexes in an ATP-dependent manner by binding and stretching ssDNA along the helical axis of the DnaA oligomer (Duderstadt et al., 2011) (**Figure 1.3B**).

Although the precise mechanism is not fully understood, the available evidence indicates that either concomitant with or following DnaA self-assembly, the ATPase domains of the initiator deform and open the DUE directly (Duderstadt et al., 2011). At least two models account for how DnaA organizes both ssDNA and dsDNA to promote melting (**Figure 1.3C-D**), although the precise architecture of the nucleoprotein complex is not firmly established.

Bacterial Helicase Loading Mechanisms

The loading of ring-shaped hexameric replicative helicases onto origin DNA marks the first step in assembly of the replisome. Many bacterial species appear to employ dedicated helicase loading factors that help facilitate the appropriate deposition of two replicative helicases onto single-stranded DNA at a newly formed replication bubble. In this section, both helicase loaders belonging to the DnaC and DnaI-type families will be discussed; along with similarities and differences in their respective loading mechanisms.

Helicase loading in the Gram-negative bacterium *E. coli*

The marking and processing of origins by initiator proteins facilitates the next phase of initiation, namely, the loading of replicative helicases onto DNA (reviewed in (Soultanas, 2012)). In bacteria, a single helicase – termed DnaB in *E. coli* – serves as the front end of the newly-emerging replication fork. DnaB forms a two-tiered, ring-shaped hexamer (**Figure 1.4A**) (Bailey et al., 2007b; Lo et al., 2009; Wang et al., 2008), in which a conserved **N**-**T**erminal **D**omain (**NTD**) structurally homologous to the helicase-interaction domain of the DnaG primase protein comprises one tier, and a **C**-**T**erminal RecA-type ATPase **D**omain (**CTD**) forms the other (Bailey et al., 2007a, b; Su et al., 2006; Syson et al., 2005). Adjoining NTDs in the DnaB hexamer self-assemble into a trimer-of-dimers configuration (Bailey et al., 2007b; Biswas and Tsodikov, 2008; Lo et al., 2009; Wang et al., 2008), creating a collar that binds ssDNA (Lo et al., 2009). The CTD tier also interacts with nucleic acid substrates, and serves as the DNA translocation motor during duplex DNA unwinding (Biswas and Biswas, 1999; Lo et al., 2011; Nakayama et al., 1984; Nitharwal et al., 2012).

During replication, DnaB encircles the lagging template-DNA strand (Jezewska et al., 1998), moving 5′→3′ with the ATPase domains oriented toward the duplex DNA (Jezewska et al., 1998; Kaplan, 2000; LeBowitz and McMacken, 1986; Lee et al., 1989). DNA unwinding is thought to occur by a steric mechanism that excludes the leading template strand from the helicase interior during translocation (Hacker and Johnson, 1997; Kaplan, 2000). *E. coli* DnaB is loaded onto the single-stranded DUE regions of *oriC* by the concerted action of both DnaA and a dedicated loading factor, DnaC (Davey et al., 2002a; Fang et al., 1999; Marszalek and Kaguni, 1994; Seitz et al., 2000; Wickner and Hurwitz, 1975).

DnaC is an AAA+ ATPase and paralog of DnaA (Koonin, 1992; Mott et al., 2008), but lacks the C-terminal, duplex-DNA binding domain of the initiator. DnaC, like DnaA, bears a DnaB-binding domain at its N-terminus (Ioannou et al., 2006; Ludlam et al., 2001); however, the folds of these regions are unrelated between the two protein families (Abe et al., 2007; Loscha et al., 2009; Lowery et

al., 2007). DnaC also binds ssDNA in a cooperative and ATP-dependent manner (Biswas et al., 2004; Mott et al., 2008), using its AAA+ domains to form a right-handed helical oligomer (**Figure 1.4B**) that exhibits a bipartite ATPase site highly similar to that of DnaA (Mott et al., 2008). DnaC represses DnaB activity when bound to ATP or poorly-hydrolyzable ATP analogs (Allen and Kornberg, 1991; Davey et al., 2002a; Wahle et al., 1989). Although ATP binding is not required for DnaC to load DnaB onto a ssDNA circle, productive association with nucleotide is necessary for DnaC to support the DnaA-dependent initiation of DNA replication on an *oriC* substrate *in vitro* and *in vivo* (Makowska-Grzyska and Kaguni, 2010). Overall, the role of nucleotide binding and ATP hydrolysis in DnaC function has remained enigmatic. Work I have conducted to help clarify this issue is described in **Chapter 2**.

How DnaB is placed onto a melted origin has been a central question in the field. DnaC forms a 6:6 complex with DnaB (Galletto et al., 2003; Kobori and Kornberg, 1982), and has been proposed to "crack" open the helicase ring to allow ssDNA to engage the motor interior (Ahnert et al., 2000; Davey and O'Donnell, 2003; Soultanas, 2012). Consistent with these proposals, recent EM studies have demonstrated that *E. coli* DnaC indeed functions by a DnaB ring breaker mechanism (Arias-Palomo et al., 2013).

Recruitment of DnaB to *oriC* is mediated, at least in part, by an interaction between domain I of DnaA and the NTD region of the helicase (Marszalek and Kaguni, 1994; Sutton et al., 1998). Co-precipitation studies using *A. aeolicus* DnaC further has shown that the helicase loader, whose N-terminus binds to the C-terminal face of DnaB (Galletto et al., 2003; Ludlam et al., 2001) can use its ATPase domain to bind the AAA+ domain of DnaA initiator in a nucleotide-dependent manner (Mott et al., 2008). Together with biochemical studies showing that DnaA preferentially loads DnaB onto the "bottom" strand of the DUE *in vitro* (Weigel and Seitz, 2002), and that two DnaB hexamers are loaded onto opposite strands and in opposing orientations from one another at *oriC* (Fang et al., 1999), DnaA and DnaC have been proposed to collaborate in orienting DnaB hexamers on the complementary strands of a melted DUE (**Figure 1.4C**). Recent studies have shown that the DnaG primase can bind to the DnaB•DnaC complex, stimulating ATP hydrolysis by the loader and causing DnaC to release the helicase (Makowska-Grzyska and Kaguni, 2010). Efforts to clarify how DnaA and DnaC coordinately faciliate the loading of DnaB rings will also be presented in **Chapter 2**.

Helicase loading in Gram-positive bacteria

Replicative helicase loading mechanisms in Gram-positive bacteria, particularly those with low G+C content, are less well defined than their Gram-negative cousins, such as *E. coli*. Although these bacteria exhibit many similarities with *E. coli*, distinct differences nonetheless exist (Soultanas, 2012). For example, while *B. subtilis* contains homologs of *E. coli* DnaA, replicative helicase, primase, helicase loader and DNA polymerase, additional replication initiation factors (called DnaD and DnaB) are required for promoting replicative helicase loading. The nomenclature for replication proteins between Gram-negative and Gram-positive organism is unfortunately cumbersome, with replicative helicase and loader in Gram-negative bacteria called DnaB and DnaC, whereas in Gram-positive species the helicase and loader are called DnaC and DnaI, respectively.

During initiation in *B. subtilis*, DnaB and DnaD, together with their cognate initiator DnaA, associate with *oriC* in the order DnaA→D→B (Smits et al., 2010, 2011; Velten et al., 2003). DnaB and DnaD then interact with DNA, the DnaC helicase, and the DnaI•DnaC complex to facilitate helicase loading (Velten et al., 2003). As in *E. coli*, the DnaI loader can both bind ssDNA in an ATP-dependent manner and form a stable 6:6 complex with a replicative helicase target (Ioannou et al., 2006); however, data have also suggested that the *B. subtilis* helicase is assembled on the origin, rather than loaded as a preformed hexamer (Velten et al., 2003). Although the helicase loader DnaI appears to share similar biochemical activities with that of the *E. coli* DnaC loader (Ioannou et al., 2006), the particular roles *B. subtilis* DnaB and DnaD play in replication initaition remain ill-defined. The research presented in **Chapter 3** aims to enhance our current understanding of DnaI helicase loader activity in Gram-positive bacterial species.

Helicase loading in bacteria that lack a helicase loader

Efforts to establish a general framework for helicase loading in bacteria have been confounded by the apparent lack of DnaC/DnaI loader orthologs in many species (e.g., *Helicobacter pylori* and *Mycobacterium tuberculosis* (Alm and Trust, 1999; Cole et al., 1998)). This absence raises the question as to whether certain bacteria rely on as yet unrecognized loading factors, or whether their helicases are self-loading. In this respect, *H. pylori* DnaB has been observed to form an distinctive double-hexamer, which appears predicated on a six-fold symmetric configuration of the N-terminal domains that differs from the trimer-of-dimers state seen in other DnaB orthologs (Stelter et al., 2012). Moreover, expression of *H. pylori* DnaB in *E. coli* can complement a temperature-sensitive mutation in the *dnaC* helicase loader gene (Soni et al., 2003). These data suggest that dedicated helicase-loading proteins may not be required in all bacterial species; DnaA may serve as the sole factor responsible for mediating the recruitment of the hexameric motor to replication origins in these instances (Ozaki and Katayama, 2009). Overall, much remains to be discovered concerning the mechanisms by which initiation factors collaborate to facilitate helicase loading, and the extent to which these strategies differ between bacterial species.

Regulation of Bacterial DNA Replication

Although cellular organisms utilize a complex array of distinct mechanisms to control initiation certain parallels exist in how initiation is regulated between species. For example, origin accessibility can be controlled by DNA architecture factors such as histones in eukaryotes and nucleoid-associated proteins in bacteria (see reviews (Dorn and Cook, 2011; Leonard and Grimwade, 2011; Luijsterburg et al., 2008)); initiation proteins can similarly be regulated by post-translational modifications and/or protein-protein interactions. However, even within bacteria, there exists a variety of approaches to restrict access to replication origins and to modulate initiator activity (Katayama et al., 2010; Leonard and Grimwade, 2010, 2011; Mott and Berger, 2007; Skarstad and Katayama, 2013; Zakrzewska-Czerwinska et al., 2007).

Control of bacterial origin accessibility

Origin accessibility is one highly regulated aspect of initiation that serves to help prevent inappropriate re-initiation. For example, following initiation in *E. coli*, a dedicated protein known as SeqA binds to newly replicated origins, enforcing synchronous DNA replication (Odsbu et al., 2005). There are 11 GATC sites located in *E. coli oriC*, interspersed throughout both the DnaA box region and the DUE, which are normally fully methylated by Dam methylase. Following the passage of a replication fork through *oriC*, the origin enters into a transient, hemi-methylated state that allows SeqA – whose affinity for hemi-methylated DNA is greater than for fully-methylated substrates (Brendler et al., 1995; Slater et al., 1995) – to engage specific GATC sequences within the region (Nievera et al., 2006; Oka et al., 1980; Zyskind and Smith, 1986). As SeqA associates with *oriC*, it assembles into a filamentous oligomer, organizing the origin into a stable nucleoprotein complex. This SeqA-dependent assembly occupies low-affinity DnaA sites to block initiator binding to *oriC* and impede re-replication (Guarne et al., 2005; Nievera et al., 2006; Taghbalout et al., 2000). Upon the dissociation of SeqA from DNA, the Dam methylase fully methylates *oriC* to prevent SeqA from rebinding the origin (Kang et al., 1999), thereby re-establishing initiation competency. SeqA's crucial role in regulating initiation has been demonstrated genetically, as deletion of the *seqA* gene results in premature initiation events, abnormal nucleoid localization, and asynchronous replication (Brendler et al., 2000; Von Freiesleben et al., 1994; Lu et al., 1994; Slater et al., 1995).

Nucleoid Associated Proteins help regulate DnaA-*oriC* assembly

In *E. coli*, the ability of DnaA to access its binding sites within *oriC* is closely tied to the action of dedicated DNA-binding proteins that either compete for origin sites or that stimulate DnaA association and action (**Figure 1.5**). For example, as mentioned previously, the IHF and HU proteins of *E. coli*, are two Nucleoid Associated Proteins (NAPs) that synergistically potentiate the assembly of DnaA on *oriC* (Hwang and Kornberg, 1992). Both proteins significantly bend DNA (Rice et al., 1996; Sugimura and Crothers, 2006; Swinger et al., 2003), an activity that can either help destabilize duplex origin DNA directly (HU) (Funnell et al., 1987; Hwang and Kornberg, 1992; Ryan et al., 2002), or that can promote the assembly of ATP-bound DnaA on *oriC* to drive DUE melting (IHF) (Craig and Nash, 1984; Hwang and Kornberg, 1992; Kuznetsov et al., 2006; Leonard and Grimwade, 2011; McGarry et al., 2004; Rice et al., 1996). By contrast, a third NAP – Fis (Factor for Inversion Stimulation) – can prevent the binding of IHF to *oriC* and thereby block DnaA assembly (Hiasa and Marians, 1994; Koch and Kahmann, 1986; Pan et al., 1994; Ryan et al., 2004; Wold et al., 1996). Although neither IHF nor Fis are essential for viability, both factors are involved in maintaining initiation synchrony during rapid *E. coli* growth (Boye, 1993; Ryan et al., 2002).

Origin control in *Bacillus subtilis* and *Caulobacter crescentus*

Based on phylogenetic data, other bacteria do not appear to rely on the NAPs and SeqA system used in *E. coli*. Nevertheless, the use of sequence-specific DNA binding proteins to compete for DnaA access to cognate replication origins is a general trend. For example, in *B. subtilis,* an origin-binding protein called SpoA both recognizes specific sites in *oriC* and prevents DNA melting *in vitro,* possibly through an origin sequestration mechanism (Castilla-Llorente et al., 2006). In *C. crescentus,* a master regulatory protein known as CtrA silences the chromosomal origin (C_{ori}) by binding next to one or more DnaA boxes, thereby preventing the initiator from appropriately engaging DNA (Marczynski and Shapiro, 2002; Quon et al., 1996; Quon et al., 1998; Siam and Marczynski, 2000). Notably, control of CtrA function utilizes several cell-cycle dependent strategies reminiscent of those found in eukaryotes. For example, CtrA can be phosphorylated by the histidine kinase CckA (Cell cycle histidine kinase), an event that allows CtrA to productively associate with C_{ori} (Siam and Marczynski, 2000). CtrA levels also are regulated by controlled proteolysis through the ClpXP degradasome (Gorbatyuk and Marczynski, 2005; McGrath et al., 2006). Given the relative abundance of DNA-binding and remodeling proteins in bacterial cells (Grainger et al., 2006), it seems likely that studies of other bacterial species will turn up analogous, albeit distinct, systems for controlling origin accessibility.

Control of DnaA availability and activity

The model bacterial species (*E. coli, B. subtilis, and C. crescentus*) discussed in this section all contain a single circular chromosome with a single replication origin. In these organisms, DnaA activity can also be controlled directly by replication-coupled proteins, which stimulate ATP hydrolysis by the initiator, to produce an inactive ADP-bound state (discussed below) (Keyamura and Katayama, 2011; Su'etsugu et al., 2005, 2008, 2013; Xu et al., 2009). Other, alternate control systems have also been characterized in *E. coli*. For example, DnaA binding sites located outside *oriC*, known as DARS, have been shown to control the subcellular localization of DnaA or re-activation (Fujimitsu et al., 2009; Katayama et al., 2010), stimulating the exchange of bound ADP to ATP (Fujimitsu and Katayama, 2004; Su'etsugu et al., 2006). *E. coli* DnaA is also controlled at the transcriptional level through an auto-regulatory feedback mechanism centered on the *dnaA* gene (Atlung et al., 1985). Fresh DnaA synthesis is known to be required to initiate a new round of DNA replication during each cell cycle (Kimura et al., 1979; Leonard and Grimwade, 2010), and while only roughly 20 DnaA molecules are required to form the "open" DnaA-*oriC* initiation complex (Crooke et al., 1993; Ryan et al., 2004), it has been estimated that approximately between 500-2000 monomers of the DnaA can be found in any given cell, dependent on strain and variable growth rates (Chiaramello and Zyskind, 1989; Hansen et al., 1991; Sekimizu et al., 1988b).

Given the abundance of DnaA, an amount significantly exceeding the number of molecules sufficient to promote initiation, it is perhaps unsurprising that the specific oligomerization and origin assembly activities of DnaA are tightly and precisely controlled. *E. coli* prevents recurrent initiation events by keeping DnaA in an "inactive," ATP-bound state until initiation is desired, and the timing of bacterial replication initiation thus relies heavily on stringent control of a relatively small pool of the active ATP-bound form of the initiator. Multiple coordinated mechanisms govern this "active initiator pool" by controlling availability, protein synthesis, access to initiator binding sites, and ATP hydrolysis.

Although DnaA's affinity for both ATP and ADP is high (K_d = 30 and 100 nM, respectively) (Sekimizu et al., 1987), newly synthesized DnaA becomes primarily bound to ATP as the concentration of ATP greatly exceeds ADP in the cell. Notably, expression of new DnaA, and therefore production of active ATP-DnaA, necessitates careful regulation of ATP-DnaA levels in order to accommodate the fluctuating number of origins per cell during different rates of growth. ATP-DnaA levels are monitored through repressive auto-regulation of the *dnaA* gene by DnaA; providing flexible DnaA-ATP expression during different growth rates (Atlung et al., 1985). Once the active ATP-DnaA pool reaches a particular concentration within the cell, the active ATP-DnaA

cooperatively assembles at *oriC* resulting in origin melting and recruitment of the replicative helicase.

Following self-assembly, ATP hydrolysis by DnaA is stimulated by exogenous proteins in several interesting ways. In *E. coli,* the initiator's ATPase activity is stimulated through a replication-coupled pathway involving an AAA+ protein called Hda. Hda mediates a process known as RIDA ('Regulatory Inactivation of DnaA'), in which the presence of a polymerase sliding-clamp promotes ATP hydrolysis in DnaA (Katayama et al., 2010). Hda elicits the RIDA response through two interactions: a canonical AAA+/AAA+ contact between an arginine-finger on Hda and the nucleotide-binding site of DnaA (Nakamura and Katayama, 2010; Su'etsugu et al., 2005), and a specific interaction between domain IV of DnaA and a DNA-bound clamp•Hda complex (Keyamura and Katayama, 2011).

Hda-type strategies appear to exist in a number of bacterial species. For example, l*ike E. coli*, the α-proteobacterium *C. crescentus* contains an Hda ortholog, termed HdaA, which co-localizes with the sliding clamp and inhibits re-initiation (Collier and Shapiro, 2009). Although *B. subtilis* and other Gram-positive bacteria do not appear to have a clear Hda homolog, they do possess a functionally analogous protein termed YabA. As with Hda, YabA binds to both DnaA and the sliding clamp to block further DnaA binding to *oriC*, thereby preventing inappropriate re-initiation (Hayashi et al., 2005; Noirot-Gros et al., 2002; Noirot-Gros et al., 2006). How YabA and Hda-like proteins associate with DnaA remains to be established.

In addition to negative-regulation, bacteria have evolved means for positively controlling DnaA function directly. For example, the DnaA-binding protein DiaA is a potentiator of initiation that, in *E. coli*, enhances the assembly DnaA onto *oriC* and aids DUE unwinding, (Ishida et al., 2004; Keyamura et al., 2009; Keyamura et al., 2007). DiaA and its orthologs appear to function by forming homo-tetramers that bind to the N-terminus of DnaA (Keyamura et al., 2009; Natrajan et al., 2009), facilitating cooperative interactions between initiator protomers to maintain replication synchrony (Keyamura et al., 2009). Other proteins also bind to the N-terminal domain of *E. coli* DnaA; however, some of these interactions (such as with the L2 ribosomal subunit) interfere with DnaA assembly to negatively regulate initiator activity and assembly at *oriC* (Chodavarapu et al., 2011). *B. subtilis* utilizes a different set of factors that bind to and control DnaA activity. To date, three such proteins – SirA, Soj and SpoOJ – have been found to collectively govern how the initiator associates with both itself and *oriC* (**Figure 1.5**) (Lee and Grossman, 2006; Murray and Errington, 2008; Ogura et al., 2003; Rahn-Lee et al., 2009; Scholefield et al., 2011; Wagner et al., 2009). SirA is specifically expressed during *B. subtilis* sporulation, and blocks initiation of chromosome replication by binding directly to *B. subtilis* DnaA

(*Bs*DnaA) to prevent *oriC* binding and to stimulate dissociation of the initiator from the origin (Rahn-Lee et al., 2009; Wagner et al., 2009). By comparison, Soj – a Walker-type ATPase that binds both DNA and DnaA – functions through a complex mechanism involving its partner protein, SpoOJ (Lee and Grossman, 2006; Murray and Errington, 2008; Ogura et al., 2003; Scholefield et al., 2011). During replication onset, Soj specifically associates with a site proximal to *oriC*, termed *parS* (Lee and Grossman, 2006), forming a complex that promotes the DnaA-dependent initiation of replication (possibly by altering the local structure of the *oriC-parS* region) (Murray and Errington, 2008; Ogura et al., 2003). Once replication begins, SpoOJ stimulates ATP hydrolysis by Soj, resulting in the dissociation of an ADP-bound Soj dimer from *parS* that subsequently binds to DnaA and sequesters the initiator to prevent re-initiation (Scholefield et al., 2011) (**Figure 1.5**). The differences between the protein-dependent strategies used by *E. coli, B. subtilis* and *C. crescentus* for controlling DnaA function and origin accessibility imply that a diverse array of regulatory mechanisms likely exists among bacterial species indicating that many new factors and pathways await discovery.

Intersections between Bacterial and Phage Replication Processes

During replication, viruses face distinct challenges from those encountered by cellular organisms. For example, viruses must carefully coordinate their enzymatic activities with those of their host, while at the same time evading defense systems, in order to ensure rapid proliferation of viral progeny. In this section, replication initiation mechanisms utilized by a few bacteriophages will be discussed. In many phage genomes, there exists a common theme whereby genes encoding replication functions are often found located close to one another. These regions are sometimes referred to as 'replication modules' (Weigel and Seitz, 2006). Many phage replication modules, such as those of phage λ, have been characterized experimentally (e.g., see (Alfano and McMacken, 1989; Dodson et al., 1985; Klinkert and Klein, 1978; Learn et al., 1997; LeBowitz and McMacken, 1984a, 1984b; Schnos et al., 1988; Struble et al., 2007; Wold et al., 1982)).

At present, the initiation mechanisms of multiple circular and linear dsDNA phage replicons have been established in detail. Three common initiation strategies employed by phages include: (1) cutting or 'nicking' of the phosphodiester bond between two adjacent bases on one DNA strand; (2) 'melting' or breaking the hydrogen bonds holding two complementary DNA strands together; and (3) unwinding the terminal ends of linear double-stranded DNA (reviewed in (Weigel and Seitz, 2006)). All of these strategies produce a single-stranded template required for DNA synthesis and have been studied extensively in a variety of phages.

One of the most studied bacteriophages, the temperate phage lambda (λ), has been influential in enhancing our understanding of some of the general principles of DNA replication initiation. In this section, the replication initiation mechanism utilized by lambda phage will be highlighted to give just one example of a well-characterized phage replication module and its corresponding initiation strategy. In addition, replication modules from *Staphylococcus* specific phages, which are poorly understood, will be discussed as the particular phage replication module investigated in this dissertation work (presented in **Chapter 3**) belongs to the *Staphylococcus aureus* specific family of bacteriophages.

Lambda phage DNA replication initiation mechanism

When bacteriophage lambda (λ) infects an *E. coli* cell, the virus's linear, double-stranded DNA is circularized through the action of bacterial ligase (Furth, M.E., 1983; Kornberg and Baker, T. A., 1992). Once circularized, λ DNA is further processed by gyrase, which introduces negative supercoils into the phage DNA. Replication of the phage genome begins at a specific DNA sequence called

*ori*λ and proceeds bi-directionally from this site (Furth, M.E., 1983; Schnos and Inman, 1991; Stevens, W.F., Adhya, W., Szybalski, W., 1971). Phage replication assembly at *ori*λ involves a complex set of interactions between λ phage proteins and the *E. coli* host DNA replication machinery. The phage origin contains two key features: (i) four, 19 bp direct repeats, each of which is an inverted repeat (iterons are shown in Figure 1.2B); and (ii) an adjacent ~40 bp AT-rich region that is melted during initiation (Denniston-Thompson et al., 1977; Schnos et al., 1988; Tsurimoto and Matsubara, 1981).

Bacteriophage λ (lambda) encodes two proteins, "O" and "P," that initiate phage genome replication (Alfano and Mcmacken, 1988; Alfano and McMacken, 1989; Dodson et al., 1986; Lebowitz and Mcmacken, 1984; LeBowitz and McMacken, 1984b; Mallory et al., 1990; Mensa-Wilmot et al., 1989; Wickner, 1978; Wold et al., 1982). The λO and λP proteins, the initiator and helicase loader, respectively, are the only phage-encoded proteins required for viral DNA replication (LeBowitz and McMacken, 1984b; Tsurimoto and Matsubara, 1981; Weigel and Seitz, 2006; Wickner, 1978), while host replication proteins and accessory factors required to complete lambda DNA synthesis include gyrase, DNA ligase, PolA, and Topo IV (reviewed in (Weigel and Seitz, 2006)). The initiation of λ DNA replication begins with the binding of λO to the four direct repeats sequences within *ori*λ (located within the center of the λO gene) (Tsurimoto and Matsubara, 1981; Zahn and Blattner, 1985) (see **Figure 1.2B**).

Although λO can associate with either the linear or relaxed form of λ DNA, λO requires a negatively-supercoiled substrate to promote the assembly of an λO-*ori*λ initiation complex, termed the "O-some", which is competent to promote origin melting (Dodson et al., 1985; LeBowitz and McMacken, 1984b; Taylor and Wegrzyn, 1995; Tsurimoto and Matsubara, 1981). Host gyrase transforms the lambda genome into an appropriate substrate for initiation by introducing negative supercoils into the now circularized lambda dsDNA (Schnos et al., 1988). Adjacent to the "O-some" initiation complex is an AT-rich region thought to serve as the site for origin melting during initiation (Denniston-Thompson et al., 1977; Hobom et al., 1979).

To promote loading of the host replicative helicase, λO must first associate with λP (Friedman, 1992; Furth and Yates, 1978; Wickner and Zahn, 1986; Zylicz et al., 1984), which forms a direct association with DnaB (Friedman, 1992; Liberek et al., 1990; Mallory et al., 1990; Wickner, 1978). Though the λP phage helicase loader is not an ATPase, both λP and ATP-dependent DnaI/C bacterial helicase loaders share a cryptic ssDNA-binding activity, which is only uncovered when each of the proteins bind to the bacterial replicative helicase (Ioannou et al., 2006; Learn et al., 1997). This pattern suggests that lambda phage has independently

evolved a DNA replication initiation and helicase loading strategy that is functionally analogous to that of its host.

Replication modules in *Staphylococcus aureus* bacteriophages

To date, relatively little is known about the biology of the large family of staphylococcal siphoviridae bacteriophages. Some members of this family, such as phage strains 80 and 80α that specifically infect the Gram-positive bacterium *Staphylococcus aureus*, contain replication modules with genes that appear to encode for a putative helicase loader (Christie et al., 2010). Both 80 and 80α's putative helicase loaders are homologs of *E. coli* DnaC. Although these proteins are highly conserved among these particular phages, they contain variable N-terminal domains, a feature typical of bacterial helicase loaders. Just downstream of their putative helicase loader genes, the 80 and 80α phages each contain single, short open reading frames termed ORF22 in ϕ80α and ORF19 in ϕ80. ϕ80α ORF22 and ϕ80 ORF19 turn out to be homologous to the ORF104 protein of phage 77, another virus that also infects Gram-positive bacteria. Interestingly, ORF104 has been shown to inhibit DNA synthesis in *S. aureus* by binding directly to the host helicase loader *S. aureus* DnaI (Dehbi et al., 2009; Liu et al., 2004).

ORF104-type genes are present in many phages belonging to the staphylococcal siphoviridae family (although they are absent in phage ϕ11). Moreover, the DnaI-inhibitor gene from ϕ80α (ORF22) has recently been shown to be required for the derepression of *S. aureus* pathogenicity islands (SaPIs) by ϕ80α (and has been given the name *sri*) (Tormo-Más et al., 2010; Úbeda et al., 2008). SaPIs are mobile elements that are induced by helper bacteriophages. Upon induction, these mobile elements excise themselves from the host chromosome, replicate, and become encapsidated into phage-like particles, leading to high-frequency transfer. The process of SaPI mobilization is helper phage specific, in that only certain SaPIs can be mobilized by a particular cognate helper phage. The absence of a 77ORF104-type DnaI-inhibitory protein from the ϕ11 genome may account for the inability of ϕ11 to induce the SaPI1 pathogenicity island of *S. aureus*. The protein ORF19 encoded by phage ϕ80 shares 53% identity with that of ORF22 of ϕ80α; ϕ80 is similarly unable to induce SaPI1 as per ϕ11, likely the result of the differences between the two ORF104-type genes that may alter their ability to bind to host DnaI proteins. Chapter 3 discusses work aimed at structurally and biochemically characterizing the molecular mechanism by which the inhibitory ORF104-type proteins block the activity of the *S. aureus* DnaI helicase loader.

Concluding Remarks

All replicating systems must perform two fundamental tasks: (*a*) selecting the right time and place for initiating replication and (*b*) orchestrating DNA opening and replisome assembly. Cellular organisms have developed multiple strategies to contend with these challenges, often employing sets of proteins that appear to have evolved independently. Even though these factors can differ greatly in their specific molecular mechanisms, cells appear to have universally adopted a common initiation strategy whereby evolutionarily related AAA+-family ATPases serve to mark replication origins and to promote recruitment of ring-shaped hexameric helicases. Hence, while common themes exist in how initiation is executed and controlled, the specific pathways and players that promote this process can vary dramatically.

Tables

Table 1.1 Replication Initiation factors

Replication Factor	***Gram (-) bacteria***	***Gram (+) bacteria***	***Bacteriophage***
Model organism	***E. coli***	***S. aureus***	**λ *phage***
Initiator	DnaA	DnaA	λO
Replicative helicase	DnaB	DnaC	host *EcDnaB*
Helicase loader	DnaC	DnaI	λP
Co-loader factor	----------	DnaB, DnaD	----------

Table 1.2 High-affinity DnaA-boxes from various bacterial species

Organism	**High-affinity DnaA Box sequence**
Escherichia coli	TTATCCACA
Pseudomonas putida	TTATCCACA
Bacillus subtilis	TTATCCACA
Vibrio cholera	TTATCCACA
Caulobacter crescentus	TGATCCACA
Helicobacter pylori	TCATTCACA
Mycobacterium tuberculosis	TTGTCCACA
Thermotoga maritima	AAACCTACCACC
Streptomyces coelicolor	TTGTCCACA

Figures

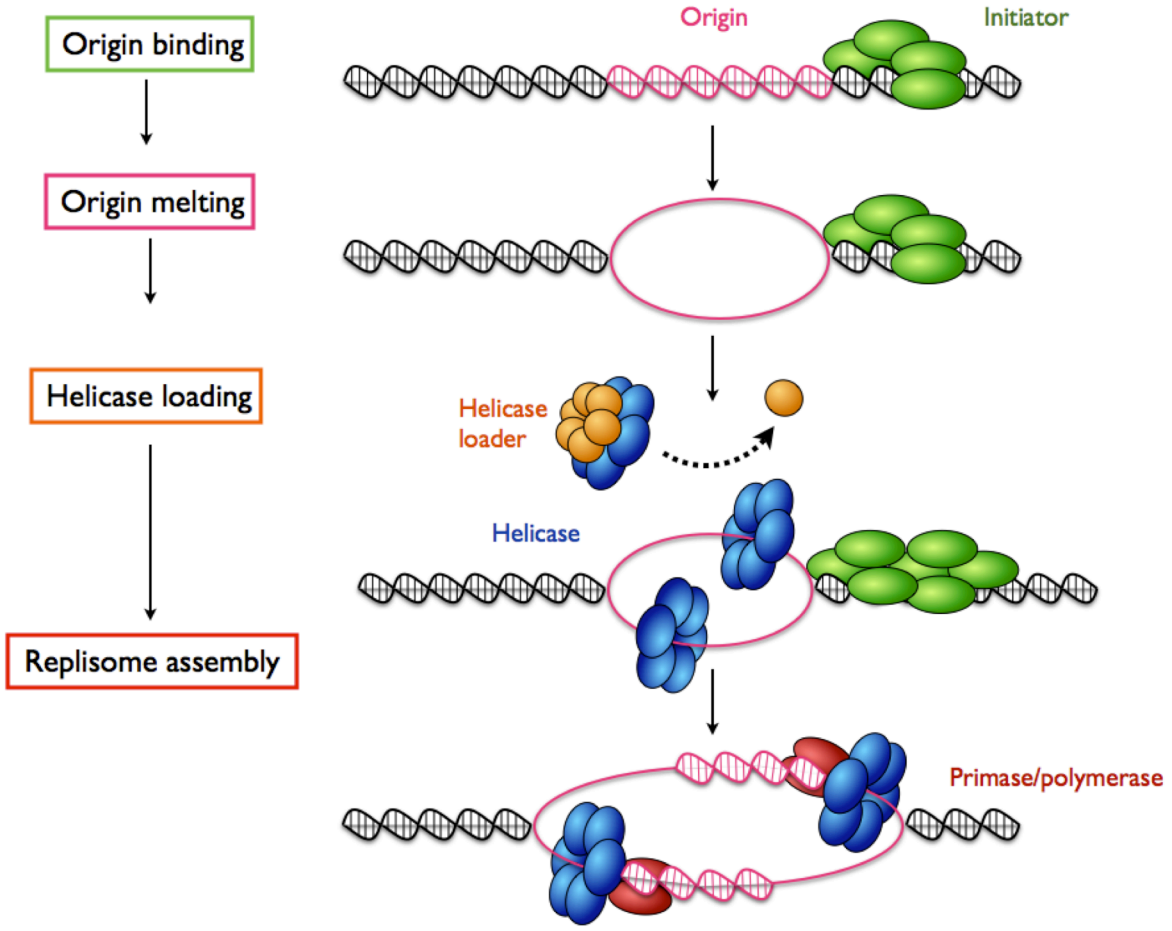

Figure 1.1. Stages of DNA replication initiation. Steps of replication initiation: (1) recognition or selection of a double-stranded DNA (dsDNA) initiation site, (2) duplex unwinding or "melting" of the replication origin (in eukaryotes and archaea helicases are loaded onto dsDNA prior to origin melting – mechanism remains unclear), (3) loading of two copies of the replicative helicase onto the origin, and (4) recruitment of primase, polymerases and other replication factors leading to assembly of a bi-directional replication fork.

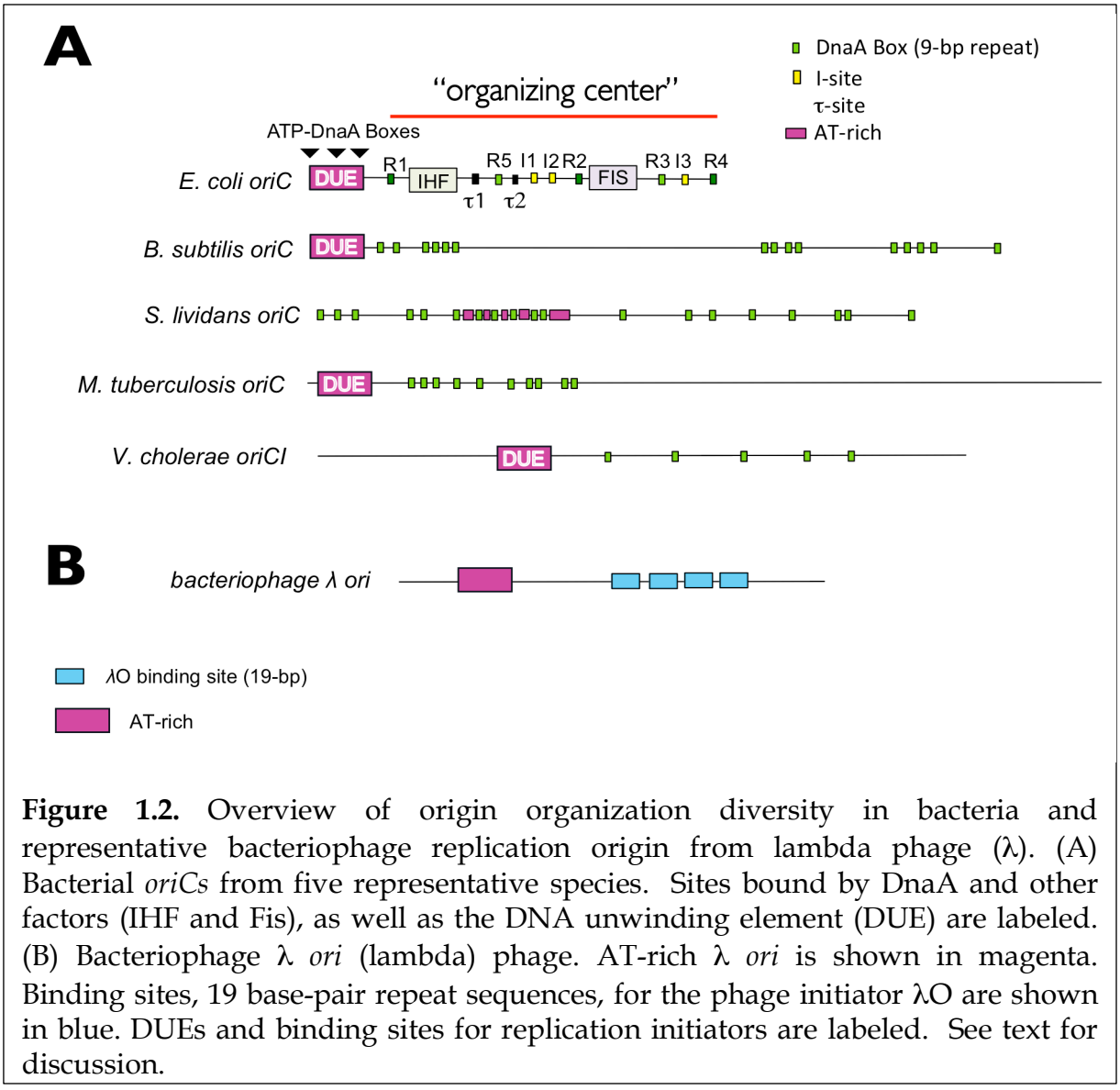

Figure 1.2. Overview of origin organization diversity in bacteria and representative bacteriophage replication origin from lambda phage (λ). (A) Bacterial *oriCs* from five representative species. Sites bound by DnaA and other factors (IHF and Fis), as well as the DNA unwinding element (DUE) are labeled. (B) Bacteriophage λ *ori* (lambda) phage. AT-rich λ *ori* is shown in magenta. Binding sites, 19 base-pair repeat sequences, for the phage initiator λO are shown in blue. DUEs and binding sites for replication initiators are labeled. See text for discussion.

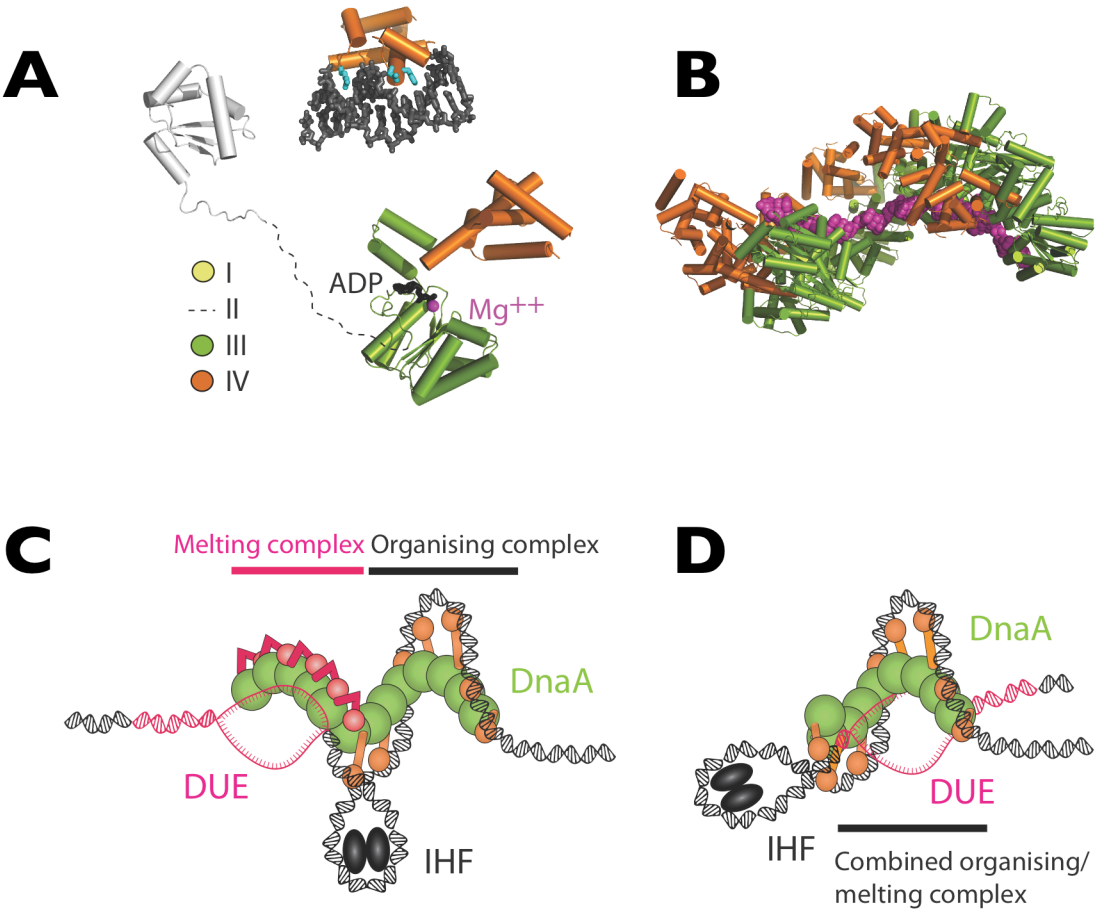

Figure 1.3. Structure and mechanism of bacterial initiator DnaA. (A) Domain architecture of DnaA. PDB models for domain I and an ADP-state of domains III/IV of DnaA are shown (Abe et al., 2007; Erzberger et al., 2006; Lowery et al., 2007). Inset – structure of domain IV bound to duplex DNA (Fujikawa et al., 2003). (B) Structure of AMPPCP-assembled DnaA helix (domains III and IV) bound to an extended single-stranded DNA substrate (magenta) (Duderstadt et al., 2011). (C) Two-state model for IHF-assisted DnaA melting of *oriC* (Erzberger et al., 2006). This mechanism accounts for the existence of two different DnaA oligomers (Bramhill and Kornberg, 1988; Duderstadt et al., 2010), one of which wraps the organizing center of *oriC* and another that melts the DUE. (D) Loopback model for IHF-assisted melting, in which a single DnaA complex bound at the organizing center of *oriC* opens the DUE (Ozaki and Katayama, 2012).

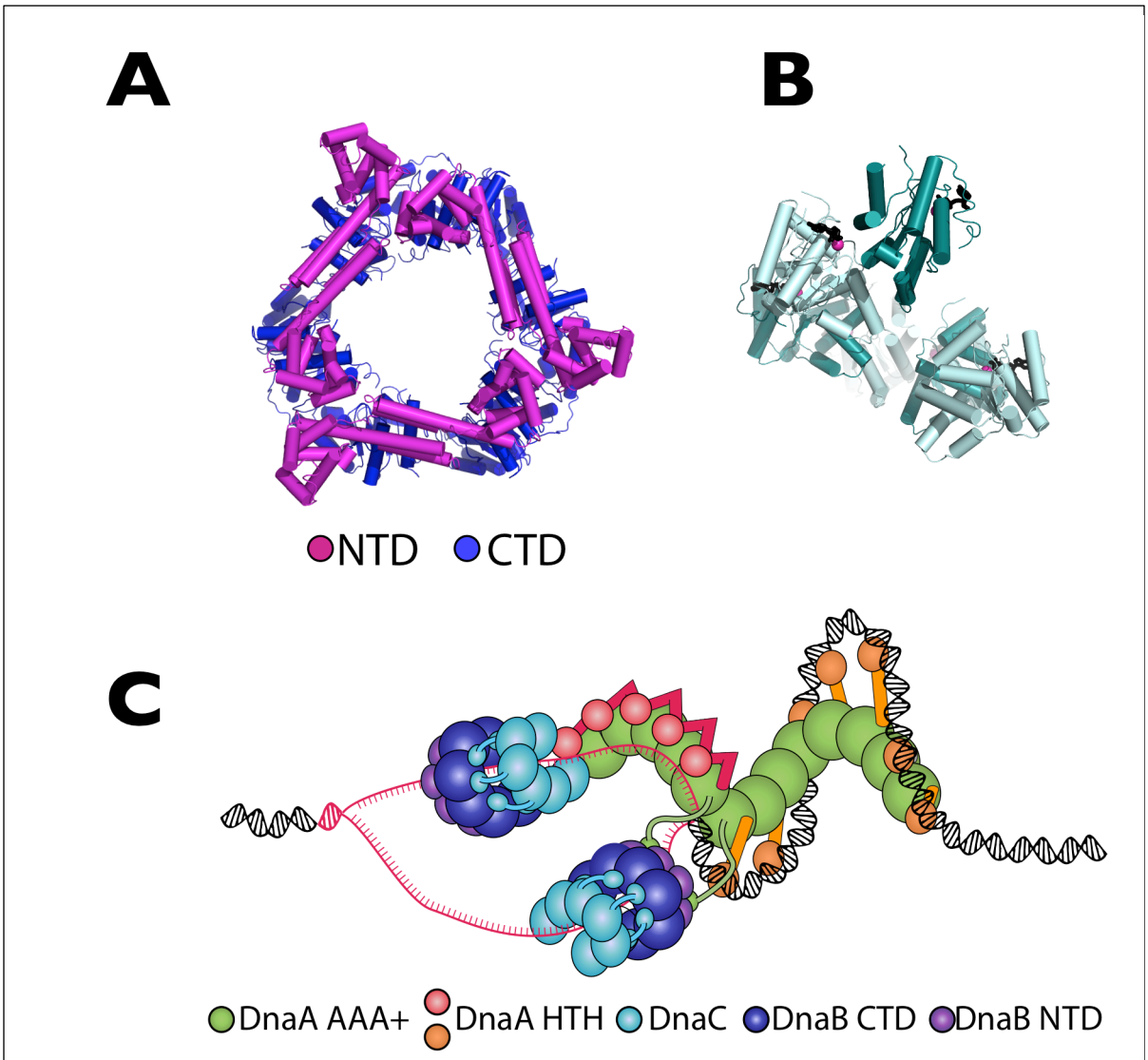

Figure 1.4. Replicative helicase, DnaB, and helicase loader, DnaC, structures and helicase loading mechanism. (A) Closed-ring DnaB hexamer from *B. stearothermophilus* (Bailey et al., 2007b). (B) Structure of spiral DnaC oligomer (containing six AAA+ domains) bound to nucleotide. Individual DnaC AAA+ monomers are alternately colored dark and light cyan for perspective (Mott et al., 2008). (C) Model for loading of DnaB onto *oriC* following the two-state mechanism.

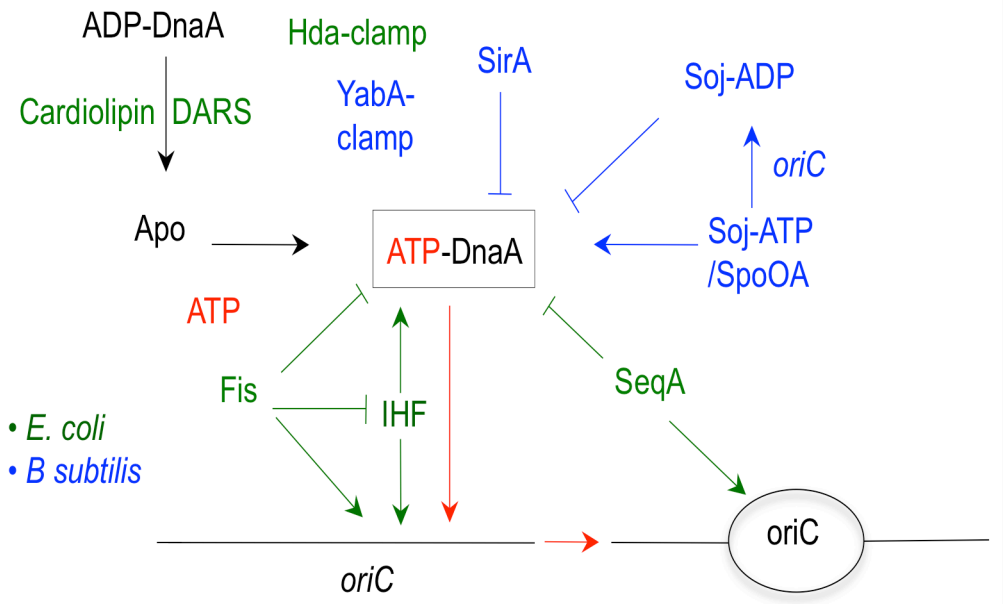

Figure 1.5. Overview of initiation factor regulation in bacteria**.** Regulation of DnaA in bacteria, comparing and contrasting *E. coli* and *B. subtilis* systems.

Chapter 2: Biochemical studies of DnaA and DnaC in helicase loading & activation

(portions reproduced from Arias-Palomo E.*, O'Shea V.L.*, Hood, I.V., and Berger, J.M. (2013). The bacterial DnaC helicase loader is a DnaB ring breaker. Cell. 153(2):438-48.)

* These authors contributed equally to this work.

Abstract

In all cellular organisms, the appropriate loading of hexameric replicative helicases onto initiation start sites, called replication origins, marks a critical committing event towards duplication of a cell's genomic DNA. Precisely how replicative helicases are physically deposited onto chromosomes, which lack free single-stranded DNA ends that would otherwise allow threading of the helicase onto DNA, has been a long-standing question in the field. Throughout the three domains of life, as well as in certain viruses, specialized AAA+ ATPases serve essential roles in solving the topological problem of chaperoning ring-shaped helicases onto DNA by a variety of mechanisms. In bacteria, such as the Gram-negative model system *E. coli*, the initiation of DNA replication is accomplished by two proteins: an initiator protein, DnaA, and a helicase loading factor, DnaC. Working together, DnaA and DnaC load the DnaB replicative helicase onto newly melted origin DNA strands in an ATP-dependent manner; how DnaA and DnaC collaborate to ensure that two copies of DnaB are properly deposited onto complementary strands in opposing orientations, and how ATP binding and hydrolysis by DnaC help control loader activity, are unknown. To better understand these issues, I developed several fluorescence-based helicase assays to study the individual roles of DnaA and DnaC in helicase loading onto a simple DNA fork and a synthetic, pre-melted origin-like substrate. The work presented in this chapter reveals that: 1) the N-terminal, helicase-binding domain of DnaA performs an important role in recruiting and loading DnaB to both strands of a DNA fork, 2) DnaC not only helps promote helicase loading, but also stimulates the motor's DNA unwinding activity, and 3) ATP binding and hydrolysis by DnaC, while dispensable for loader function *per se*, help to increase the efficiency of helicase activation.

Introduction

The proliferation of all cellular organisms relies on the precise and faithful transmission of genetic information. The copying of DNA is performed by a multi-component macromolecular machine called the replisome, which couples duplex DNA unwinding of parental DNA with the synthesis of new daughter strands (Baker and Bell, 1998; MacNeill, 2011; Pomerantz and O'Donnell, 2007; Schaeffer et al., 2005). During replication, ring-shaped hexameric helicases utilize the energy of ATP hydrolysis to unwind duplex DNA and drive progression of replication forks (McGlynn, 2011). To maintain genetic integrity, replicative helicases must be properly recruited and transferred to replication origins at the correct time and location such that chromosomal DNA is duplicated only once per cell cycle (Katayama et al., 2010; Nielsen and Lobner-Olesen, 2008; Soultanas, 2012).

How replicative helicases are loaded onto cellular chromosomes, which lack free DNA ends, has been a long-standing question. There appear to be two dominant strategies employed by cells to promote helicase loading onto DNA, both of which rely on dedicated ATP-dependent loading factors (Davey and O'Donnell, 2003; O'Shea and Berger, 2014). One approach is to physically open and deposit a preformed hexameric ring onto target substrates. The other is to assemble a hexamer around DNA from monomeric subunits. Examples of both strategies have been found in many different species (Soultanas, 2012); for instance, in eukaryotes pre-formed MCM-family hexameric helicases are loaded by the eukaryotic initiator complex Origin Recognition Complex (ORC) (Bowers et al., 2004; Evrin et al., 2009; Remus et al., 2009), while the E1 replicative helicase of papillomaviruses assembles onto origins directly (Enemark et al., 2002; Sanders and Stenlund, 1998; Schuck and Stenlund, 2005; Sedman and Stenlund, 1998).

For bacterial systems, such as *E. coli*, the establishment of a bidirectional fork begins with assembly of the initiator protein DnaA onto a series of duplex DnaA binding sites, called DnaA boxes, within *oriC*. In its ATP-bound form, DnaA self-associates on these sites into a large nucleoprotein complex that stimulates local unwinding of an AT-rich region within the origin termed the DNA Unwinding Element (DUE) (Bramhill and Kornberg, 1988a; Kowalski and Eddy, 1989; Leonard and Grimwade, 2005; Speck et al., 1999). Following origin unwinding, DnaA assists the bacterial helicase loader DnaC in properly positioning one copy of the replicative helicase DnaB onto each strand of the melted origin, an event involving a direct interaction between the N-terminal domains of DnaA and DnaB (Kobori and Kornberg, 1982b; Marszalek and Kaguni, 1994; Marszalek et al., 1996; Seitz et al., 2000; Wickner and Hurwitz, 1975), and a direct interaction between the DnaC N-terminal domain and DnaB

C-terminal RecA ATPase domain (Ludlam et al., 2001) (see domain organization in **Figure 2.1**). Structural and biochemical studies have shown that DnaA forms a nucleoprotein complex, which forms on one side of the unwound DNA Unwinding Element (DUE) (Erzberger et al., 2006; Funnell et al., 1987). This observation raises a paradox as to how an asymmetric organization of the initiator can lead to the proper deposition of two helicases in a symmetric manner onto a melted origin.

Both *E. coli* DnaC and DnaA – like many helicase loading factors and initiators – belong to the AAA+ (ATPases Associated with various cellular Activities) superfamily of nucleotide hydrolases (Koonin, 1992; Mott et al., 2008). DnaC and DnaA are paralogs of one another and self-associate via their AAA+ ATPase domains to form open helical filament assemblies (Duderstadt et al., 2011; Erzberger et al., 2006; Mott et al., 2008), rather than the closed-ring assemblies adopted by a majority of AAA+ ATPases (Duderstadt and Berger, 2008; Erzberger and Berger, 2006; Neuwald et al., 1999; Ogura and Wilkinson, 2001). For the *E. coli* DnaB/DnaC complex, numerous studies have indicated the loader and helicase interact with a 6:6 stoichiometry (Galletto et al., 2003; Kobori and Kornberg, 1982c). Interestingly, the right-handed helical assembly as observed in the crystal structure of an isolated DnaC AAA+ domain, which recapitulates formation of a bipartite ATPase active site (Mott et al., 2008), has also been observed by negative-stain EM in the context of the *E. coli* DnaB-DnaC complex (Arias-Palomo et al., 2013). These results, combined with *in vivo* genetic studies (Mott et al., 2008), strongly indicate that the spiral configuration of the AAA+ domains DnaC seen crystallographically represents a physiological state of the loader. This assembly, combined with the observation that DnaA can associate with DnaC, has led to a model suggesting that DnaC may dock onto the opened ended face of the DnaA helical filament at a melted origin to participate in positioning one DnaB helicase on one strand of a melted DUE, while direct interactions with DnaA help position a second DnaB onto the complementary strand in an opposing orientation (Mott et al., 2008). Many aspects of this model have not been explicitly tested, however. To begin to address how DnaA and DnaC collaborate in helicase deposition, we developed several fluorescence-based helicase assays to study specific functions of the two proteins. Together, our data show: 1) that DnaA's N-terminal domain serves an important role in recruiting DnaB to ssDNA at a melted origin, 2) that both DnaC and its isolated N-terminal helicase binding domain appear to overcome an auto-repressed "inactive" state of the replicative helicase by switching DnaB into an active configuration, and 3) that the ATP binding and hydrolysis activities of DnaC are important for enhancing the efficiency of helicase activation.

Results

The DnaA N-terminal helicase binding domain aids in recruiting DnaB to a melted origin

Although it is known that different faces of DnaB associate with DnaA and DnaC, with the N-terminal domain (NTD) of DnaA binding to the NTD of the helicase and the NTD of DnaC binding to the C-terminal face (**Fig. 2.1**), relatively little is known as to the precise mechanism by which the DnaA facilitates appropriate deposition of DnaB in the proper orientation onto ssDNA at a melted origin. Previous *in vitro* studies have suggested that DnaA may be specifically involved in loading the helicase to only one strand of the melted origin (the so-called "lower strand" of the DUE, **Fig. 2.2A**) (Masai and Arai, 1995; Mott et al., 2008; Weigel and Seitz, 2002). Several lines of evidence have supported this strand-specific DnaA-mediated loading model. For example, electron microscopy and biochemical work have shown that the DnaA nucleoprotein complex is located off to one side of the DUE (Fuller et al., 1984), indicating the action of the initiator is asymmetric in loading two copies of DnaB. In addition, the ATPase domains of DnaA and DnaC are highly homologous and interact (Mott et al., 2008), suggesting that one DnaB is loaded by a direct DnaA-DnaB association, while the other is loaded through a DnaA-DnaC contact (Duderstadt et al., 2011; Erzberger et al., 2006; Mott et al., 2008) (**Fig. 2.2A**).

To test whether DnaA has a strand-specific preference for directing loading of DnaB to either strand of a melted origin, we developed a DnaA-dependent, helicase loading and unwinding assay, employing a substrate that mimics a melted replication origin and that reports on both helicase loading events to either the "upper" or "lower" strand of a melted origin. This substrate will be hereafter referred to as the *oriC* fork (shown in **Figure 2.2B**). Our *oriC* fork design was inspired and modified based on previous work, which used a similar synthetic substrate to examine DnaA-dependent loading (Weigel and Seitz, 2002). The substrate was designed to mimic an open replication bubble based on the known 28bp 'footprint" of DnaB (Fang et al., 1999); random non-complementary ssDNA strands were used to provide the appropriate regions for helicase loading. A duplex region offset on one side the *oriC* fork contains a single high-affinity DnaA binding site, called the R1 DnaA-box, which is normally found directly adjacent to the DUE element in *oriC*.

Based on the model of both Weigel and Seitz, and Mott et al., along with the predicted binding polarity of DnaA filaments along duplex *oriC* regions (Duderstadt et al., 2011; Erzberger et al., 2006), we expected that upon the binding of DnaA to the DnaA-box R1 site, the initiator would help facilitate recruitment and loading of the helicase primarily to the "lower strand" of the synthetic origin (**Figure 2.2B**). Nonetheless, our substrate was designed such that

loading events in both orientations could be monitored, either by release of a Cy3-labelled "upper" strand or a Cy5-labelled "lower" strand as helicase activity ensued. To prevent the helicase from non-specifically threading onto a free DNA end, an oligo was annealed to the "upper strand" as a block. To verify successful annealing of the *oriC* fork substrate we ran our hybridized forks on 4-20% native TBE gels. For visualization purposes, strands not containing quencher labels were used to ensure visualization of all DNA strand species. The same annealing conditions were used to prepare the *oriC* fork substrate intended for time-resolved measurements by a plate reader-based helicase assay to simultaneously monitor loading and unwinding events to both the "upper" and "lower" strand. DnaA binding to the fork was verified by a band-shift assay (**Figure 2.3)**.

To carry out the loading/unwinding reactions, 100 nM of prepared forks were first mixed with 200 nM of *E. coli (*$DnaB)_6$ hexamer on ice. After 5 min, 1.2 μM of DnaC were added and the reactions incubated at 37˚C for 3o min, after which the reactions were quenched. Parallel assays were measure both by TBE gels and by plate-reader to ensure consistency between the two assays. In the fork assay, helicase loading to the "upper strand" is measured by an increase in Cy3 fluorescence, as helicase loading and duplex unwinding should release the Cy3-labeled strand from the quencher–labeled strand resulting in an increase in Cy3 fluorescence (**Figure 2.4-2.6**). By contrast, loading of the helicase to the "lower strand" and subsequence unwinding of the duplex region would release the Cy5-labeled strand from its complementary quencher-labeled strand (**Figure 2.4-2.6**). To our surprise, and in contrast to previous studies using radiolabeled substrates (Weigel and Seitz, 2002), we were able to observe DnaA-mediated effects on helicase loading and unwinding of both strands of our *oriC* fork (**Fig. 2.4-2.6)**. This result indicated that DnaA does not preferentially load the helicase to a single strand but rather facilitates loading to both strands of our synthetic melted origin.

Because the observed DnaA-dependencies on loading/unwinding were unexpected, we elected to further test the need for the initiation using mutant initiator proteins. Single point alanine mutations in the N-terminal DnaB-binding domain of DnaA of either the Asp21 or Phe46 have been reported to disrupt association with the helicase (Abe et al., 2007; Keyamura et al., 2009). We therefore cloned, expressed and purified these mutants using established DnaA purification protocols (Duderstadt et al., 2010; Li and Crooke, 1999). Interestingly, the mutants displayed different results in our oriC fork assay for "upper" and "lower" strand helicase loading and unwinding (**Figure 2.7**). The F46D mutant was deficient for loading to both "top" and "lower" strands. By contrast, the E21A mutant appears wild-type for loading to the "top" strand and displayed a modest reduction in loading to the "lower strand". Overall, our results show that DnaA serves an important is recruiting the helicase to both strands of a melted origin, rather than just preferentially loading to the "lower"

strand, and that the DnaA N-terminal helicase binding domain serves a critical but differential role in recruiting the helicase to both strands.

During the course of conducting our assays, we noticed that the DnaBC complex alone was sufficient to elicit a low level of DNA unwinding (**Figure 2.7**). To reduce this amount of non-specific helicase loading, we incubated the with excess dT_{20} ssDNA as a competitor. Under these conditions, helicase loading became strikingly dependent on the presence of DnaA (**Figure 2.8**). Again, however, the F46D mutant was completely inactive for helicase loading to the upper and lower strands, further demonstrating the vital role DnaA serves in recruiting the helicase to a melting origin.

To complete our tests, we next turned to a truncation of DnaA that lacked the N-terminal helicase-binding domain, *Ec*DnaC$^{\Delta NTD}$, of the initiator. This construct contains a hexa-histidine tag and lacks the first 130 residues (**Figure 2.1**). When tested the *Ec*DnaC$^{\Delta NTD}$ for its effect in our *oriC* fork assay. The NTD truncation was unable to sufficiently recruit the helicase to either the "upper" or "lower" strands of our synthetic origin (**Figure 2.9**). Taken together with the point mutant data, these findings demonstrate that DnaA serves an important role in recruiting the helicase to DNA through a direct interaction with its N-terminal domain, and suggest that initiator may help promote loading on both strands of a melted origin, as opposed to only one as previously suggested.

DnaC activates DnaB in an ATP-independent manner

Although *E. coli* DnaB can thread onto a free 5'-ssDNA end and unwind a downstream duplex fork (Jezewska et al., 1998), a curious biochemical feature of the helicase is relative inefficiency by which DnaB unwinds DNA duplexes (**Figure 2.11**). Instead, others have reported that robust activity requires either DnaC or a large excess of the helicase over DNA (Galletto et al., 2004a; Kaplan, 2000; Kaplan and Steitz, 1999). These findings, together with structural data demonstrating that an N-terminal region of DnaB can adopt multiple conformational states (Arias-Palomo et al., 2013; Bailey et al., 2007; Itsathitphaisarn et al., 2012; Lo et al., 2009; San Martin et al., 1998, 1995; Strycharska et al., 2013; Tsodikov and Biswas, 2011; Wang et al., 2008), suggested to us that DnaB might not only rely on DnaC for loading, but also for proper activity.

To test this idea further, we developed a fluorescent-based DnaC-dependent helicase assay using a synthetic fork substrate (**Figure 2.10**). To validate the fork as a reagent, we compared the signal of the annealed quenched fork with that of a melted fork, in which the Cy3 label is free from the quencher. Single time points for reactions were analyzed by a gel-based assay, using 4-20%

gradient TBE gels (**Figure 2.11B**), whereas time-resolved measurements were obtained on a plate reader (**Fig 2.11A**). At a 2:1 ratio of *Ec*DnaB hexamers to fork substrate, we were unable to observe substantial helicase unwinding activity when quantified by either gel- or plate reader-based experiments, indicating that both of our assays corroborate one another (**Figure 2.11**). By contrast, we observed that significant helicase unwinding activity occurred only when a stoichiometric (1:1) amount *Ec*DnaC was added (**Figure 2.11A**). For both our gel-based and plate reader assays, robust DnaC-dependent helicase activity necessitated the addition of a complementary "capture strand", designed to anneal only to the duplex region of the fork after the helicase successfully unwound the duplex region (**Figure 2.11**). These data indicate that, on its own, DnaB forms inactive hexamers, and that DnaC helps to switch DnaB into an active double-stranded unwinding state (**Figures 2.12**).

With our helicase assay in hand, we next set out to define the individual contributions that each domain of the loader serves in promoting helicase activity. Previous studies had established that an *Ec*DnaC ATP-binding mutant (K112R) retains the ability to load DnaB helicase onto DNA (M13ssDNA) (Davey & O'Donnell), suggesting that the C-terminal AAA+ domains of DnaC may be dispensable for the ability of DnaC to activate DnaB DNA unwinding activity. To test this idea, we analyzed the effect of the isolated DnaC's N-terminal helicase-binding domain in our fluorescence-based DnaC-dependent helicase assay. The DnaC NTD was found to be nearly as efficient as full-length DnaC in promoting dsDNA unwinding by the helicase, indicating that it exerts a similar effect on the helicase as the intact loader, despite lacking its ATPase domain (**Figure 2.12**). To test whether the DnaC NTD could also load the helicase onto a closed circular ssDNA substrate, Dr. Valerie O'Shea, a post-doc in the Berger lab, also tested the DnaC NTD in an established M13 helicase loading assay as well (Davey et al., 2002). DnaC NTD was observed to load the helicase, albeit at a significantly reduced level compared to wild-type, demonstrating that NTD is sufficient for helicase loading (data not shown) (Davey et al., 2002).

ATP binding and hydrolysis by DnaC increases efficiency of helicase activation

Although ATP has been shown to be required for DnaC function during *oriC*-dependent initiation, it has remained unclear what role the ATPase domains of DnaC serve during this process (Fang et al., 1999). Indeed, it has been debated as to whether or not DnaC is a functional ATPase and if so, how nucleotide turnover might be utilized by the loader. Although our observations that the ATPase domain is not required for DnaC to promote either helicase loading or unwinding on forked DNA substrates, DnaC does possess the complete set of

amino acid motifs known to promote ATPase activity in AAA+ ATPases (Koonin, 1992; Mott et al., 2008). We therefore elected to explore whether mutants in these element might alter the action of the loader in promoting DnaB function. In making our prospective ATPase mutants, we made changes to four well-known signature regions of the AAA+ superfamily, including the Walker-A (K112R), Walker-B (D169A), Arginine Finger (R220A/D) and Sensor-II (R236A/D) motifs. In addition, we also altered a second, conserved arginine with in the Box VII (R216A/D). To determine that the ATPase mutants were indeed inactive for ATP hydrolysis, a post-doctoral fellow in the Berger lab Dr. Valerie O'Shea first tested these mutants using a radioactive ATPase assay (data not shown). As expected, with the exception of the second Box-VII arginine mutants R216A/D, the ATPase mutants displayed barely detectable ATP hydrolysis activity. However, in the presence of high concentrations of ATP, at 3.2 mM ATP or higher, the Walker-B mutant (D169A) displayed activity. Interestingly, the R216A mutant had more activity than wild-type indicating that R216 may be involve in regulating DnaC ATPase activity. We then tested the mutants for activity in our fork based helicase-activation assay (**Figure 2.13**). Inspection of the effects of the ATPase mutants shows that all DnaC ATP hydrolysis mutants (Walker-B, Arg-finger, Sensor-II) were completely unable to stimulate DNA unwinding by DnaB. By contrast, a mutant which blocks only ATP binding (Walker-A, K112R), as well as the mutant bearing a change in the second conserved Box-VII arginine (R216A), were nearly as active as the DnaC N-terminal domain alone (**Figure 2.13**). These findings indicate that although ATP binding *per se* is not important for DnaC-dependent activation of DnaB, an inability of the loader hydrolyze any ATP that might be bound is critical for such a function.

Discussion

How DnaA and DnaC collaborate to ensure that two copies of DnaB are properly deposited onto complementary strands in opposing orientations has remained poorly defined. Moreover, to what extent ATP binding and hydrolysis by the bacterial helicase loader may play in modulating DnaC's activities on DnaB has remained unknown. To address these issues, we developed several fluorescence-based assays designed to study the individual roles of DnaA and DnaC in promoting helicase loading and DNA unwinding. Using a model, melted origin to assess DnaA-dependent loading, we found that both a single mutation of Phe46 to an aspartic acid (F46D) in DnaA's N-terminal domain and a truncation of the DnaA NTD results in the inability of the initiator to recruit the helicase to either strand in our origin-mimicking helicase assay. These findings were unexpected as previous work suggested that loading to each strand of the melted origin might require different protein-protein interactions given the asymmetric nature of the DnaA-oriC initiation complex; indeed, an association between DnaA and DnaC had been predicted to load the helicase to upper or "top" strand of the melted origin while DnaB was proposed to DnaA directly for loading onto the bottom strand. At a minimum, our data suggest that DnaA may be required for DnaB loading regardless of which strand the helicase is loaded onto. Future studies looking at DnaB loading in the context of a full *oriC* substrate, rather than a synthetic fork bearing only a single DnaA box, will be needed to test this model further. Likewise, it will be important to establish whether direct DnaA/DnaC contacts occur during DnaB loading onto a *bone fide* origin. The mutants described here will be useful for such efforts.

Why DnaC is an AAA+ ATPase homolog, and the role its ATPase domain might play during helicase loading has similarly been unclear. To investigate this issue further in the context of promoting helicase activity by DnaB, we developed a DnaC-dependent helicase assay using a forked substrate containing a free 5'-ssDNA end. Interestingly, we not only found that DnaC stimulates DnaB activity on such a substrate, but that the ATPase domain of loader was dispensable for this function (**Figure 2.12 and 2.14**). However, we also found that mutations expected to play a role in ATP hydrolysis by DnaC also are important for activation, and that trapping the loader in an ATP bound state blocked helicase function. This finding corroborates prior studies suggesting that DnaB needs DnaC to dissociate before it can unwind DNA (Davey et al., 2002; Makowska-Grzyska and Kaguni, 2010); in this regard, hydrolysis likely traps DnaC as an oligomer on DnaB, preventing subsequent activity by the helicase (**Figure 2.15**). Moreover, our data suggest that bacterial replicative helicases, like those of eukaryotes, may bear auto-regulatory domains responsible for controlling DNA unwinding activity. Together these findings highlight how bacterial helicase loading may be tightly regulated to ensure helicase activation at the correct time

and location during loading of the helicase onto the melted origin, preventing futile cycling of the loader. Future studies looking at the stability of DnaC•DnaB complexes as a function of ATP binding and/or hydrolysis will be necessary to test this model further.

Materials and Methods

Protein Expression and Purification

E. coli DnaC and DnaB proteins were independently expressed in strain C41 (Lucigen) from pET28b-derived plasmids by induction with 0.5 mM IPTG at 37 °C for 2.5 or 3 hours, respectively. Following induction, cells were harvested by centrifugation, resuspended in respective lysis buffers (for DnaB: 20 mM HEPES-KOH pH 7.5, 500 mM NaCl, 10 % glycerol, 10 mM $MgCl_2$, 0.1 mM ATP, 1 mM b-mercaptoethanol, 1 mM PMSF, 1 mg/mL Pepstatin A, and 1 mg/mL Leupeptin; for DnaC: 50 mM HEPES-KOH pH 7.5, 1 M KCl, 10 % glycerol, 30 mM imidazole, 10 % $MgCl_2$, 0.1 mM ATP, 1 mM b-mercaptoethanol, 1 mM PMSF, 1 mg/mL Pepstatin A, and 1 mg/mL Leupeptin), flash frozen in liquid nitrogen, and lysed by sonication. *E. coli* DnaB migrated as a hexamer by sizing exclusion chromatography (s300), whereas E. coli DnaC migrated as a monomer (s200 column).

Full-length DnaC and the DnaC N-terminal domain (amino acids 1 – 75) were constructed as TEV-protease-cleavable 6xHis-MBP fusions to allow removal of both tags; removal was carried out by incubation with TEV protease (1 mg TEV protease per 20 mg protein) at 4°C for 16 - 20 hrs. Purification for these constructs was performed by Ni Sepharose (GE Healthcare) and amylose (New England Biolabs) affinity resins, followed by gel filtration on a HiPrep 16/60 Sephacryl S-200 column (GE Healthcare) in buffer containing 50 mM HEPES pH 7.5, 500 mM KCl, 10 % glycerol, 10 mM $MgCl_2$, 0.1 mM ATP, 1 mM b-mercaptoethanol, 1 mM PMSF, 1 mg/mL Pepstatin A, and 1 mg/mL Leupeptin. For DnaC-NTD, $MgCl_2$ and ATP were omitted from the buffers. DnaB was purified by ammonium sulfate precipitation (30 % cut) and anion exchange chromatography on a HiTrap Q HP column (GE Healthcare), followed by gel filtration on a HiPrep 16/60 Sephacryl S-300 column (GE Healthcare) in buffer containing 20 mM Tris-HCl pH 8.5, 800 mM NaCl, 10 % glycerol, 5 mM $MgCl_2$, 1 mM b-mercaptoethanol, 0.1 mM ATP, 1 mM PMSF, 1 mg/mL Pepstatin A, and 1 mg/mL Leupeptin. Protein purity of > 95% was determined by SDS-PAGE with Sypro Orange protein stain (Invitrogen). Concentration of combined pure fractions was determined using the Bradford method with Coomassie Plus Protein Assay Reagent (Thermo Scientific) and a BSA standard curve. Purified proteins were aliquotted, flash frozen in liquid nitrogen and stored at –80˚C.

E. coli DnaA (*Ec*DnaA) was previously cloned into a pET28b vector lacking the MBP tag, by Dr. Karl E. Duderstadt, generating a hexa-histidine (His6-*Ec*DnaA) fusion construct containing a linker sequence encoding the TEV-protease cleavage site. QuickChange mutagenesis (Stratagene) was used to generate mutations were into this His6-EcDnaA. All primers for QuickChange

were designed using the web-based program PrimerX (Automated design of mutagenic primers for site-directed mutagenesis. Available: www.bioinformatics.org/primerx). All His6-EcDnaA proteins were expressed in *E. coli* C41 cells (Miroux and Walker, 1996). Cells were grown at 37°C in LB media containing 0.05% glucose. Once the cultures reached an A600 cell density of 0.6, cultures were induced with 1 mM IPTG (Isopropyl β-D-1-thiogalactopyranoside) and allowed to express 1.5 hours. All His6-*Ec*DnaA proteins were purified as previously described (Li and Crooke, 1999), except for the following modifications. Protease inhibitors (1 μM pepstatin-A, 1 μM leupeptin, 1 mM PMSF) were included in all buffers throughout purification, which was performed using a 1 ml HiTrap Chelating HP column (GE Healthcare) charged with 0.2 M NiSO4. Aggregated protein was separated from soluble species by size exclusion chromatography using an S-200 column. *Ec*DnaA monomeric fractions were pooled, concentrated and flash frozen in liquid nitrogen for storage in a final buffer of 50 mM PIPES-KOH pH 6.8, 10 mM magnesium acetate, 200 mM ammonium sulfate, 20% (v/v) sucrose, 0.1 mM EDTA and 2 mM DTT.

Annealing helicase assay substrates

All oligonucleotides used in this study (**Table 2.2**) were synthesized by IDT. Helicase fork substrates were annealed at a final concentration of 20 μM fluorescently labeled stranded with a 1.2-Fold molar excess of quencher labeled stranded. 10.5 μl of 10× fork annealing buffer containing 200 mM Tris-acetate, 100 mM Mg^{2+}-acetate, 500 mM K^{+}-acetate, pH 7.9, in a total volume of 35 μl was heated to 95°C in a heating block for 5 minutes. After the 5 minute incubation the heating block was transferred to a Styrofoam contained and allowed to cool down overnight for ~ 12 hours to room temperature. The following morning, annealed reactions were aliquotted and flash frozen in liquid nitrogen and stored at −80°C. Prior to setting up helicase assays, aliquots were thawed on ice and diluted to 2 μM in H_2O. Hybridization status was verified by native 4-20% PAGE using 1× TBE running buffer containing: 89 mM Tris-borate, 2.0 mM EDTA, pH 8.0 (Sambrook, J., Fritsch, E.F., and Maniatis, 1989).

E. coli DnaA oriC fork binding gel shift assay

DnaA was incubated with o*riC* fork in binding buffer (20 mM HEPES-KOH pH 7.5, 5 mM Mg Acetate, 5% Glycerol, 1 mM ATP, 4 mM DTT, 0.2 mg/ml BSA). Reactions containing DnaA (at final concentrations 50 nM, 100 nM, 150 nM, 300 nM, 500 nM and 1 mM) and 100 nM *oriC* fork were pre-incubated on ice for 5 minutes before being incubated at 37°C for 5 minutes. Samples were run on a 4.5%, 8% and 12% (80:1) acrylamide:bis-acrylamide TBE gels in 1X TBE running

buffer for 55 minutes. Gels were scanned for Cy5 on a typhoon. 1X TBE running buffer contained: 89 mM Tris-borate, 2.0 mM EDTA, pH 8.0 (Sambrook, J., Fritsch, E.F., and Maniatis, 1989). Gels were stained with SYBR Gold for 15 minutes at room temp and destained with for 15 minutes.

DnaA/DnaC-dependent oriC fork helicase assay

Unwinding of *oriC* forked DNA substrates was carried out by first annealing a 5′-Cy3- and 5′-Cy5 labeled oligonucleotides, with a 1.2 molar excess of a 3′-black hole quencher-labeled strand and Top strand oligo (see **Table 2.1**). Capture oligos complementary to the base-paired region of the Cy3- or Cy5-labeled strands were added to all reactions to prevent re-annealing of the unwound substrate and recycling of DnaB by the loader (see **Table 2.1**). Reactions containing 200 nM DnaB hexamer (with or without 1.2 mM loader monomer), 100 nM fork substrate, 400 nM DnaA, and 200 nM capture oligos were monitored at 37 °C for 15-30 minutes in assay buffer (20 mM HEPES-NaOH pH 7.5, 5 mM magnesium acetate, 50 mM potassium glutamate, 5 % glycerol, 4 mM DTT, 0.2 mg/mL BSA and 1 mM ATP).

HPLC-purified DNA oligonucleotides were purchased from Integrated DNA Technologies. The *oriC* forked DNA substrates were formed by annealing the fork such that both the 5′-Cy3 and 5′-Cy5-labeled oligonucleotides were annealed in the presence of a 1.2 molar excess of a quencher strands at a final concentration of 20 mM each in annealing buffer (10 mM Tris-HCl, 1 mM EDTA, and 100 mM NaCl, pH 7.5). Helicase and loader were pre-mixed on ice and incubated for 10 minutes, followed by addition of substrate DNA and incubation for an additional 10 minutes. Capture strand DNAs (complementary to the base-paired regions of either the Cy3-labeled or Cy5-labeled oligos, along with ATP, was then added immediately prior to reading the plate at 37 °C. The resultant 75 µL reactions containing 200 nM DnaB hexamer (with or without 1.2 mM loader monomer), 100 nM fork substrate, and 200 nM capture strand were monitored for fluorescence increase at 37 °C for 30 minutes on a Victor V3 plate reader (Perkin Elmer). The final assay buffer consisted of 20 mM HEPES-KOH pH 7.5, 5 mM magnesium acetate, 50 mM potassium glutamate, 5 % glycerol, 4 mM DTT, 0.2 mg/mL BSA and 1 mM ATP. Data were analyzed and plotted in Excel (Microsoft).

DnaC-dependent forked substrate helicase assay

Unwinding of forked DNA substrates was carried out by first annealing a 5′-Cy3-labeled oligonucleotide (5′-Cy3-TACGTAACGAGCCTGC$(dT)_{25}$-3′) to a 1.2 molar excess of a 3′-black hole quencher-labeled strand (5′-$(dT)_{25}$-GCAGGCTCGTTACGTA-BHQ2-3′).

A capture oligo (5′-GCAGGCTCGTTACGTA-3′) complementary to the base-paired region of the Cy3-labeled strand was added to all reactions to prevent re-annealing of the unwound substrate and recycling of DnaB by the loader. Reactions containing 200 nM DnaB hexamer (with or without 1.2 mM loader monomer), 100 nM fork substrate, and 200 nM capture oligo were monitored at 37 °C for 15 minutes in assay buffer (20 mM HEPES-KOH pH 7.5, 5 mM magnesium acetate, 50 mM potassium glutamate, 5 % glycerol, 4 mM DTT, 0.2 mg/mL BSA and 1 mM ATP).

HPLC-purified DNA oligonucleotides were purchased from Integrated DNA Technologies. The forked DNA substrate was formed by annealing a 5′-Cy3-labeled oligonucleotide (5′-Cy3-TACGTAACGAGCCTGC$(dT)_{25}$-3′) with a 1.2 molar excess of a 3′-black hole quencher-labeled strand (5′-$(dT)_{25}$-GCAGGCTCGTTACGTA-BHQ2-3′) at a concentration of 20 mM each in annealing buffer (10 mM Tris-HCl, 1 mM EDTA, and 100 mM NaCl, pH 7.5). Helicase and loader were pre-mixed on ice and incubated for 10 minutes, followed by addition of substrate DNA and incubation for an additional 10 minutes. A capture strand DNA (complementary to the base-paired region of the Cy3-labeled oligo (5′-GCAGGCTCGTTACGTA-3′), along with ATP, was then added immediately prior to reading the plate at 37 °C. The resultant 75 µL reactions containing 200 nM DnaB hexamer (with or without 1.2 mM loader monomer), 100 nM fork substrate, and 200 nM capture strand were monitored for fluorescence increase at 37 °C for 15 minutes on a Victor V3 plate reader (Perkin Elmer). The final assay buffer consisted of 20 mM HEPES-KOH pH 7.5, 5 mM magnesium acetate, 50 mM potassium glutamate, 5 % glycerol, 4 mM DTT, 0.2 mg/mL BSA and 1 mM ATP. Data were analyzed and plotted in Excel (Microsoft).

Tables

Table 2.1 *oriC* fork DNA oligonucleotides

	DNA oligonucleotides sequences
Top45_BHQ2 (upper) strand	5′-GGATCCTAGAGATCTGTTCTATTGTGATCTCTTATTAGGATCGCACTGCCCTGTGGATAACAAGGA-BHQ2-3′ DnaA R1 Box is underlined, 13-mer AT-rich DUE elements (M and R) are colored red and green, respectively.
Cy3-lower strand-/3IAbRQSp/	5′-Cy3-TCCTTGTTATCCACAGGGCAGGCGCTAGGGTTGTTAGTCATTGCTCGTCCGGTCTGTGAGCACGTG-/3IAbRQSp/
Cy5-lower strand reporter	5'- /5Cy5/CACGTGCTCACAGACCGTTTTTTT -3'
Cy5 capture strand (lower)	5'- CGGTCTGTGAGCACGTG -3′
Top (upper) strand oligo 17nt	5′-ACAGATCTCTAGGATCC-3'
Cy3 capture strand	5'- TCC TTG TTA TCC ACA GGG CAG -3'

Figures

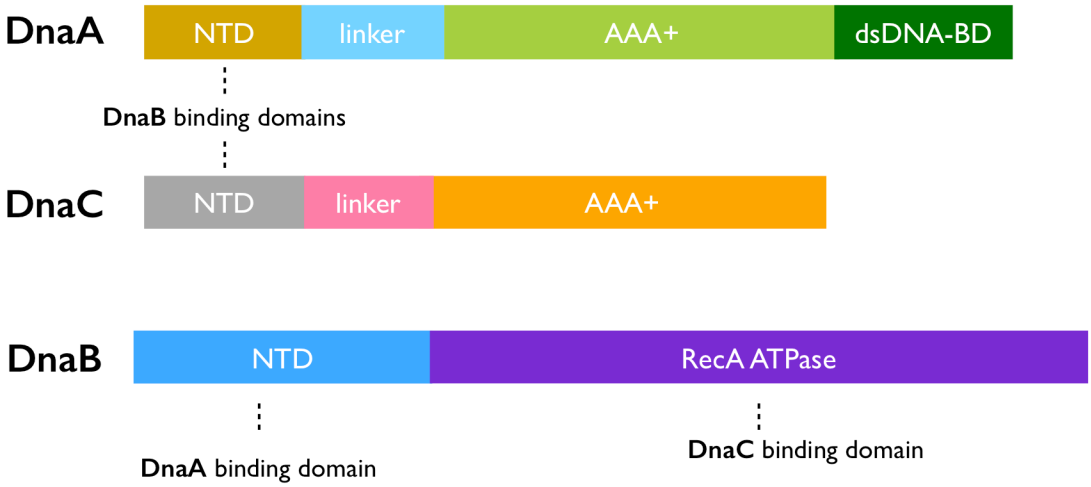

Figure 2.1. Domain organization of *E. coli* DnaA, DnaB and DnaC. Specific domains and protein-protein interacting domains are labeled.

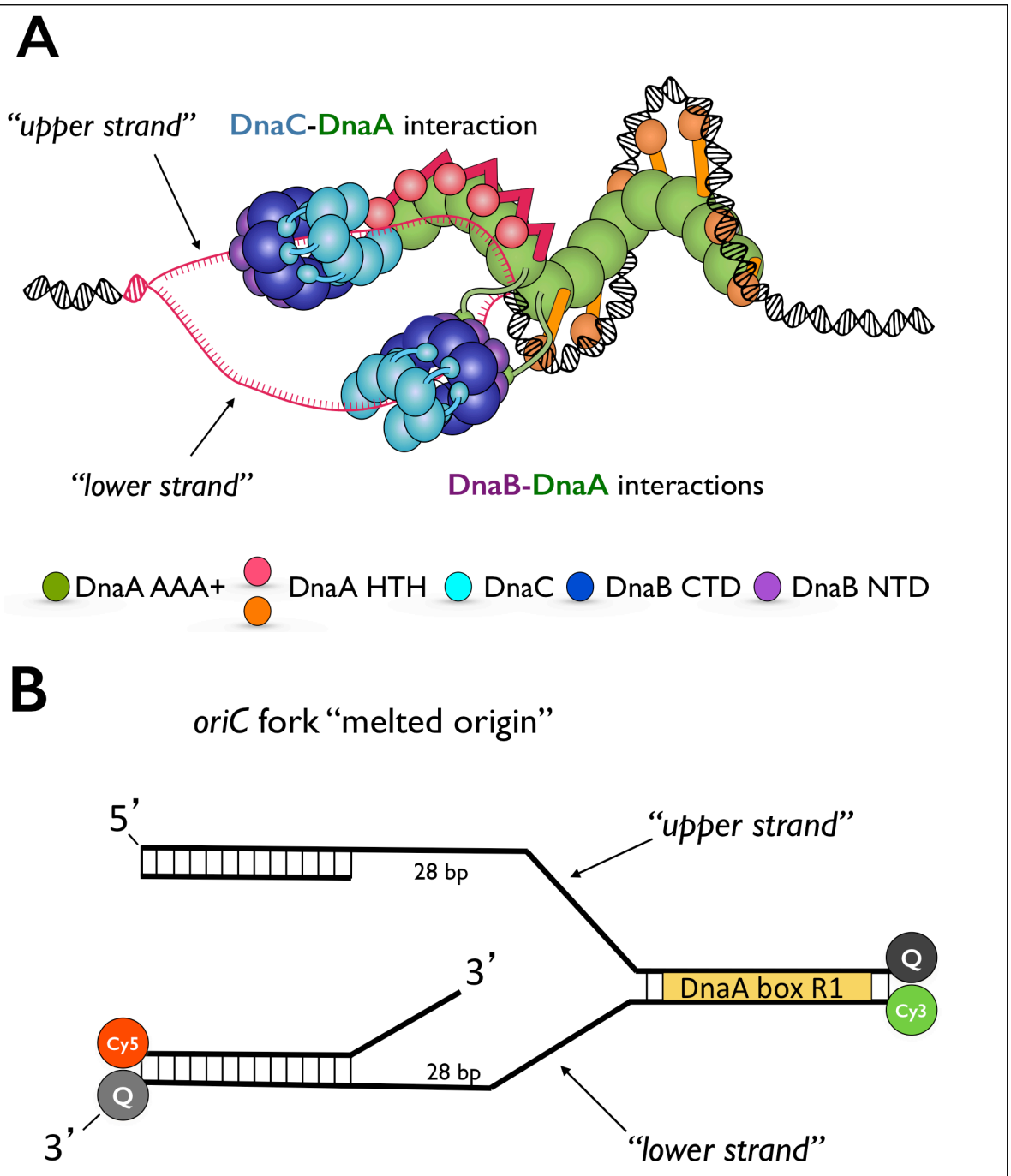

Figure 2.2. Model for strand-specific replicative helicase loading by the bacterial initiator DnaA and helicase loader DnaC and design of synthetic *oriC* forked "melted origin" helicase loading and unwinding substrate. (A) Model for strand-specific helicase loading by DnaA- and DnaC-specific interactions. Loading to the "upper strand" is predicted to occur through an association between DnaA and DnaC while loading to the "lower strand" is predicted to occur through interactions between the N-terminal domains of DnaA and the replicative helicase DnaB helicase. (B) Cartoon diagram of synthetic *oriC* forked "melted origin" substrate.

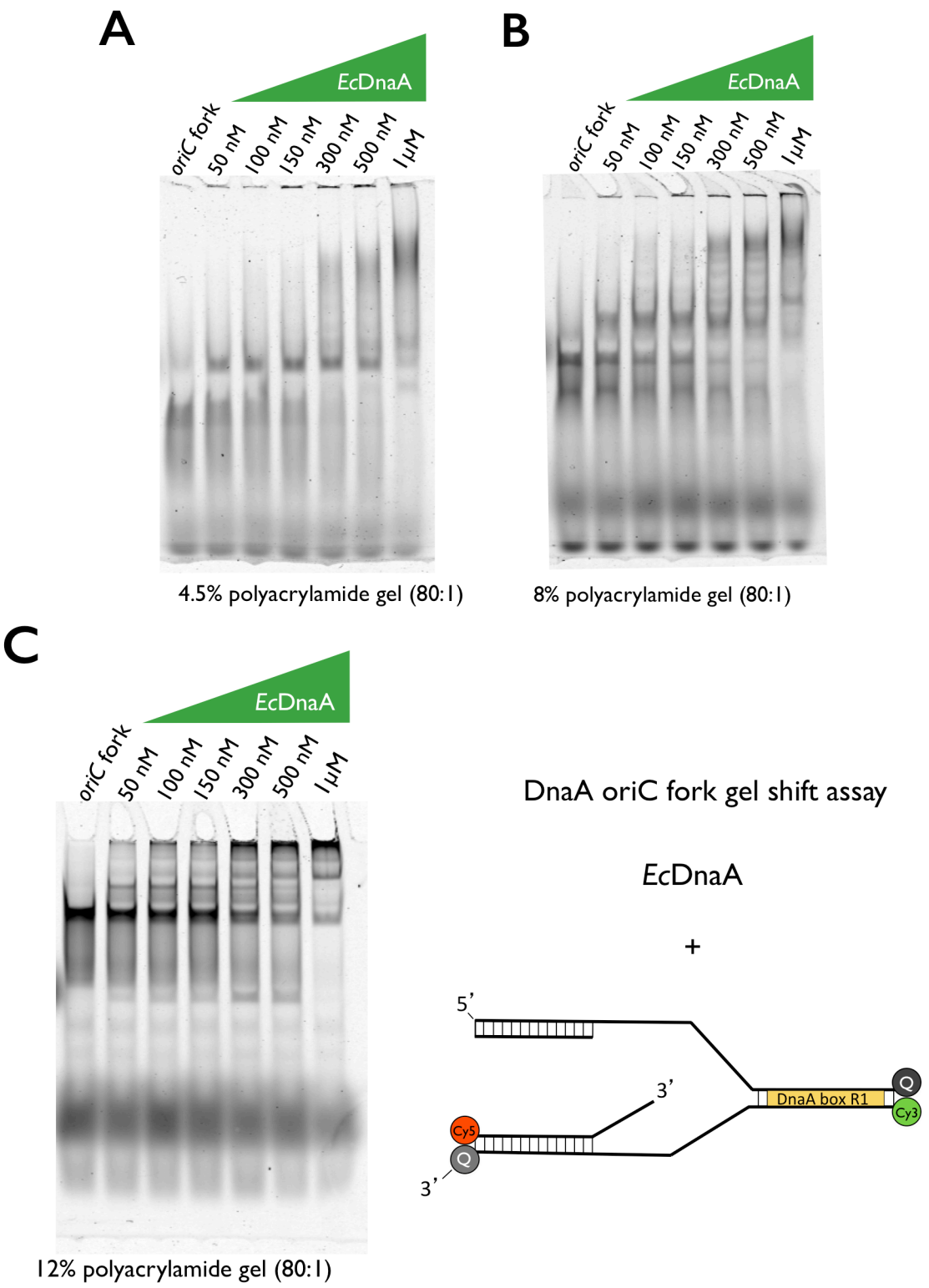

Figure 2.3. Gel shift assay of *E. coli* DnaA titration for binding to *oriC* fork substrate. *E. coli* DnaA *oriC* fork binding reactions were run on 4.5% (A), 8% (B) and 12% (C) polyacrylamide gels.

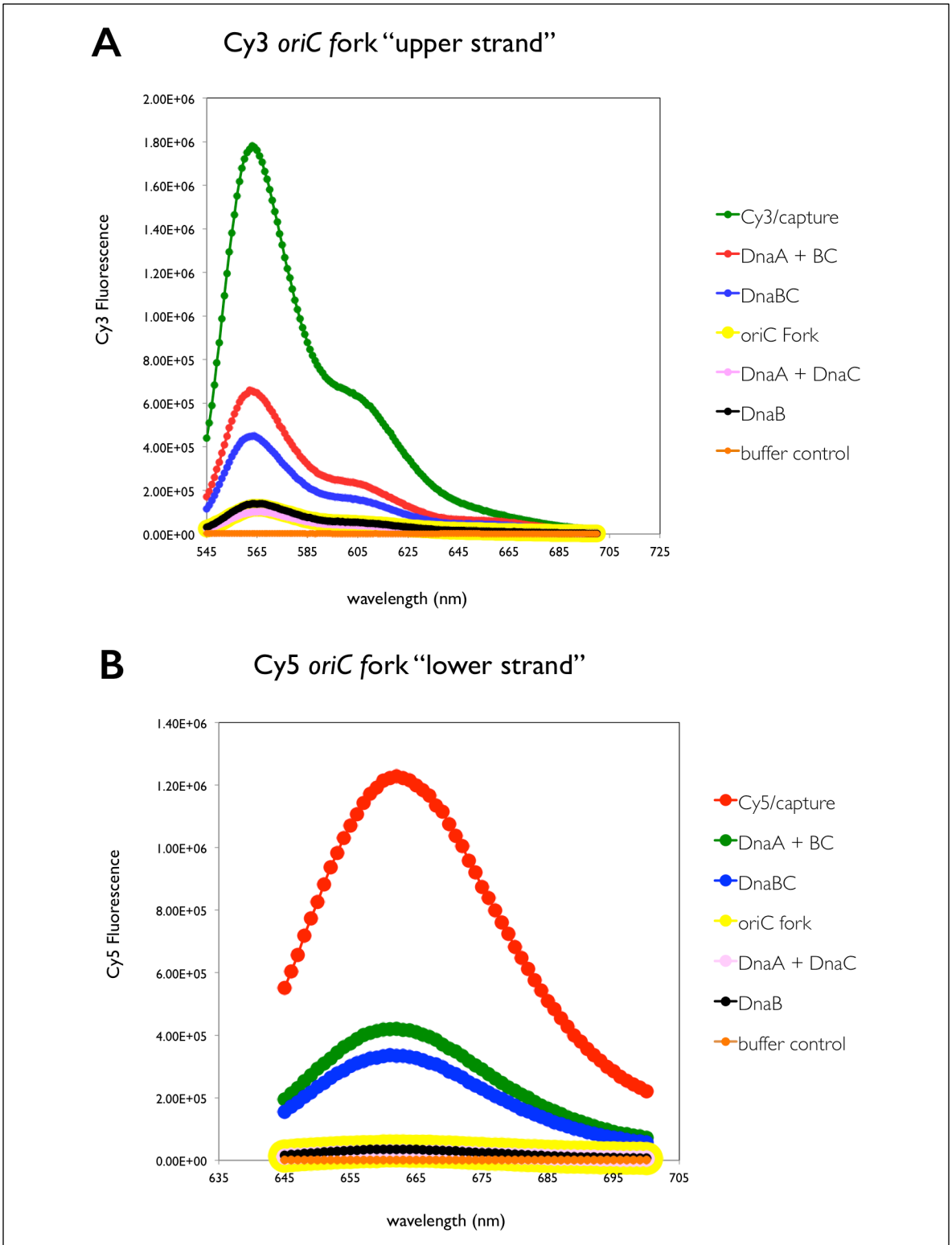

Figure 2.4. "Upper" and "lower" stranding oriC fork unwinding observed in DnaA-dependent helicase assay. Raw fluorescence scans of Cy3 (upper strand) and Cy5 (lower strand). Data was collected on a FluoroMax-4 spectrophotometer (HORIBA, Ltd.).

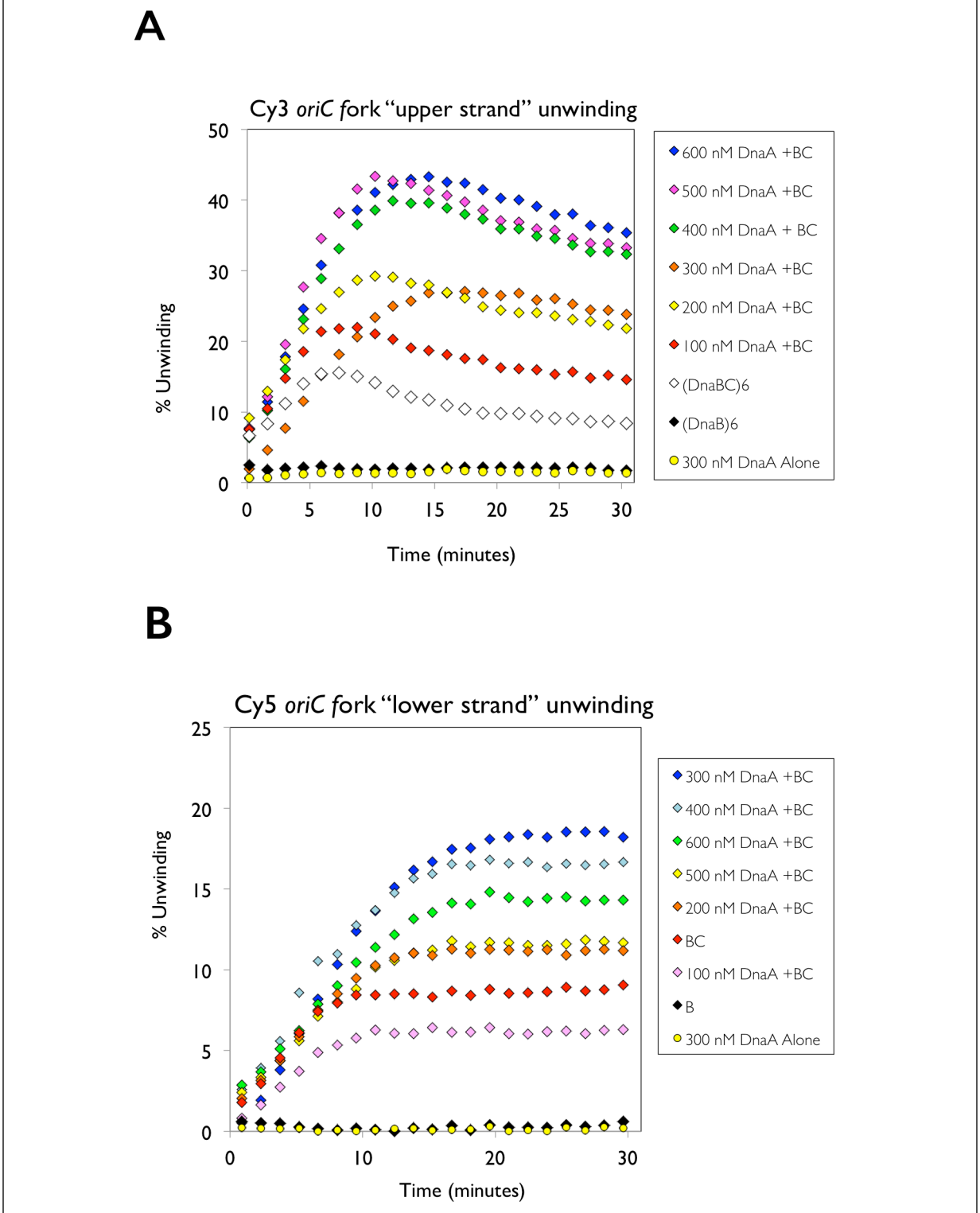

Figure 2.5. DnaA titration with *oriC* fork. "Upper" and "lower" strand unwinding by DnaB helicase measured by plate reader.

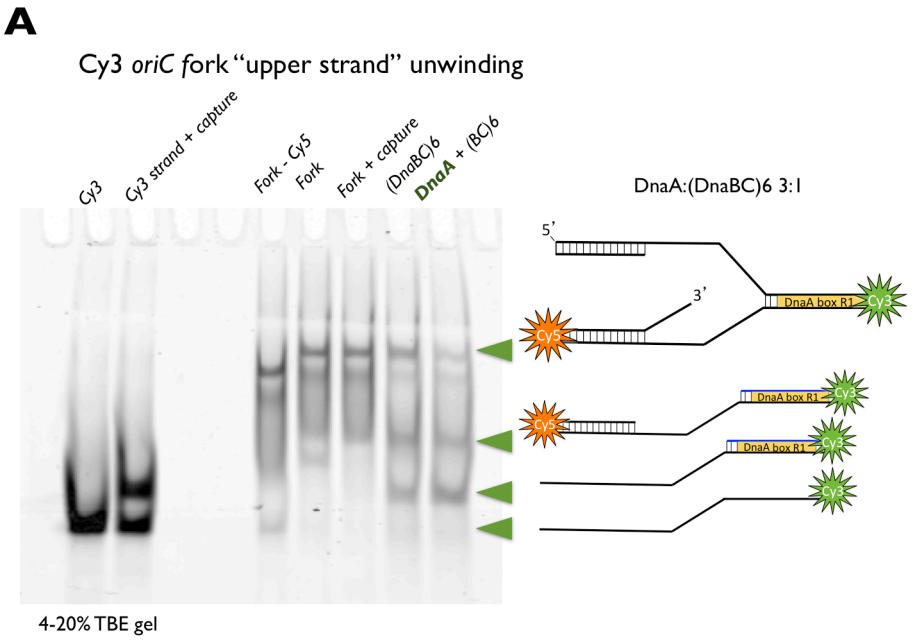

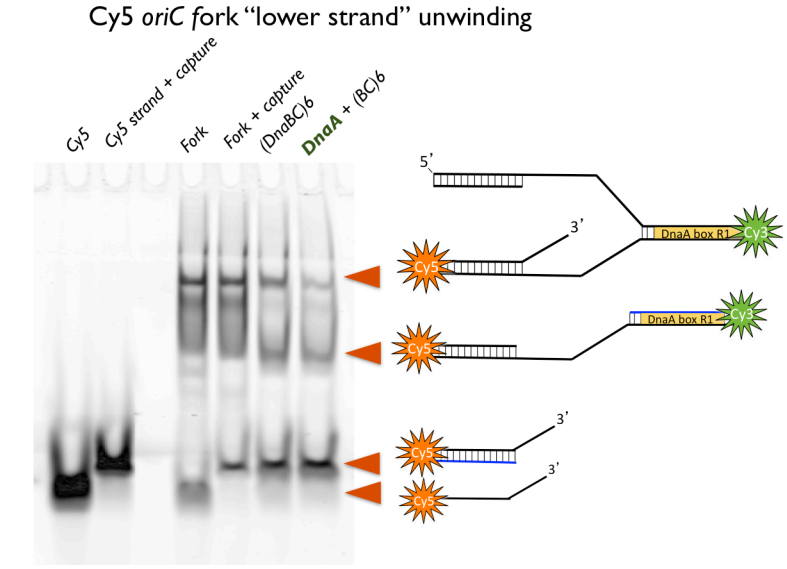

Figure 2.6. DnaA enhanced "upper" and "lower" strand unwinding measured by a 4-20% TBE gel.

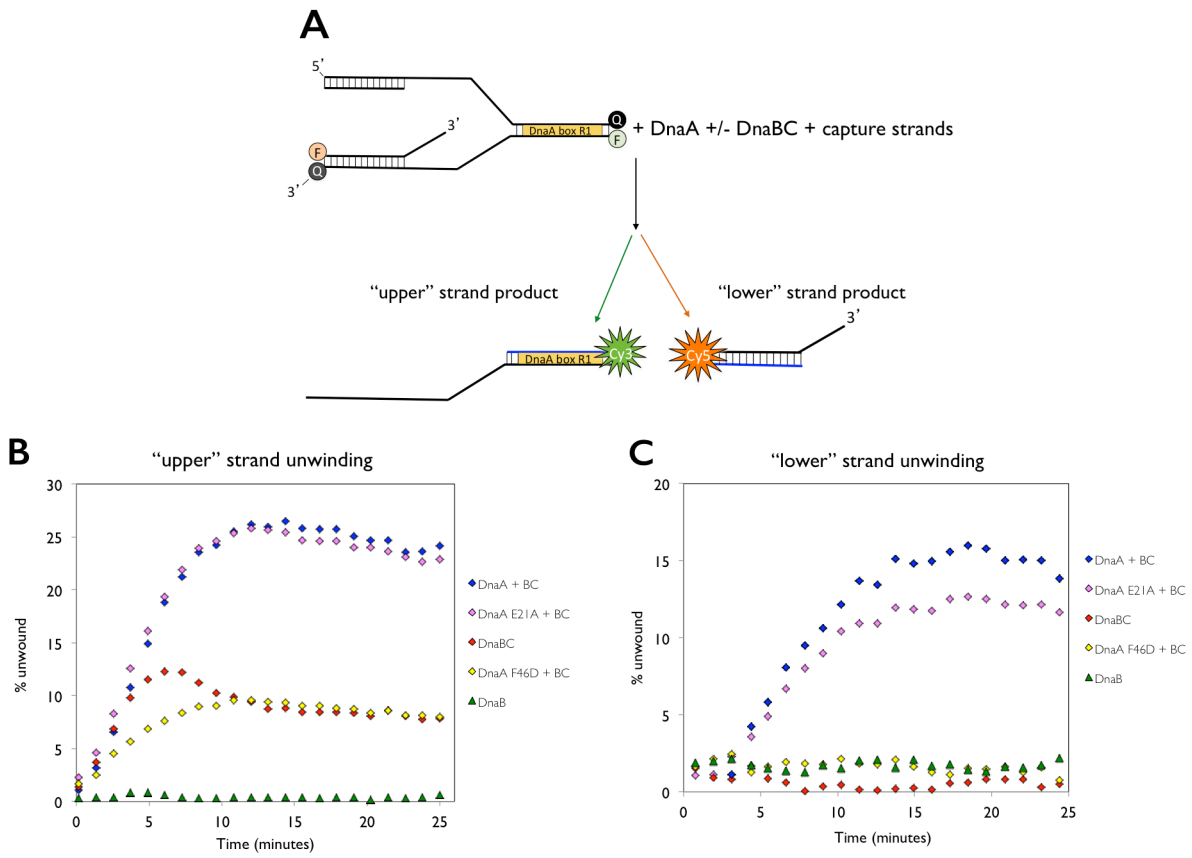

Figure 2.7. DnaA mediated recruitment to both strands of a melted *oriC* fork. DnaB binding mutant (F46D) is unable to recruit the DnaB to both strands of the *oriC* forked substrate resulting in an inability to unwind the fork. E21A mutant shows wild-type activity for loading to the "upper strand" but is modestly reduced for loading to the "lower strand".

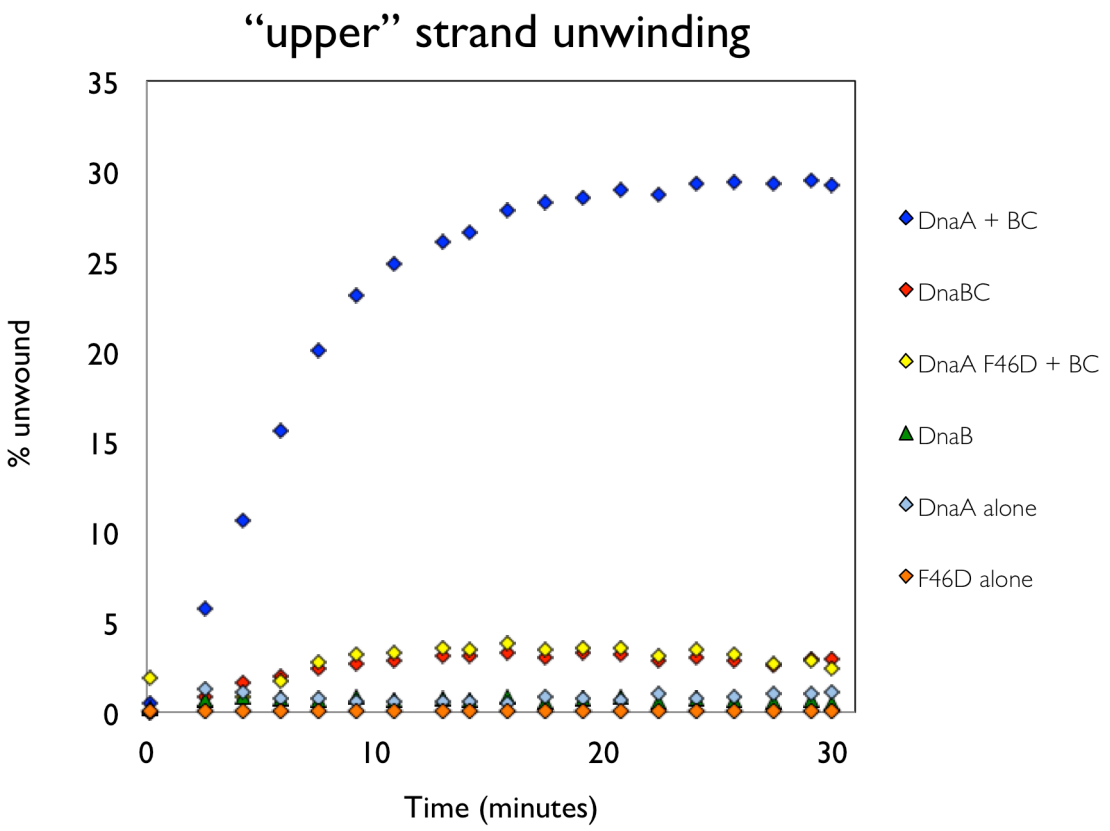

Figure 2.8. DnaA mediated recruitment to "upper strand" of melted *oriC* fork. DnaB binding mutant (F46D) is unable to recruit the DnaB to the *oriC* forked substrate resulting in an inability to unwind the fork. *dT20 ssDNA is added to prevent non-specific association of DnaBC with fork.

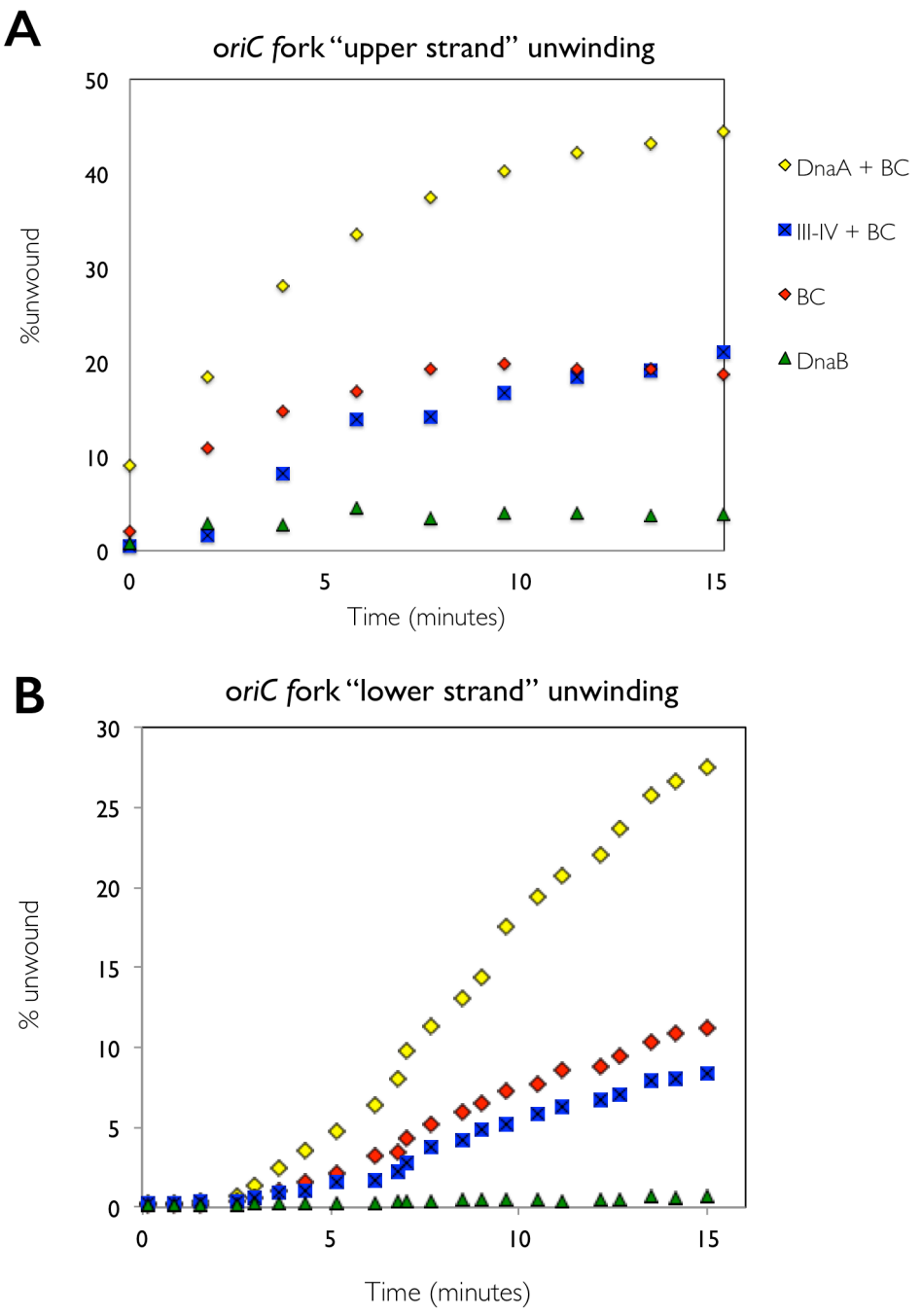

Figure 2.9. DnaA N-terminal domain is required for recruitment of the helicase to both the "upper" and "lower" strands of melted *oriC* fork. (A) DnaA recruitment to "upper" strand of *oriC* fork. (B) DnaA recruitment to "lower" strand of *oriC* fork. DnaA N-terminal domain truncation, labeled III-IV, which contains only domain III (AAA+) and IV (dsDNA binding domain) is unable to enhance recruitment of the helicase to either the "upper" or "lower" strand. Reaction conditions did not include excess dT_{20}.

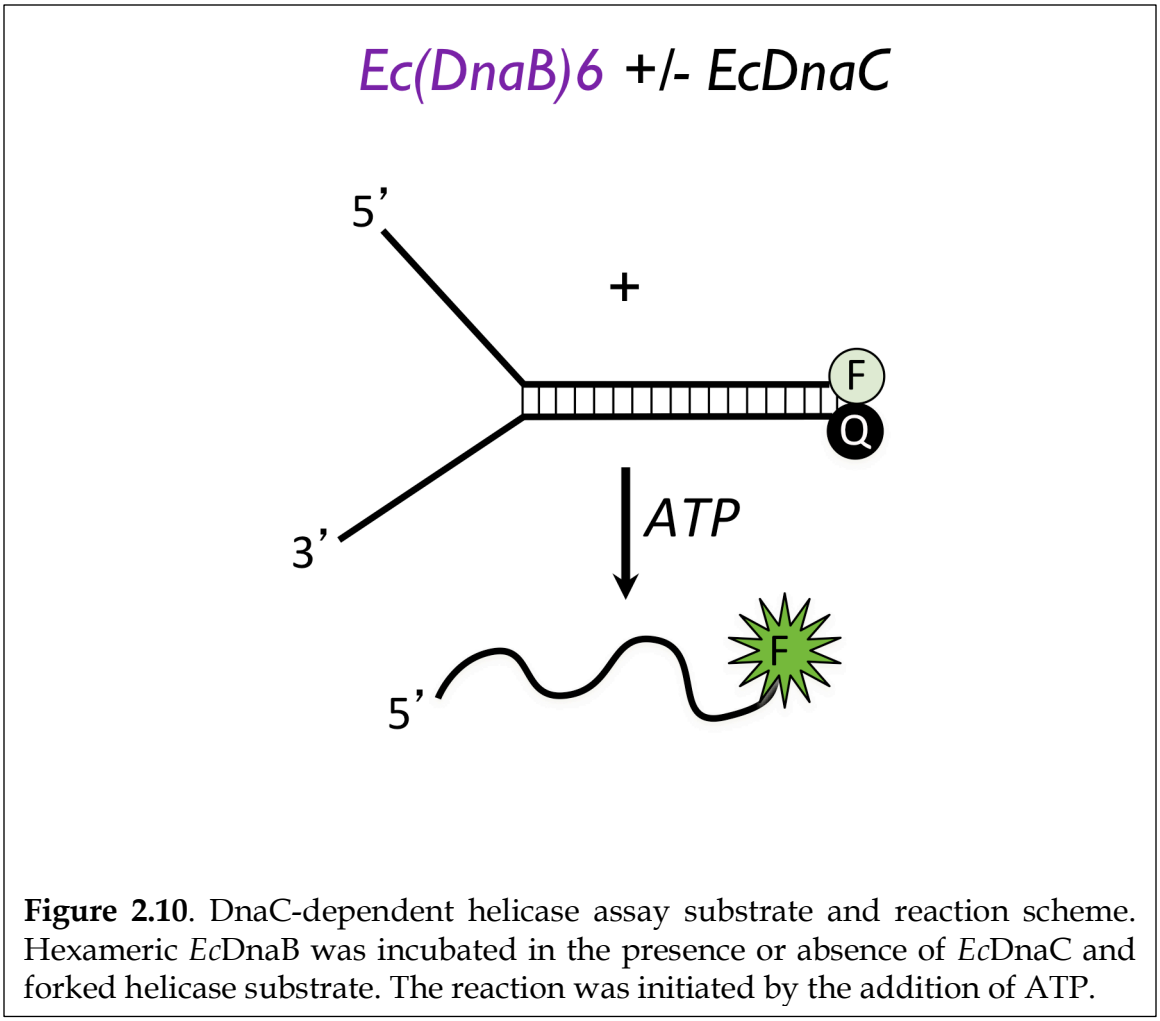

Figure 2.10. DnaC-dependent helicase assay substrate and reaction scheme. Hexameric *Ec*DnaB was incubated in the presence or absence of *Ec*DnaC and forked helicase substrate. The reaction was initiated by the addition of ATP.

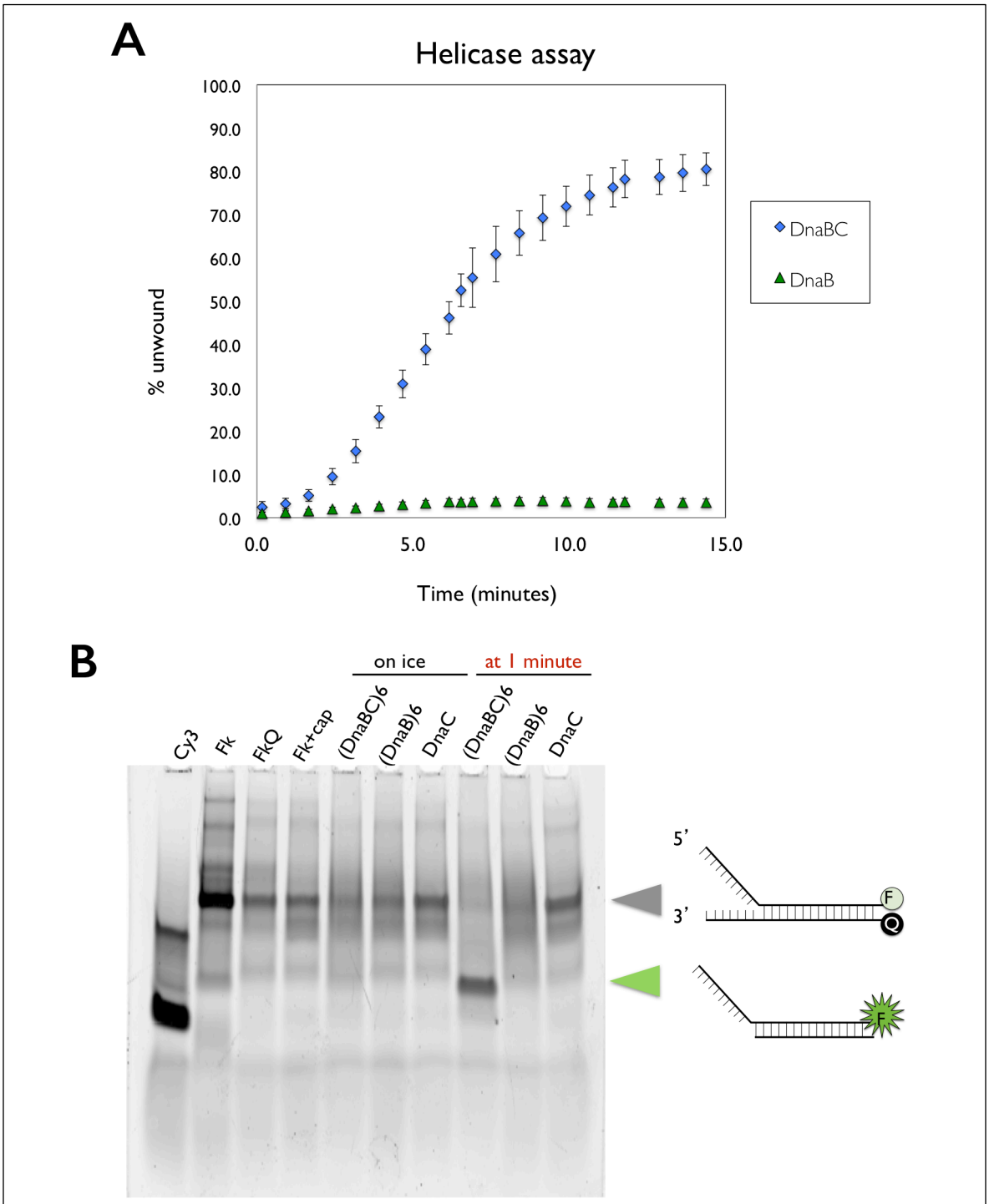

Figure 2.11. Development of an *E. coli* DnaB helicase assay. (A) Plate reader based analysis. (B) Gel-based analysis on 4-20% TBE gel. Cartoon of duplexed fork substrate is shown. Robust DNA unwinding activity is observed only in the presence of both *E. coli* DnaB and *E. coli* DnaC. DnaB and DnaC alone controls show no unwinding.

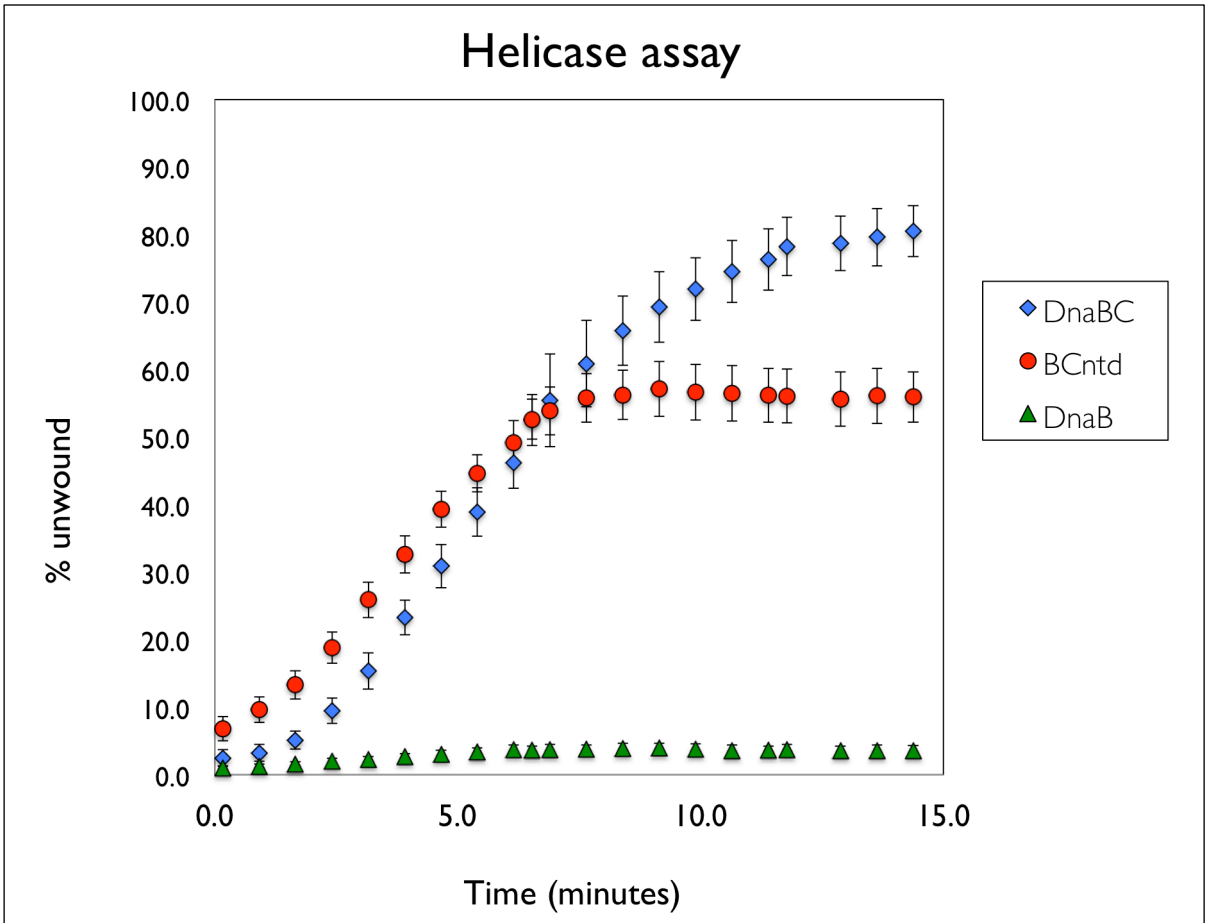

Figure 2.12. *E. coli* DnaC N-terminal binding domain (DnaC-NTD) activates DnaB-dependent unwinding of a topologically accessible forked DNA substrate. Plot shows unwinding of a fluorophore/quench-labeled DNA by DnaB in the presence or absence of DnaC or the $DnaC_{NTD}$. Data points and error bars represent the average and standard deviation, respectively, from at least six measurements.

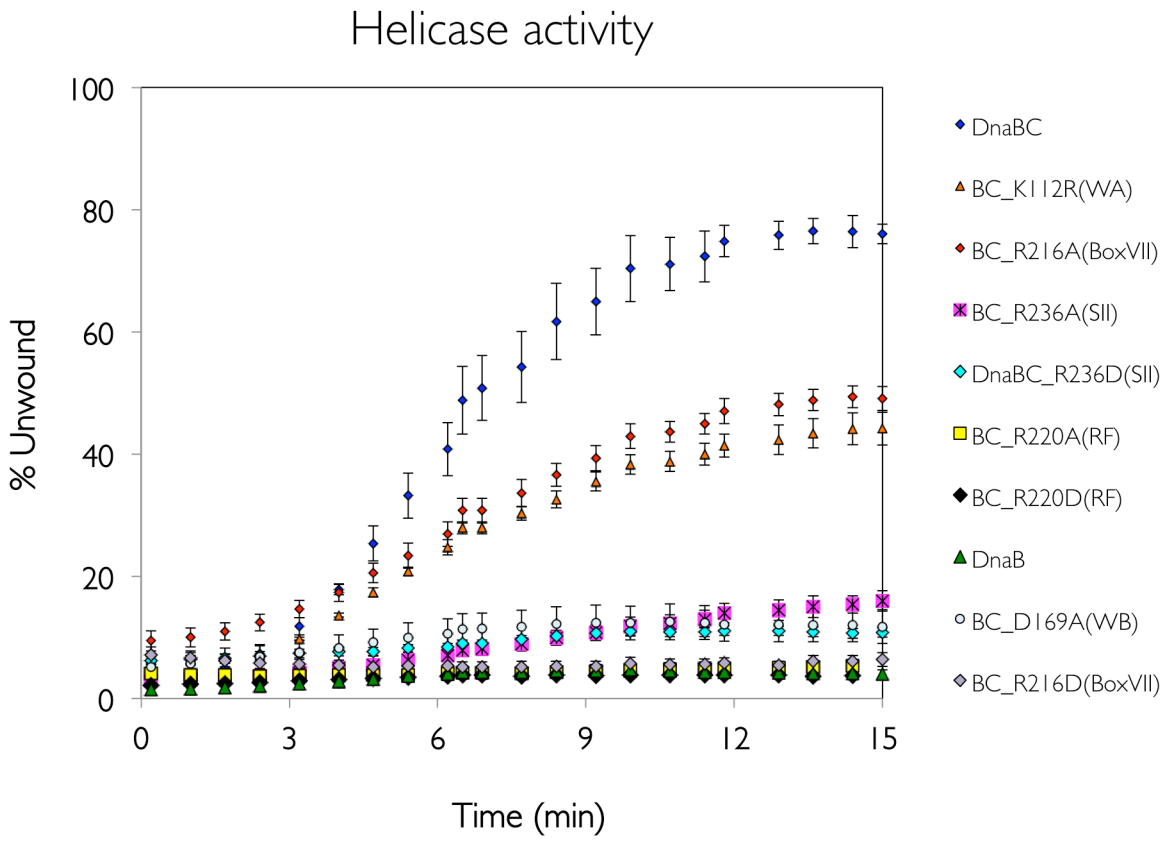

Figure 2.13. *E. coli* DnaC mutants defective for ATP hydrolysis are unable to promote DnaB helicase activity. Wild-type DnaC and DnaC mutants Walker A mutant (K112R), Walker B (D169A), Sensor II (R236A and R236D), Arginine Finger (R220A and R220D) are shown in blue, orange, grey, magenta, cyan, yellow, and black respectively. DnaB alone is shown in green. Plot shows unwinding of a fluorophore/quench-labeled DNA by DnaB in the presence or absence of DnaC or the $DnaC_{NTD}$. Data points and error bars represent the average and standard deviation, respectively, from at least six measurements.

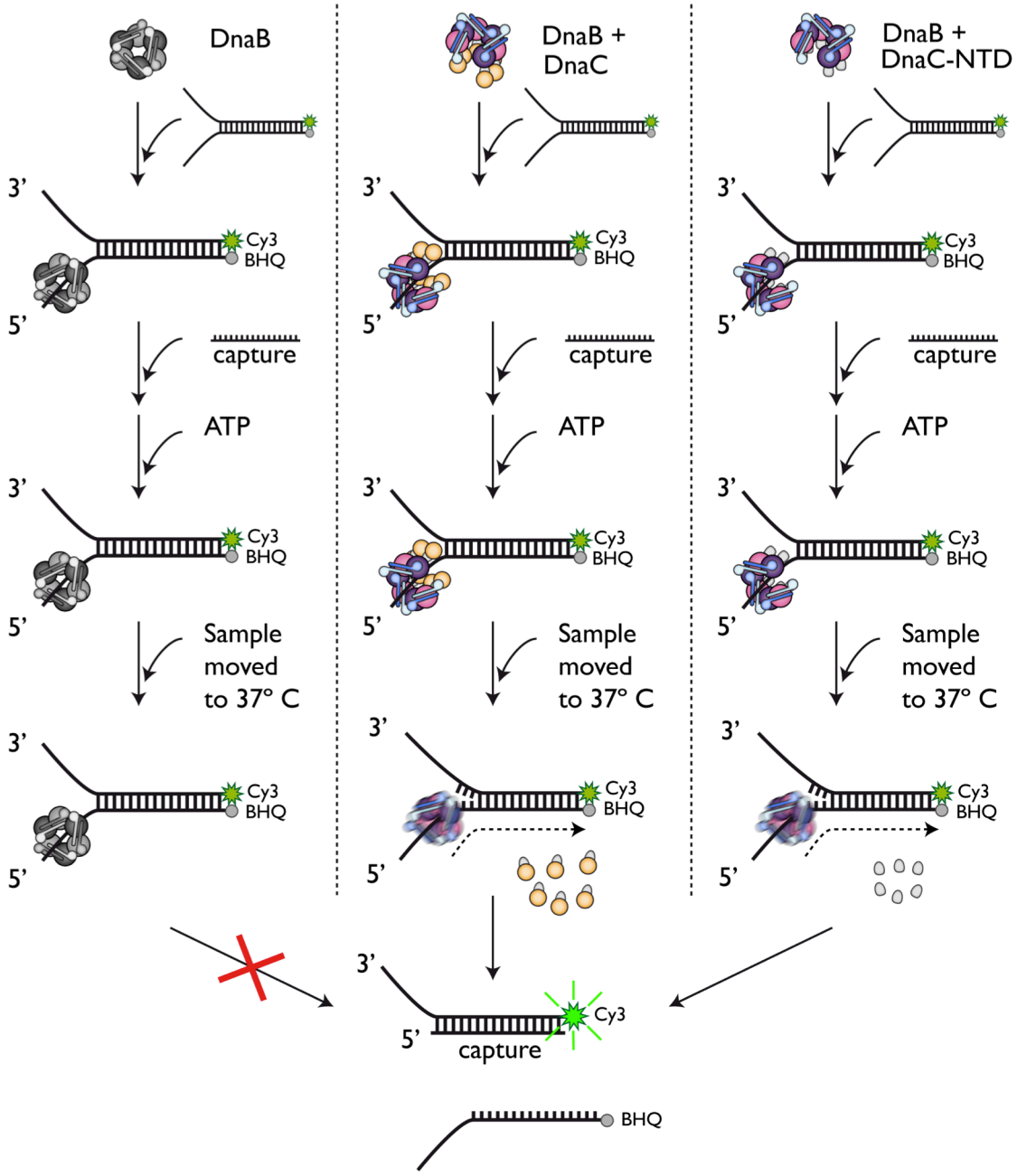

Figure 2.14. Helicase assay reaction schematic for forked DNA substrate. DNA unwinding experiment using a forked substrate, DnaB, alone or together with loader, was pre-incubated on ice with the forked DNA substrate at a 2:1 ratio for 10 min. A capture strand was next incorporated to prevent re-annealing of the unwound substrate, along with ATP immediately prior to moving the sample from 4°C to 37°C to start the reaction. DnaBC and DnaBC$_{NTD}$ show high levels of activity, monitored by fluorescent emission of the unwound Cy3 strand re-annealed with the capture strand. By contrast, DnaB alone shows almost no helicase activity.

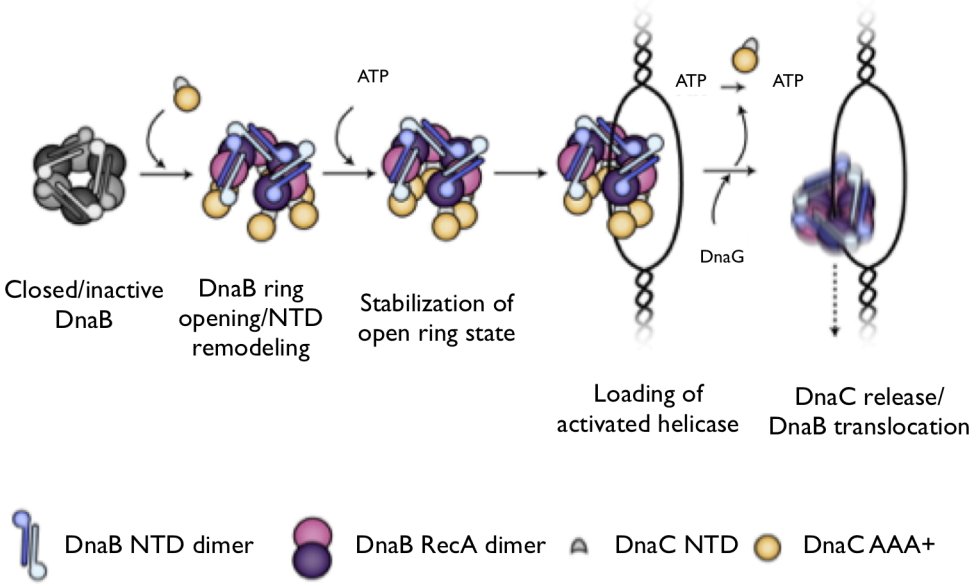

Figure 2.15. Mechanism of DnaC Action. DnaC opens and remodels DnaB to facilitate DNA loading and unwinding. Closed-ring DnaB cannot engage a topologically closed DNA substrate. DnaC associates with the helicase, remodeling the N-terminal collar, and triggering helicase opening. In the presence of ATP, DnaC AAA+ domains further assemble into a helical conformation that stabilizes the open-ring complex and assists with DNA binding. ATP hydrolysis by DnaC and/or DnaG helps disengage the loader (Davey et al., 2002; Makowska-Grzyska and Kaguni, 2010), leaving an active helicase encircled around DNA.

Chapter 3: Structural and biochemical studies of *Staphylococcus aureus* helicase loader DnaI and loader inhibition by phage peptide 77ORF104

(Iris V. Hood and James M. Berger, manuscript in preparation. 2015.)

Abstract

The assembly of cellular replisomes depends upon efficient loading of ring-shaped hexameric helicases onto DNA by ATP-dependent helicase loading factors. How nucleotide turnover is coupled to helicase loader function and how loader activity is appropriately regulated remains unclear. In many organisms, replication machineries – including those used for initiation – can be subverted or co-opted by viruses to produce progeny; the study of such systems provides invaluable insights into mechanism. To better understand the function of the helicase loader DnaI from *Staphylococcus aureus (S. aureus)*, we performed structural and biochemical analyses to establish that an antimicrobial protein from phage 77, ORF104, interferes with the function of *S. aureus* DnaI (*Sa*DnaI) by binding directly to the loader's C-terminal AAA+ ATPase domain. A crystal structure of the 77ORF104 phage peptide bound to ADP•BeF_3-bound *Sa*DnaI^{AAA+}, determined to 1.9 Å resolution, reveals that the 77ORF104 inhibitor directly engages DnaI's nucleotide-binding site. This complex, together with a second structure of the uninhibited loader ATPase domain, shows that ORF104 interferes with loader self-assembly both sterically and through an induced conformational change in an element important for loader oligomerization called the Initiator-specific motif (ISM). Comparative structural analysis of related DnaI/DnaC-family loaders reveal that the helicase loader's variable N-terminal linker region occupies the same location as the C-terminus of 77ORF104, suggesting that the phage protein exploits an existing, unanticipated regulatory "hotspot" that normally prevents aberrant helicase loader auto-association. Biochemical studies demonstrate that while the inhibitory phage protein does not block association with the replicative helicase, 77ORF104 inhibits DnaI ATPase activity; we further find that phage 77 encodes a cognate, phage-encoded helicase loader homolog and show that it is not affected by the phage peptide, but instead directly binds the host's replicative helicase. Together, these findings reveal a new mechanism by which viruses can hijack host replication processes, highlighting the prospects of mining the virosphere as a promising reserve for antibiotic drug discovery.

Introduction

All cellular organisms duplicate their genomic DNA concurrently with cell cycle signals, a step vital for both cell survival and the maintenance of genetic stability (Ding and MacAlpine, 2011; Heller and Marians, 2006; Sutera Jr. and Lovett, 2006). To synthesize DNA, active multi-component replication machines must first be assembled at correct chromosomal loci in the genome, termed replication origins. Dedicated proteins, called initiators, serve essential roles in selecting the correct start site and in remodeling the origin DNA to provide the appropriate platform for delivery of replicative helicases prior to strand synthesis (Bell and Stillman, 1992; Bramhill and Kornberg, 1988a; Dueber et al., 2007; Fang et al., 1999; Kaguni and Kornberg, 1984).

Although specific helicase recruitment and loading mechanisms vary across the three domains of life, all appear to rely on replication initiation factors belonging to the AAA+ superfamily of ATPases. Replicative helicases are ring-shaped hexameric motors that likewise rely on ATP hydrolysis, unwinding parental duplex DNA at the head of the replication fork to drive fork progression (McGlynn, 2011). Appropriate deposition of replicative helicases onto origin DNA by dedicated loading factors is highly regulated to ensure the faithful copying of the genome once per cell cycle. The molecular basis by which replicative helicases are loaded onto replication origins remains an outstanding and fundamental issue.

In bacteria, DNA replication initiation relies on an initiator protein, DnaA, which recognizes and melts the bacterial replication origin (Bramhill and Kornberg, 1988a; Gille and Messer, 1991; Hsu et al., 1994). During initiation, DnaA actively opens a region of the origin, termed the DNA unwinding element (DUE) (Kowalski and Eddy, 1989), and then helps recruit two copies of the replicative helicase to the newly melted single strands. In Gram-negative bacteria, a protein known as DnaC frequently assists loading of the helicase, many Gram-positive species retain a homolog of DnaC termed DnaI. Both DnaC and DnaI are composed of an N-terminal helicase binding domain and a C-terminal AAA+ ATPase domain connected to each other by a variable linker region of unknown function (Loscha et al., 2009)(**Figure 3.1A**). At present, it remains unknown how specific events in a nucleotide hydrolysis cycle helps control the activity of DnaC/DnaI family helicase loaders. There is evidence that ATPase activity by these proteins controls aspects of the helicase loading cycle and may even be auto-regulated (Davey et al., 2002; Ioannou et al., 2006; Learn et al., 1997); however, the mechanism by which this occurs is likewise poorly understood.

Over the past few decades, there has been a marked rise in multi-drug resistant bacterial strains, such as MRSA (Methicillin-resistant *Staphylococcus aureus*), along with associated human fatalities (Klein et al., 2007, 2013; Salgado et al., 2003). As a consequence, there has been renewed interest in exploring bacteriophage genomes to discover new antimicrobial agents. In one such example, a high-throughput screen identified several phage-encoded proteins that inhibit growth of *S. aureus* cells by

blocking DNA replication (Liu et al., 2004). This work revealed that a small, 52 amino acid peptide from phage strain 77, encoded by the *ORF104* gene, interacts with the *S. aureus* helicase loader, DnaI (*Sa*DnaI). The discovery of ORF104 marks the first known instance in which the replication initiation machinery of a bacterium can be inhibited by an exogenous factor (Liu et al., 2004); however, where ORF104 associates with DnaI and how it exerts its function has yet to be determined.

To better understand the activity of DnaI-type helicase loaders and the mechanism used by the phage77 ORF104-type protein inhibits *S. aureus* DnaI (*Sa*DnaI) function, we performed structural, biochemical, and comparative studies on both the isolated and peptide-inhibited loader. We found that the phage peptide binds directly to DnaI's AAA+ ATPase domain, where it both remodels a region critical for loader self-assembly and sterically masks a known subunit-subunit interaction site. This action, which represses the loader's ATP hydrolysis activity, is found to exploit a binding site normally occupied by a portion of the N-terminal linker region that connects the N- and C-terminal regions of DnaI. Together, these findings not only reveal a new mechanism for the viral inhibition of bacterial DNA replication, but also indicate that bacterial helicase loaders bear an existing, unanticipated auto-regulatory element, located within their variable linker region, that likely exists to help prevent premature loader self-assembly.

Results

77ORF104 binds *Sa*DnaI C-terminal AAA+ domain in a nucleotide independent manner

To begin to probe the interaction between 77ORF104 and *Sa*DnaI, we first cloned, expressed, and purified both full-length proteins. We then used limited proteolysis studies both in the presence and absence of 77ORF104 to determine whether the phage peptide might protect a particular region of *Sa*DnaI. Inspection of the reactions using SDS-PAGE showed relatively rapid degradation of *Sa*DnaI when peptide was omitted. By contrast, when 77ORF104 was added to the full-length loader, a distinct 20 kDa species appeared (**Figure 3.2**). Together these data indicate that the peptide associates not with full-length DnaI, but with a particular region of the loader.

The size of the species produced by limited proteolysis suggested the inhibitor might bind to C-terminal AAA+ domain of *Sa*DnaI, which is also ~20 kDa in mass (**Figure 3.2**). To test this idea, we cloned, expressed and purified truncated variants of *Sa*DnaI that encompassed the N-terminal helicase binding domain (*Sa*DnaI^{NTD}, residues 1-117), the C-terminal AAA+ ATPase domain *(Sa*DnaI^{AAA+}, residues 136-306), and the AAA+ domain plus the linker region that connects to the NTD (*Sa*DnaI^{CTD}, residues 117-306) (see domains in **Figure 3.1A**). With these constructs in hand, we next performed pull down assays using His_6MBP-tagged 77ORF104 as bait and the untagged, truncated DnaI domains as prey. In agreement with our limited proteolysis data, analysis of the amylose pull-downs by SDS-PAGE revealed that the phage protein was capable of retaining both the native DnaI protein and the isolated C-terminal domain containing its AAA+ ATPase domain (**Figure 3.3A-B**) but not the N-terminal domain (**Figure 3.3C**). Given that 77ORF104 bound to *Sa*DnaI's ATP binding domain, we also tested whether nucleotide was required for DnaI's association with 77ORF104. In the absence of nucleotide, our pull-downs revealed that ATP was dispensable for association with either full-length or the C-terminal AAA+ domain of *Sa*DnaI (**Figure 3.4**). Together, these findings establish that the phage inhibitor directly binds to the ATPase fold of DnaI but that this interaction is not dependent on nucleotide.

Structure of ADP•BeF_3-bound *Sa*DnaI^{AAA+}•77ORF104 complex

Having identified the interacting regions of 77ORF104 and *Sa*DnaI, we next set out to determine a crystal structure of the complex. To define a minimal *Sa*DnaI construct for crystallization screening, we fluorescently labeled the N-terminus of wild-type 77ORF104 (**Methods**) and performed fluorescence anisotropy-based binding assays. In accord with our pull-down studies, the core AAA+ domain of *Sa*DnaI^{AAA+} proved sufficient for binding to 77ORF104 (**Figure 3.5**), while the N-terminal domain showed no evidence for binding in this assay. The calculated apparent K_d (K_d =49 nM ±

19 nM) for the peptide-AAA+ domain interaction proved comparable to that previously reported for the peptide and full-length *Sa*DnaI (K_d =51 nM) by Liu and co-workers (Liu et al., 2004). Together, these data show that only the core AAA+ domain is required for high affinity association with the 77ORF104 peptide, and suggested that this region of *Sa*DnaI might serve as a promising candidate for co-crystallization studies.

To crystallize a *Sa*DnaI^{AAA+}•77ORF104 complex, we first purified both proteins individually, expressing *Sa*DnaI^{AAA+} in minimal media containing seleno-methionine for labeling purposes. We then mixed *Sa*DnaI^{AAA+} together with a 2-fold molar excess of 77ORF104 and purified the complex by size-exclusion chromatography (**Figure 3.6**). Following the successful acquisition of crystals and data collection (**Methods**), the structure was solved using single-wavelength anomalous dispersion for phasing. Following several rounds of refinement in PHENIX, the model stabilized at an R_{work}/R_{free} of 18.0%/21.8% for the resolution range of 47.4-1.9Å (**Table 3.I**). The final model contains residues (136-300) for DnaI and all residues (1—52) for 77ORF104, and displays good stereochemistry as reported by MOLPROBITY (Chen et al., 2010; Davis et al., 2004).

Examination of the ADP•BeF3-bound-*Sa*DnaI^{AAA+}•77ORF104 complex revealed that the phage protein binds to the AAA+ domain of *Sa*DnaI in a 1:1 manner (**Figure 3.7)**. *Sa*DnaI's core AAA+ domain forms a αβα fold typical of AAA+ nucleotide-binding domains, and exhibits all of the canonical motifs involved in nucleotide binding, such as the Walker-A, Walker-B and Sensor-I elements (Walker et al., 1982); these motifs adopt a configuration similar to that seen in structures of other nucleotide-bound AAA+ ATPases except that the last six C-terminal residues of the structure, which included the Sensor-II element (Arg304), were unresolved (**Figure 3.8A**). Inspection of the electron density in the active site revealed clear density for nucleotide binding, permitting modeling of ADP, BeF_3, and a single Mg^{2+} ion and its associated waters (**Figure 3.8B**). Interestingly, 77ORF104 can also been seen to directly engage the bound nucleotide (**Figure 3.8**). In this regard, Lys39 of ORF104 makes one of the more notable contacts, projecting into the *Sa*DnaI^{AAA+} active site to engage the BeF_3 moiety in a manner analogous to that of AAA+ type ATPase "arginine fingers" (**Figure 3.8A**). The 77ORF104-*Sa*DnaI^{AAA+} interaction also manifests several electrostatic and polar contacts (e.g., residue Ser14 with His269, Lys20 with Glu265, Lys39 with Asp226, Arg46 with Asp225, and Glu51 with Lys212 – amino acid numbers lower than 50 correspond to ORF104 residues, and those greater than 100 to *Sa*DnaI^{AAA+})(**Figure 3.9**), as well as a buried tyrosine (Tyr17), which both makes hydrophobic contacts to several *Sa*DnaI^{AAA+} residues (Phe166, Phe261 and Ala229) and helps to coordinate a water molecule associated with the BeF_3 moiety (**Figure 3.9**).

Structurally observed interactions are important for loader-peptide interactions

Having established that 77ORF104 specifically binds to *Sa*DnaI's C-terminal AAA+ ATPase domain, we next sought to test whether the interactions observed in our crystal structure were indeed important for stable association of the peptide with *Sa*DnaI. Upon inspection of the 77ORF104•*Sa*DnaI^{AAA+} binding interface, it became evident that the interactions can be clustered into roughly three "hotspots". One such locus involves the last five C-terminal residues of the peptide, which form a β-strand that associates laterally with one edge of the β-sheet in *Sa*DnaI's AAA+ domain core (**Figure 3.10A**). The other two loci involve two single residues, Tyr17 and Lys39, which make contacts to or around the nucleotide-binding site of *Sa*DnaI and the associated protein-peptide interaction surface (**Figure 3.10A**).

To establish whether specific contacts observed in the ADP•BeF3-bound *Sa*DnaI^{AAA+}•77ORF104 complex are important for the inhibitor's association with DnaI, we designed, cloned and purified several 77ORF104 mutants based on the structure and tested them for binding to *Sa*DnaI^{AAA+} (**Figure 3.10A**). Lys39 and Tyr17 were each mutated to glutamate in the full-length peptide, and the last 5 amino acids of the peptide's C-terminus were truncated (ORF104$^{\Delta 47\text{-}52}$). We then turned to a fluorescence anisotropy-based competition assay to assess the ability of different peptide mutants to displace fluorescently labeled, wild-type 77ORF104 from the *Sa*DnaI AAA+ domain. Unlabeled wild-type peptide, which was first used as a positive control, showed a robust ability to compete away dye-labeled 77ORF104 for binding to *Sa*DnaI^{AAA+} ($K_{i,app}$=1.625 μM ± 0.07 μM) (as evidenced by a sharp fall-off in anisotropy as the concentration of the unlabeled peptide was increased) (**Figure 3.10B**). Examination of the K39E mutant revealed to a modest reduction in the ability of the phage inhibitor to displace the wild-type peptide, indicating this amino acid serves a relatively peripheral role in stabilizing the peptide-DnaI nucleotide-binding interface (**Figure 3.10B**). By contrast, both removal of the C-terminal tail of 77ORF104 and the Y17E mutant were essentially unable to compete for binding of the native phage peptide over the concentration range tested (**Figure 3.10B**). Together, these data corroborate the structural interactions seen in the 77ORF104•*Sa*DnaI^{AAA+} complex, demonstrating that both last five residues of the C-terminal tail of 77ORF104 and Tyr17 are critical for promoting the activity of the phage inhibitor. The results with the K39E mutant also corroborate our binding studies, which had shown that the 77ORF104-*Sa*DnaI interaction does not require nucleotide for stable association (**Figure 3.4B**).

77ORF104 blocks DnaI self-assembly by two mechanisms

Having validated the importance of the observed contacts manifest in the structure of the *Sa*DnaI^{AAA+}•77ORF104 complex, we sought next to determine how peptide binding might interfere with specific loader functions. Most AAA+ ATPase systems follow a pattern whereby oligomeric interactions are supported by inter-ATPase domain contacts between the active site of one subunit and a catalytically important basic amino acid (the arginine finger) of another. In the case of ORF104, the peptide binds to the nucleotide binding face of *Sa*DnaI; superposition of the AAA+ domain of one subunit from an *Aquifex aeolicus* DnaC dimer onto the AAA+ domain of *Sa*DnaI in our complex shows that the 77ORF104 peptide occupies the same location as that of the neighboring protomer (**Figure 3.11**) This arrangement indicates that the phage inhibitor blocks *Sa*DnaI activity by sterically blocking loader self-assembly.

Within AAA+ ATPases, one specialized feature that phylogenetically distinguishes helicase loaders such as DnaI and bacterial replication initiator proteins from other superfamily members is the existence of an extra α-helix that is inserted into one edge of the core AAA+ fold (Iyer et. al., 2004). This element, which is termed the **I**nitiator/loader-**S**pecific **M**otif (ISM) (Dueber et al., 2007), has been shown to be important for self-assembly and function in bacterial helicase loaders and initiators (Duderstadt et al., 2011; Mott et al., 2008). In nucleotide-oligomerized DnaA and DnaC structures, the ISM introduces a significant out-of-plane displacement of adjacent ATPase folds, and appears responsible for pushing these assemblies into a helical, as opposed to closed-ring, formation. As anticipated, based on structures of its closest homologs, the ISM of ORF104-bound *Sa*DnaI^{AAA+} forms a V-shaped projection from the central ATPase domain. Inspection of this region, however, indicated that one of the α-helices of the *Sa*DnaI ISM was sharply bent compared to other helicase loaders, such as that of *Aquifex aeolicus* DnaC^{AAA+} (*Aq*DnaC^{AAA+}), *Streptococcus pyogenes* DnaI^{AAA+} (*Spyo*DnaI^{AAA+}) and *Geobacillus kaustophilus* DnaI^{AAA+} (*Gka*DnaI^{AAA+}) (**Figure 3.12B**).

To determine whether the conformational change seen in *Sa*DnaI corresponded to a natural state of *S. aureus* protein, or resulted from peptide binding, we crystallized and determined the structure of the *Sa*DnaI AAA+ domain in absence of peptide (**Figure 3.12A**). Structural alignment of the "apo" and peptide-bound *Sa*DnaI^{AAA+} models shows that the inhibitor free ISM is straight, as in other helicase loader structures. This result indicates that the conformation change visualized for the ISM is a consequence of ORF104 binding, rather than a favored state of the *Sa*DnaI protein alone (**Figure 3.12**). This finding indicates that, in addition sterically blocking partner protein binding, ORF104 remodels a critical self-assembly element in DnaI to further block loader self-association.

77ORF104 does not disrupt *Sa*DnaI loader-helicase interactions

Given that the N-terminal domain of DnaI type proteins contains the portion of the loader known to bind the replicative helicase, we reasoned that the ORF104 inhibitor might not disrupt the ability of DnaI to associate with its cognate target, DnaC (*Sa*DnaC, a DnaB-family helicase not to be confused with the *E. coli* DnaI homolog and helicase loader, *Ec*DnaC). To test this idea, we performed pulldown experiments using His_6MBP-tagged ORF104 as bait to bind either untagged *Sa*DnaI or *Sa*DnaC-bound-*Sa*DnaI as prey (**Figure 3.13**). Analysis of reactions by SDS-PAGE revealed that 77ORF104 bound to both free and *Sa*DnaC-bound *Sa*DnaI equally well. By contrast, 77ORF104 did not bind to the *Sa*DnaC helicase alone (**Figure 3.13**). Overall, this result is consistent with a model in which 77ORF104 inhibits *Sa*DnaI function by preventing loader self-assembly, rather than by blocking loader/helicase associations.

77ORF104 inhibits ssDNA-stimulated ATP hydrolysis by *Sa*DnaI

If 77ORF104 targets the ability of *Sa*DnaI to self-associate, as opposed to an interaction with the host helicase, then the peptide should be expected to affect functions of DnaI that rely on loader-loader contacts. Self-oligomerization of helicase loaders has previously been shown to be required for single-stranded DNA binding (ssDNA)(Biswas et al., 2004; Mott et al., 2008), an event that in turn stimulates ATP hydrolysis directly in Gram-positive homologs such as that of *Bacillus subtilis* DnaI (Ioannou, C & Soultanas, P et. al. 2006). To test whether ORF104 would impact such a function, we carried out radioactive ATP hydrolysis assays using [γ-^{32}P]-ATP and M13-ssDNA. Although *Sa*DnaI was found to exhibit relatively modest ATPase activity on its own, the presence of M13-ssDNA significantly stimulated nucleotide turnover (**Figure 3.14A**). By contrast, when incubated with the ORF104 product from phage 77, the observed stimulation of ATP hydrolysis by ssDNA was much reduced (**Figure 3.14A**). To establish that the ATPase activity we observed was derived from DnaI and not from a potentially contaminating ATPase, we cloned, expressed and purified several active site mutants of DnaI. Both a Walker A mutant (K170A) and arginine finger mutant (R288A) showed greatly reduced ATP hydrolysis activity in the presence of ssDNA, indicating that the activity seen in our assays was indeed specific to DnaI (**Figure 3.14B**). Collective, these data further support a model in which 77ORF104 inhibits DnaI by blocking loader self-assembly and preventing proper ATPase function.

Evidence for a phage-encoded hijacking mechanism that targets the host helicase

Having established how the phage 77 ORF104 protein inhibits the host helicase loader, we next sought to gain insights into as to how the phage manages to replicate its own genome. Interestingly, within the phage 77 genome, the gene next to ORF104, termed ORF013, is annotated as an AAA+ ATPase. These two genes are located in the same operon in the phage chromosome, suggesting that they might be expressed contemporaneously and function synergistically. To determine the protein family to which 77ORF013 belongs, searched the database for homologous proteins of known function. Surprisingly, this analysis revealed that the ORF013 gene encodes a putative DnaC/DnaI-type helicase loader (**Figure 3.15A**), raising the possibility that the ORF013 protein might bind to host helicase directly. To test this idea, we cloned, expressed and purified a His_6MBP-tagged version of ORF013 and performed amylose pulldown experiments using untagged *Sa*DnaC replicative helicase as prey (**Figure 3.15B**). SDS-PAGE analysis of different pull-down fractions showed that prospective phage loader was indeed capable of binding the *Sa*DnaC replicative helicase (control pulldowns using *Sa*DnaC showed little affinity of the helicase by itself for the amylose resin) (**Figure 3.15B**). Thus, the partner open reading frame shared by ORF104 appears to encode for a phage variant of a replicative helicase loader.

The finding that ORF013 of phage 77 is a helicase loader homolog raised the question as to whether the ORF104 peptide would bind to it as well as to the host *Sa*DnaI protein. To address this question, we performed pulldowns of the His_6MBP-tagged 77ORF104 peptide with both phage 77 ORF013 and a Gram-negative, DnaC-type helicase loader (from *E. coli*). As measured by anisotropy, ORF104 proved unable to interact with either *E. coli* DnaC or ORF013 (**Figure 3.16**), indicating that the association of the phage 77 ORF104 inhibitor peptide with DnaI is specific to the *S. aureus* helicase loader. Together, these findings indicate that the phage peptide's association with *Sa*DnaI is specifically optimized to bind to only the helicase loader of a host bacterium targeted by the virus.

Discussion

In the present study, we have set out to better understand not only the function of DnaI-family bacterial helicase loaders, but also how bacteriophage can interfere with helicase loader activity to block host DNA replication. We determined two crystal structures of the *Sa*DnaI loader in a nucleotide-free state and bound to both the ATP mimic ADP•BeF3 and a DnaI-binding protein from phage 77, ORF104 **(Fig. 3.7 & 3.12)**. The structures reveal that binding of the phage inhibitor not only remodels a region known to be critical for DnaI homo-oligomerization **(Fig. 3.12)**, the Initiator Specific Motif (ISM) (Duderstadt et al., 2011; Mott et al., 2008), but also sterically occludes a principle subunit-subunit interaction surface **(Fig. 3.11)**. Binding studies of the interaction between ORF104 and *Sa*DnaI show that productive association is not dependent on nucleotide binding **(Fig. 3.4)**, but instead requires the last five C-terminal residues of the phage inhibitor peptide and a particular tyrosine residue (Tyr17) of ORF104 found buried within the binding interface **(Fig. 3.10 & Fig. 3.11)**.

The observed structural changes and regions masked by ORF104 binding would be expected to prevent DnaI self-association. This prediction is borne out by ATPase assays showing that this activity – which requires DnaI-DnaI interactions for form a competent catalytic center – is repressed by the peptide **(Fig. 3.14)**. Interestingly, ORF104 was not found to disrupt the loader's association with the replicative helicase *Sa*DnaC **(Fig. 3.13)**. This result indicates that ORF104 can likely act at multiple stages during the DNA replication cycle where helicase-loading events are required, including both initiation and replication restart (Heller and Marians, 2005a, 2005b, 2006; Kornberg and Baker, T. A., 1992).

During the course of carrying out this work, we discovered that phage 77 encodes another protein, ORF013, which is homologous to other DnaC/DnaI family loaders **(Fig. 3.15)**. In binding studies, we found that this protein binds to the host's replicative helicase, *Sa*DnaC, but not to the inhibitory ORF104 peptide that is also produced by phage 77 **(Fig. 3.16 & 3.5)**. These observations suggest that the ORF013 and ORF104, which appear to both share a common operon, serve as a two-pronged mechanism by which host replication can be inhibited and a portion of the cell's replication machinery co-opted for promoting viral DNA duplication. Surveys of other *S. aureus* phage genomes, such as phages 80 and 80α, similarly reveals the existence of both helicase loader and ORF104 inhibitor homologs (Kwan et al., 2005; Liu et al., 2004; Tormo-Más et al., 2010), indicating that the ORF013/ORF104 system may be widespread among *staphylococcus aureus* phages. The strategy of hijacking a host replicative helicase for viral replication is also generally common, and has been seen before is diverge viruses such as phage λ, phage P2, Mu, and influenza (Kawaguchi and Nagata, 2007; Mallory et al., 1990; Odegrip et al., 2000). To date, however, the existence of an associated, co-expressed inhibited helicase-loading is a feature seen thus far only in phage 77 and its relatives.

A second unexpected finding obtained from this work is that ORF104 doesn't bind to any region of the DnaI ATPase domain, but rather overlaps with a observed binding site for a portion of the linker element that connects the loader's N- and C-terminal domains **(Fig. 3.17)**. Previous studies of *Bacillus subtilis* DnaI and the related *E. coli* DnaC protein have suggested that bacterial helicase loaders are auto-regulated in some manner, such that helicase binding and/or ssDNA binding are necessary to promote ATPase activity (Ioannou et al., 2006; Learn et al., 1997), a function that directly depends on loader self assembly (Mott et al., 2008). The studies reported here show that the inter-domain linker sits at a site where subunit-subunit contacts take place during loader co-association. This observation indicates that the linker likely serves as a switch that reports on relative status of the N- and C-terminal regions, repressing loader-loader interactions until the correct helicase and DNA targets are bound. In this regard, the ORF104 peptide appears to exploit this binding locus taking advantage of the linker binding pocket to inactivate the host loader, an activity that would allow the cellular replicative helicase to be re-routed to the phage-encoded loader to promote viral replication (**Figure 3.18**). This action, which occurs within a small hydrophobic pocket on the loader AAA+ ATPase domain, suggests that the linker-binding region of the DnaI AAA+ domain could serve as an attractive site for the development of chemical inhibitors to target helicase loading and DNA replication in bacteria. Future efforts will help test and establish these concepts further.

Materials and Methods

Cloning, Expression and Protein Purification

Staphylococcus aureus DnaI full-length, DnaI AAA+(136-306), DnaI NTD (1-117), and phage 77ORF104 constructs were cloned into a pET28b (Novagen) derivative with a tobacco etch virus (TEV) protease-cleavable, N-terminal hexahistidine-MBP tag. The coding DNA sequence was verified for all constructs (Elim Biopharmaceuticals). All proteins were expressed in BL21 codon+ cells from pET28b-derived plasmids by induction with 1 mM IPTG at 37 °C for 3 hours. Cells were harvested by centrifugation, resuspended in lysis buffer and lysed by sonication. Both *S. aureus* and phage proteins were purified by Ni2+-affinity chromatography over a 5-mL General Electric HisTrap HP column. Lysis buffer consisted of 500 mM NaCl, 20 mM imidazole, 50 mM HEPES-KOH pH 7.5, 10 mM MgCl2, 10% glycerol and protease inhibitors (1 mM phenylmethylsulfonyl fluoride (PMSF), 1 mg/mL Pepstatin A, and 1 mg/mL Leupeptin). After washing in binding buffer containing 1 M NaCl proteins were eluted with 500 mM imidazole in elution buffer containing 50 mM NaCl, 50 mM HEPES-KOH pH 7.5, 10 mM MgCl2, 10% glycerol and protease inhibitors (1 mM PMSF, 1 mg/mL Pepstatin A, and 1 mg/mL Leupeptin) over 5 column volumes. His6-MBP-tags were then removed with TEV protease added at a ratio of TEV:protein 1:40 and incubated at 4°C overnight. Proteins were then exchanged into binding buffer, repassaged over a HisTrap column, and finally run over a Sepharose S-200 gel filtration column (GE) in 500 mM NaCl, 50 mM HEPES-KOH pH 7.5, 10 mM MgCl2, 10% glycerol and protease inhibitors (1 mM PMSF, 1 mg/mL Pepstatin A, and 1 mg/mL Leupeptin). Selenomethione labeled proteins were purified by the same protocol with the exception that 0.5 mM TCEP added to all buffers. Protein purity was assessed by polyacrylamide gel electrophoresis and Coomassie staining. Protein concentration was determined by absorption at 280 nm using the following extinction coefficients: 23380 M^{-1} cm^{-1} for FL *Sa*DnaI, 72310 M^{-1} cm^{-1} for H_6MBP-77ORF104, 14440 M^{-1} cm^{-1} for *Sa*DnaI$^{AAA+(136-306)}$, 4470 M^{-1} cm^{-1} for 77ORF104 and 7450 M^{-1} cm^{-1} for *Sa*DnaI$^{NTD(1-117)}$ and 15930 M^{-1} cm^{-1} for *Sa*DnaI$^{CTD(117-306)}$. Mutant staphylococcus bacteriophage 77ORF104 and *S. aureus* DnaI proteins were generated using QuickChange (Stratagene) site-specific mutagenesis and sequenced by GeneWiz. *S. aureus* DnaI and phage 77ORF104 mutants were purified as described above.

Crystallization of an ADP•BeF_3-bound SaDnaI^{AAA+}•77ORF104 complex

To crystallize the ADP•BeF_3-bound *Sa*DnaI^{AAA+}•77ORF104 complex we expressed and purified both proteins individually. We expressed the *Sa*DnaI^{AAA+} protein in minimal media containing seleno-methionine. Once each protein was purified to high purity we then formed the *Sa*DnaI^{AAA+}•77ORF104 complex using a 2-fold excess of 77ORF104 to *Sa*DnaI^{AAA+} and purified the complex by running it over a

Sepharose S200 gel filtration column (GE) (**Figure 3.6**). The purified complex was then spiked with 2 mM ADP• BeF_3 prior to setting up hanging drop vapor diffusion experiments. Large rod-like crystals grew in the space group $P6_522$ and diffracted to 1.9 Å resolution. Sparse matrix screening was performed using the hanging-drop format to find initial hits. The *Sa*DnaI^{AAA+}•77ORF104 complex was purified by adding a 2-fold molar excess of 77ORF104 to *Sa*DnaI^{AAA+} and purified as a complex by running over a Sepharose S-200 gel filtration column (GE) in sizing buffer (500 mM NaCl, 50 mM HEPES-KOH pH 7.5, 10 mM $MgCl_2$, 10% glycerol, 0.5 mM TCEP and protease inhibitors). The s200 peak containing the complex was pooled and concentrated to 6.5 mg/ml at 4°C (**Figure 3.6**). Prior to crystallization, an ATP mimic was spiked into the sample at 2 mM ADP•BeF_3. Crystallization was performed by the hanging-drop vapor diffusion method by mixing 2 µL of protein complex in s200 sizing buffer with 2 µL well solution (50 mM Tris-HCl 8.5, 20 mM MgCl2, 20% Ethanol). Large rod crystals grew within 1-2 days at 21°C using protein at 6.5 mg/mL (**Figure 3.6**). Crystals were cryo-protected by serial exchange into a harvesting buffer containing (25% PEG 400, 50 mM HEPES 7.5, 500mM NaCl, 5 mM MgCl2, 10% Glycerol, 0.5 mM TCEP, 2 mM ADP•BeF_3) before being flash frozen in liquid nitrogen. Crystals were stored in liquid nitrogen prior to data collection.

Crystallization of 'apo' SaDnaI^{AAA+}

Sparse matrix screening was performed for 'apo' *S. aureus Sa*DnaI^{AAA+} as described above. *Sa*DnaI^{AAA+} was purified over a Sepharose S-200 gel filtration column (GE) in s200 sizing buffer (500 mM KCl, 50 mM HEPES-KOH pH 7.5, 10 mM $MgCl_2$, 10% glycerol, 0.5 mM TCEP and protease inhibitors). Final crystallization conditions for *Sa*DnaI^{AAA+} contained a well solution of 0.1 M citric acid, 10 mM $MgCl_2$, and 0.8 M ammonium sulfate at pH 4.0. The s200 peak containing *Sa*DnaI^{AAA+} was pooled, concentrated, and 2 mM ADP•BeF_3 was spiked into the sample prior to crystallization. Crystals were grown by hanging-drop in 24-well plates at 21°C using protein at 5.0 mg/mL. Crystals were cryo-protected by serial exchange into a harvesting buffer containing (25% glycerol, 0.1 M citric acid pH 4.0, 0.8 M ammonium sulfate, 50 mM HEPES-KOH pH 7.5, 10 mM $MgCl_2$, 10% glycerol, and 2 mM ADP•BeF_3) before flash frozen. Crystals were flash frozen and stored in liquid nitrogen prior to data collection.

Data Collection for ADP•BeF_3-SaDnaI^{AAA+}•77ORF104 and 'apo' SaDnaI^{AAA+}

Datasets for both the structures were collected at beamline X25 at the National Synchrotron Light Source (NSLS) in Brookhaven National Lab. For the The seleno-methionine SAD dataset for the *Sa*DnaI^{AAA+}•77ORF104 complex was collected at a wavelength of 0.979 Å and processed in XDS (Kabsch, 1988, 2010). The crystals belong to the space group $P6_522$ with unit cell dimensions a= 73.17 Å, b= 73.17 Å, and c=189.72

Å with a solvent content of approximately 39.8% (**Table 3.1**). One ADP•BeF_3-*Sa*DnaI^{AAA+}-77ORF104 complex was determined per asymmetric unit. Data collection parameters include: 0.3° oscillation, 0.15 second exposures on a Pilatus 6M detector. Selenium site positions for the SeMet-*Sa*DnaI^{AAA+} were determined using HySS (Hybrid Substructure Search) as part of the PHENIX package (Adams et al., 2010; Grosse-Kunstleve and Adams, 2003). Initial experimental electron density maps were generated from AutoSol (Terwilliger et al., 2009). The structure was solved by single wavelength anomalous dispersion. Refinement was performed in PHENIX and the final model stabilized at an R_{work}/R_{free} of 18.0%/21.8% for the resolution range of 47.76-1.9Å (Adams et al., 2010) (**3.1**). The final model contains residues (136-300) for DnaI and the residues (1—52) for the 77ORF104 peptide inhibitor with bonds and angles of 0.010 and 1.27, respectively.

The "apo" dataset was collected at a wavelength of 1.5 Å and processed in XDS (Kabsch, 1988, 2010). The crystals belong to the space group $P2_12_12_1$ with unit cell dimensions a= 113.09 Å, b= 126.26 Å, and c=183.34 Å with a solvent content of approximately 52.4% (**Table 3.2**). Twelve *Sa*DnaI^{AAA+} molecules were determined per asymmetric unit. Data collection parameters included: 0.3° oscillations and 0.3 second exposures on a Pilatus 6M detector. The structure was solved by Molecular Replacement using the program MR-Phaser in the PHENIX package (McCoy et al., 2007). Refinement was performed in PHENIX and the final model stabilized at an R_{work}/R_{free} of 23.36%/28.12% for the resolution range of 47.24-2.6Å (Adams et al., 2010) (**3.2**). The final model contains *Sa*DnaI^{AAA+} residues (136-306) with bonds and angles of 0.004 and 0.96, respectively.

Limited trypsin proteolysis of S. aureus DnaI in the presence of 77ORF104

Prior to incubation with trypsin both *Sa*DnaI and 77ORF104 proteins were dialyzed overnight into a reaction buffer containing 500 mM KCl, 50 mM HEPES-KOH pH 7.5, 10 mM $MgCl_2$ and 10% glycerol. *Sa*DnaI alone or *Sa*DnaI in the presence 0f the 77ORF104 peptide were incubated for 10 minutes prior to addition of trypsin. Trypsin protease was added to reaction resulting in the final concentrations: 5 μM, 10 μM, 20 μM and 80 μM. Proteins were incubated with trypsin protease for 30 minutes at 25°C. Reactions were quenched with 200 nM PMSF. After addition of an equal volume of 2X SDS loading dye, reactions were heated at 95°C for 5 minutes before running 15 μl of each reaction on a 15% polyacrylamide gel (29:1). Protein bands were stained with coomassie blue.

Amylose pull-downs

Amylose pull-downs were performed using H_6MBP-tagged proteins and untagged proteins in a total volume of 200 µl. All H_6MBP-tagged proteins were dialyzed into the 1X binding buffer containing (20 mM HEPES-KOH pH 7.5, 100 mM NaCl, 5 mM $MgCl_2$, 10% glycerol, and 1 mM DTT) at 4°C prior to setting up the protein binding reaction. H_6MBP-tagged proteins were incubated with their untagged protein for 10 minutes at 25°C before addition of 50 µl amylose beads. After addition of the amylose beads, the binding reaction was incubated for 20 minutes at 25°C. Reactions were gently mixed every 2 minutes during the 20 minute incubation. Amylose binding reactions were spun down at 1500 RPM for 1 minute. The amylose beads were washed twice prior to either elution with maltose elution buffer containing (40 mM maltose, 20 mM HEPES-KOH pH 7.5, 100 mM NaCl, 5 mM $MgCl_2$, 10% glycerol, and 1 mM DTT) or addition of 2X SDS loading dye. Amylose pull-down inputs, washes, elution and beads samples were run on a 12% SDS-PAGE gel. SDS-PAGE gels were stained for 30 minutes with SYPRO Orange stain diluted to 1X in 10% glacial acetic acid. Gels were washed with dIH_20 three times before imaging the gels on a Kodak Gel Imager.

N-terminal labeling of 77ORF104

Purified wild-type 77ORF104 peptide was exchanged into amine-labeling buffer (50 mM HEPES-KOH pH 7.5, 500 mM KCl, 10% Glycerol, 10 mM MgCl2, 1 mM BME) by centrifugation. The neutral pH favors labeling of the amino terminus of proteins rather than surface lysines (Sélo et al., 1996). The protein was concentration to a final volume of 500 µl (final concentration 342µM). AlexaFluor 488 5-SDP (sulfodicholorphenol) ester (Life Technologies) (1 mg) was dissolved into µl DMSO. The dye was added to the concentrated protein [342µM] and the reaction was incubated at 4°C, wrapped in aluminum foil while rocking, for 1 hour. Unreacted dye was quenched by adding 20 µl of 1 M L-lysine in 20 mM Tris-HCl pH 7.5; reactions were incubated with the quench for 30 minutes at 25°C. Free dye was separated from dye-protein conjugates using a 10 mL PD-10 desalting column (GE) equilibrated in the amine-labeling buffer (see above). The labeled protein was then exchanged into a buffer containing 50 mM HEPES-KOH pH 7.5, 500 mM KCl, 30% Glycerol, 10 mM MgCl2, 1 mM beta-mercaptoethanol (BME) by centrifugation. The concentrated labeled 77ORF104 protein was aliquoted and snap frozen in liquid nitrogen, and stored at -80°C.

Anisotropy-based competition assays and protein-protein binding assays

Purified proteins were prepared in 2-fold dilutions steps in dilution buffer containing 50 mM HEPES-KOH pH 7.5, 500 mM KCl, 10% Glycerol and 10 mM MgCl2. N-terminally labeled wild-type 77ORF104 was diluted to 40 nM in a reaction buffer (50 mM HEPES-KOH pH 7.5, 10% Glycerol, 5 mM MgCl2, 1 mM DTT). For serial dilutions, purified proteins were sequentially diluted in 2-fold steps into protein dilution buffer. Proteins were mixed with N-terminally labeled 77ORF104 on ice and incubated for 10 minutes. The final reaction volume was 80µl containing the final buffer conditions (50 mM HEPES-KOH pH 7.5, 125 mM KCl, 10% Glycerol, 5 mM MgCl2, 1 mM DTT). The final concentration of labeled 77ORF104 in each reaction was 20 nM. Anisotropy measurements were recorded using CLARIOStar microplate reader (BMG LAB TECH) at 535 nm. All data points are the average of at least three independent measurements. For the 77ORF104 protein binding assays, data were plotted in GraphPad Prism Version 6 (GraphPad Prism Software, La Jolla California USA, www.graphpad.com) using the following single-site binding equation (Stein et al., 2001), by nonlinear regression,

Equation 3.1

$$\Delta\mathrm{FA} = \left[(\Delta FA_{\max} + [P_t] + K_{D,app}) - \sqrt{(\Delta\mathrm{FA}_{\max} + [P_t] + K_{D,app})^2 - 4 \times [P_t] \times \Delta FA_{max}} \right] \div 2$$

where ΔFA represents the signal at 100% ligand binding, and $[P_t]$ is the total protein concentration.

For the 77ORF104 competition experiments, reactions were prepared as previously described with the following changes. The reaction mixture contained 20 nM labeled 77ORF104 and 2µM *Sa*DnaI^{AAA+}. Wild-type 77ORF104 and peptide mutants were serially diluted (as described above) in the same dilution buffer and final buffer solution. Assays were performed as described above for the 77ORF104 mutants. Anisotropy measurements were recorded using CLARIOStar microplate reader (BMG LAB TECH). All data points represent the average of at least three independent measurements. Data points were graphed in GraphPad Prism Version 6 using the competitive binding equation between two ligands as described by Wang (Wang, 1995).

Radioactive ATP hydrolysis assays using [γ^{32}P]ATP and M13mp18 ssDNA

ATPase assays were in 30 µl of reaction buffer containing: 10 nM 4500 Ci/mmol [γ^{32}P]ATP, 100µM cold ATP, 100 mM KCl, 50 mM HEPES-KOH pH 7.5, 10 mM $MgCl_2$, 10% Glycerol and M13mp18 ssDNA (acquired from New England Biolabs, Inc.) added at a final concentration of 80 ng/uL. The 77ORF104 or *Sa*DnaI mutant proteins were added to the reactions on ice and the tubes were shifted to 37°C. After reactions were incubated for 2 hours, 3 µl was removed from the reaction and quenched by the addition of 250 mM EDTA pH 8.0 and 1% SDS (3 µl). Quenched reactions were spotted (1 µl) onto thin-layer chromatography sheets coated with polyethyleneimine cellulose (PEI-Cellulose F; EM Science) and developed in 0.4 M potassium phosphate pH 3.4 for 30 minutes. [γ^{32}P]ATP and free phosphate [γ^{32}P] migrated differently and were quantitated using a PhosphorImager and ImageJ software (Schneider et al., 2012) (U. S. National Institutes of Health, Bethesda, Maryland, USA).

Tables

Table 3.1. Data collection, phasing and refinement statistics for ADP•BeF_3-*Sa*DnaI^{AAA+}•77ORF104 complex.

Data Collection	**ADP•BeF_3-bound *Sa*DnaI^{AAA+}•77ORF104**
Wavelength (Å)	0.979
Resolution range (Å)	44.76 - 1.9 (1.968 - 1.9)
Space group	P 6_5 2 2
Unit cell dimensions a, b, c (Å), α, β, γ	73.173, 73.173, 189.727, 90°, 90°, 120°
Unique reflections	24589 (2390)
Multiplicity	2.0 (2.0)
Completeness (%)	100.00 (100.00)
Mean I/σ (I)	14.82 (1.44)
Wilson B-factor	26.6
R-merge	0.04771 (0.5436)
R-meas	0.06747
CC1/2	0.999 (0.693)
CC*	1 (0.905)
Phasing # of sites FOM[b]	 4 Se 0.90 (0.54)
Refinement R-work[c] / R-free	 0.1801 (0.3575) / 0.2183 (0.4071)
Number of non-hydrogen atoms	2020
macromolecules	1779
ligands	32
water	209
Protein residues	223
RMS(bonds)	0.010
RMS(angles)	1.27
Ramachandran favored (%)	99
Ramachandran outliers (%)	0
Clashscore	1.67
Average B-factor	31.40
macromolecules	30.40
ligands	34.90
solvent	39.80

a Numbers in parentheses refer to highest resolution shell.

b $\mathrm{FOM} = \int_0^{2\pi} P(\alpha)\, e^{i\alpha}\, d\alpha \Big/ \int_0^{2\pi} P(\alpha)\, d\alpha$ where $P(\ <\ )$ is the probability that the phage angle $<$ is corret

c $\mathrm{Rwork} = \sum \| \mathrm{Fobs} \| - | \mathrm{Fcalc} \| \Big/ \sum | \mathrm{Fobs} |$ where Fobs and Fcalc are observed and model structure factors, respectively.

*Table 3.2. Data collection and refinement statistics for "apo" SaDnaI^{AAA+}.

Data Collection	**"apo" *Sa*DnaI^{AAA+}**
Wavelength (Å)	1.5
Resolution range (Å)	47.24 - 2.6 (2.23 - 2.153)
Space group	P $2_12_12_1$
Unit cell dimensions a, b, c (Å), α, β, γ	113.09, 126.26, 183.34, 90°, 90°, 90°
Unique reflections	138458 (11644)
Multiplicity	2.0 (2.0)
Completeness (%)	97.38 (82.58)
Mean I/σ (I)	6.63 (-0.08)
Wilson B-factor	15.74
R-merge	0.06865
R-meas	0.09708
CC1/2	0.996 (-0.686)
CC*	0.999 (-0.384)
Refinement R-work[c] /R-free	0.2335(0.5840) /0.2812 (0.5900)
Number of non-hydrogen atoms	15,733
macromolecules	15,553
ligands	125
water	55
Protein residues	1980
RMS(bonds)	0.004
RMS(angles)	0.96
Ramachandran favored (%)	94.0
Ramachandran outliers (%)	2.4
Clashscore	2.4
Average B-factor	69.30
macromolecules	68.90
ligands	116.10
solvent	52.4

*Note: Table 3.2 for "apo" structure is preliminary (refinement in progress).

Figures

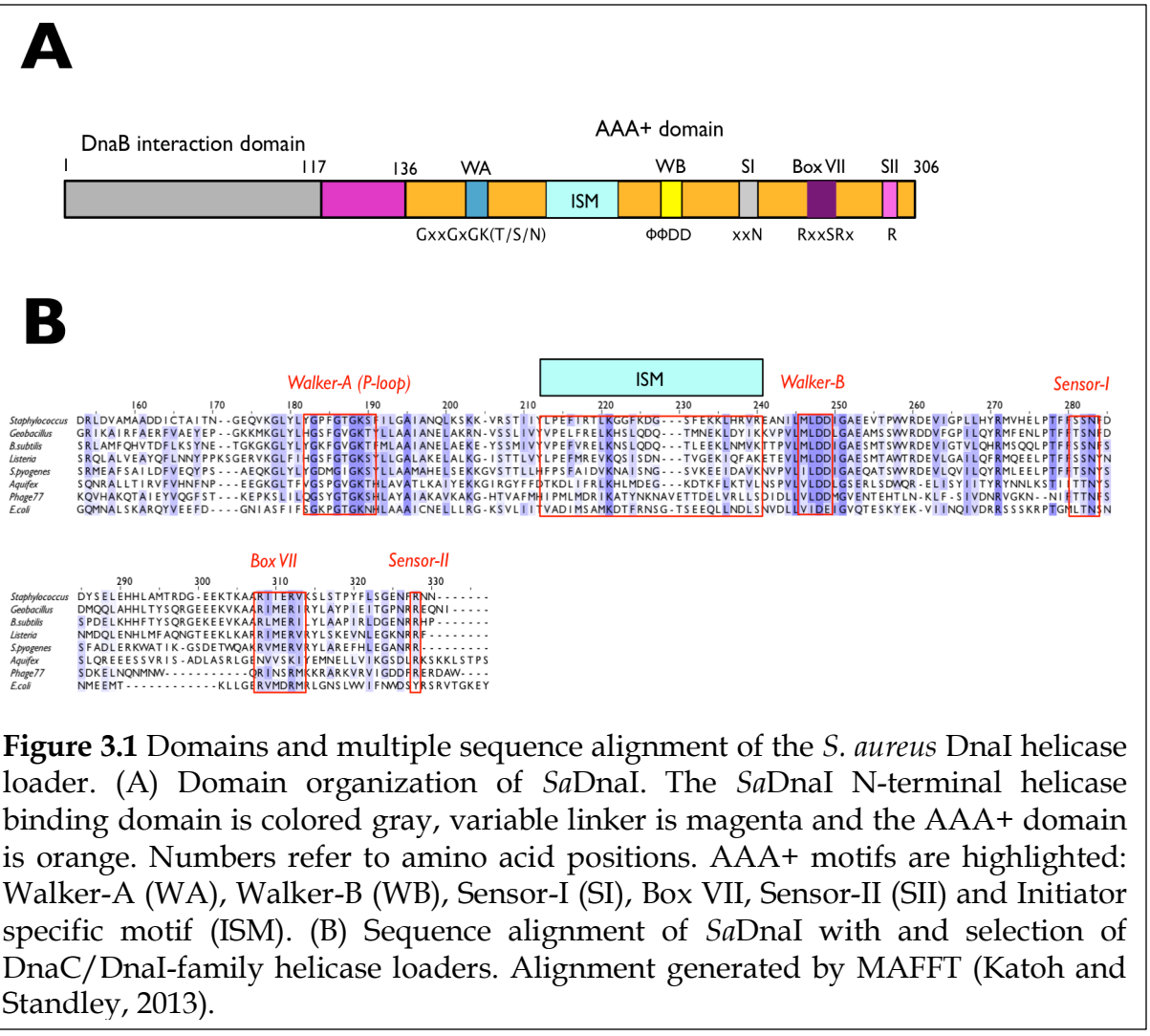

Figure 3.1 Domains and multiple sequence alignment of the *S. aureus* DnaI helicase loader. (A) Domain organization of *Sa*DnaI. The *Sa*DnaI N-terminal helicase binding domain is colored gray, variable linker is magenta and the AAA+ domain is orange. Numbers refer to amino acid positions. AAA+ motifs are highlighted: Walker-A (WA), Walker-B (WB), Sensor-I (SI), Box VII, Sensor-II (SII) and Initiator specific motif (ISM). (B) Sequence alignment of *Sa*DnaI with and selection of DnaC/DnaI-family helicase loaders. Alignment generated by MAFFT (Katoh and Standley, 2013).

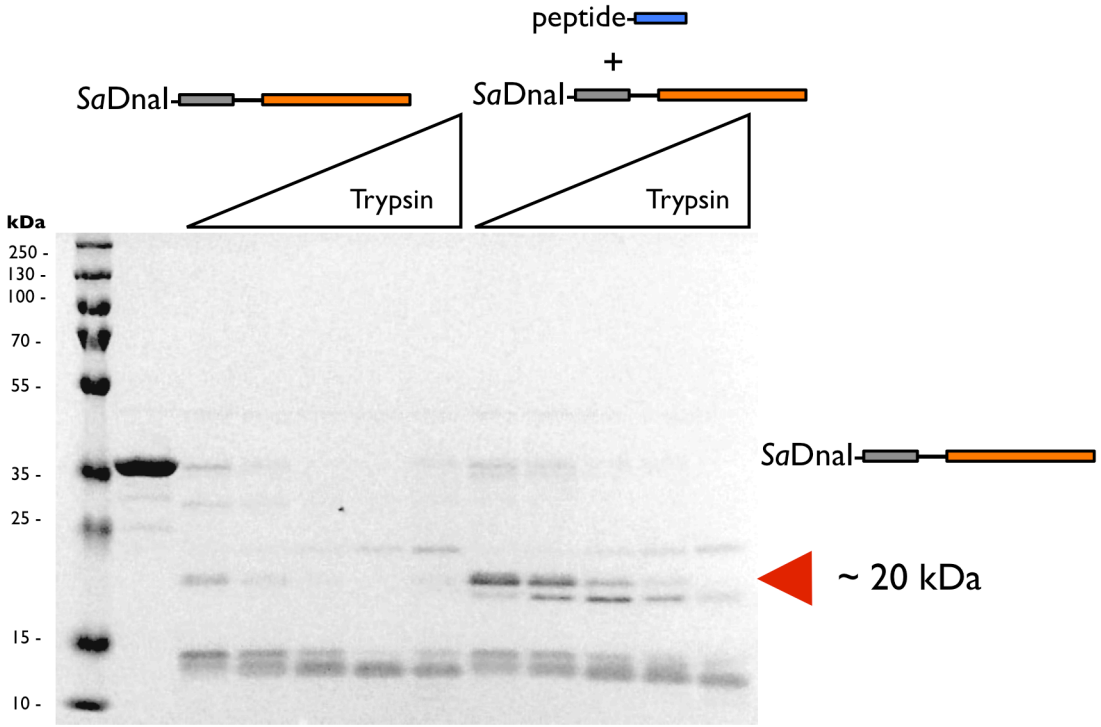

Figure 3.2. Limited trypsin proteolysis of full-length *Sa*DnaI in the presence of 77ORF104. Protein reactions were run on a 15% acrylamide:bis-acrylamide (29:1) SDS-PAGE gel. In the presence of 77ORF104 an approximately 20kDa band of *Sa*DnaI is stabilized.

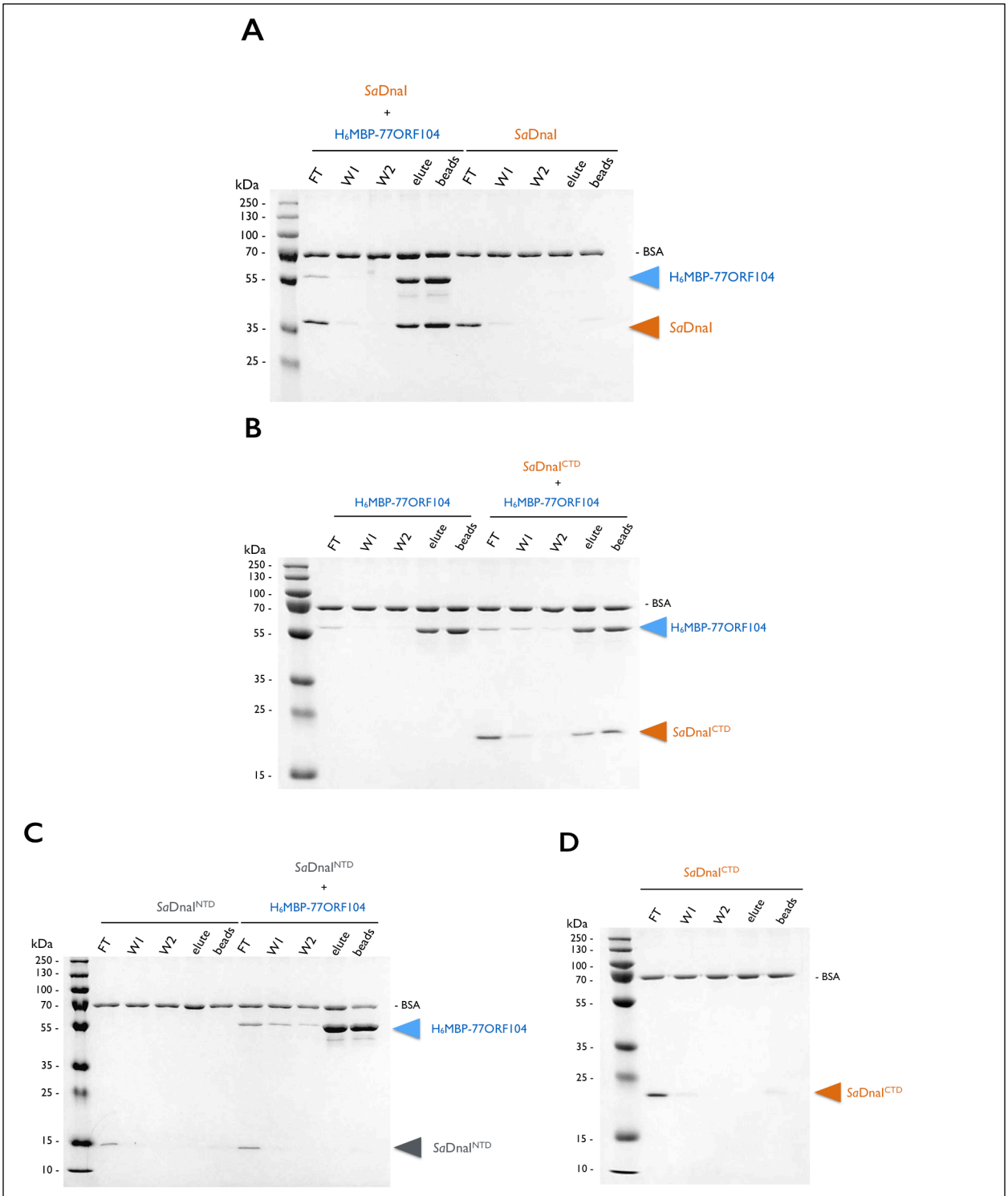

Figure 3.3. 77ORF104 interacts with the C-terminal AAA+ domain of *Sa*DnaI. SDS-PAGE analysis of amylose pull-downs between His_6MBP-77ORF104 and (A) *Sa*DnaI full-length, (B) SaDnaI^{NTD} and (C) *Sa*DnaI^{CTD}. *Sa*DnaI^{CTD} alone control is shown in (D). His_6MBP-77ORF104 associates with *Sa*DnaI full-length and *Sa*DnaI^{CTD}, but not *Sa*DnaI^{NTD}.

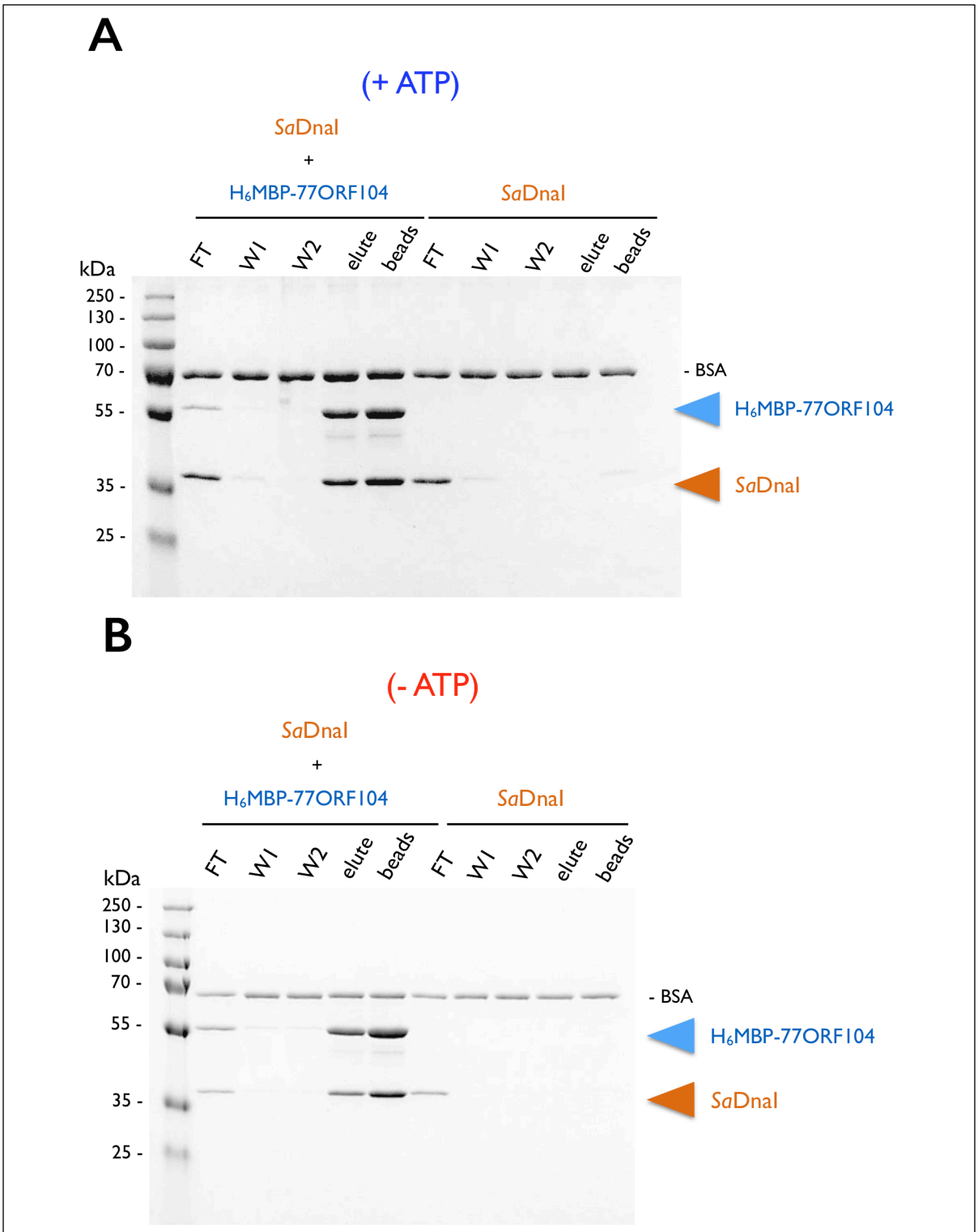

Figure 3.4. 77ORF104 associates with *Sa*DnaI in a nucleotide-independent manner. (A) Amylose pulldown of *Sa*DnaI with H_6MBP-77ORF104 in the presence of ATP. DnaI alone control is shown. (B) Amylose pulldown of *Sa*DnaI with H_6MBP-77ORF104 in the absence of ATP.

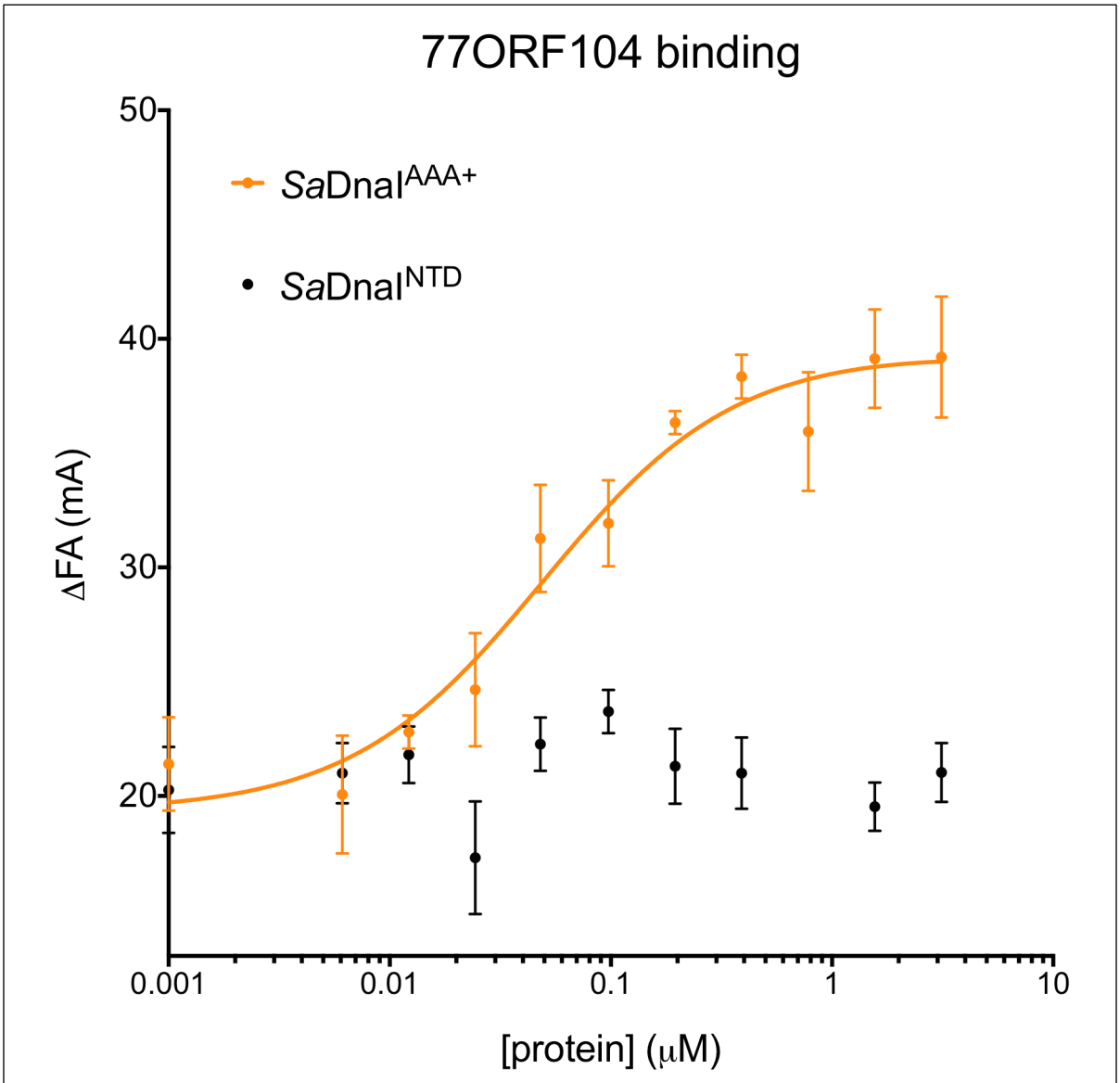

Figure 3.5. Binding to phage 77, ORF104 peptide to *Sa*DnaI^{AAA+}, *Sa*DnaI^{NTD}, as measured by a change in fluorescence anisotropy (ΔFA, milli-anisotropy units). The X-axis represents the concentration of each protein. Data points and error bars derive from three-independent experiments. No measurable binding was observed for *Sa*DnaI^{NTD}.

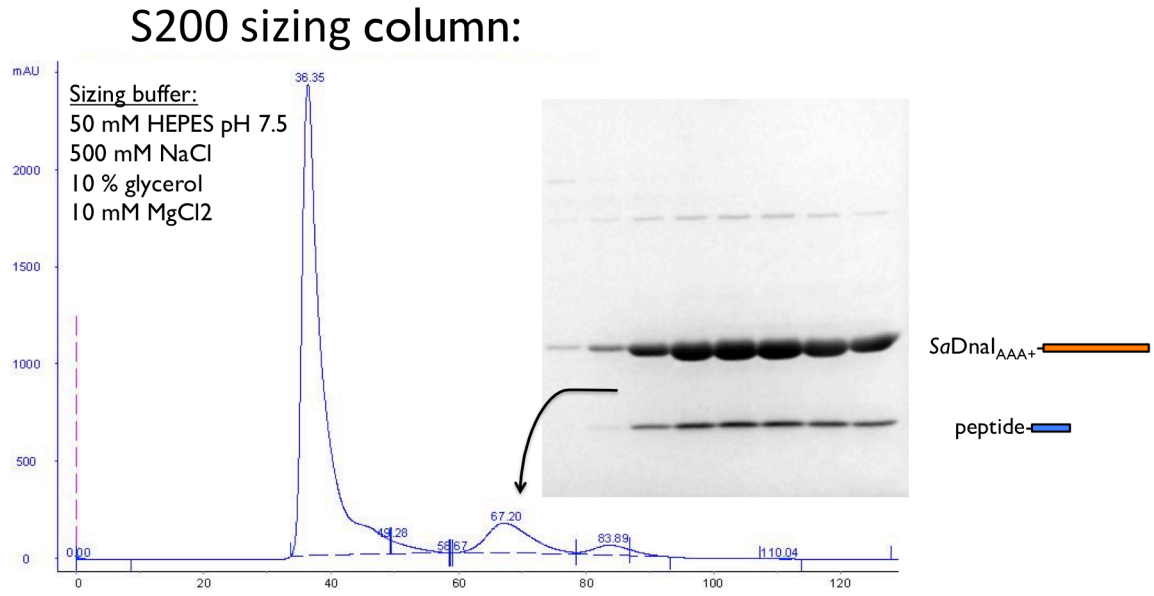

Figure 3.6. Purification of SeMet-*Sa*DnaI^{AAA+}•77ORF104 complex by size exclusion chromatography. Sizing trace and SDS-PAGE gel of peak fractions containing the SeMet-*Sa*DnaI^{AAA+}•77ORF104 complex.

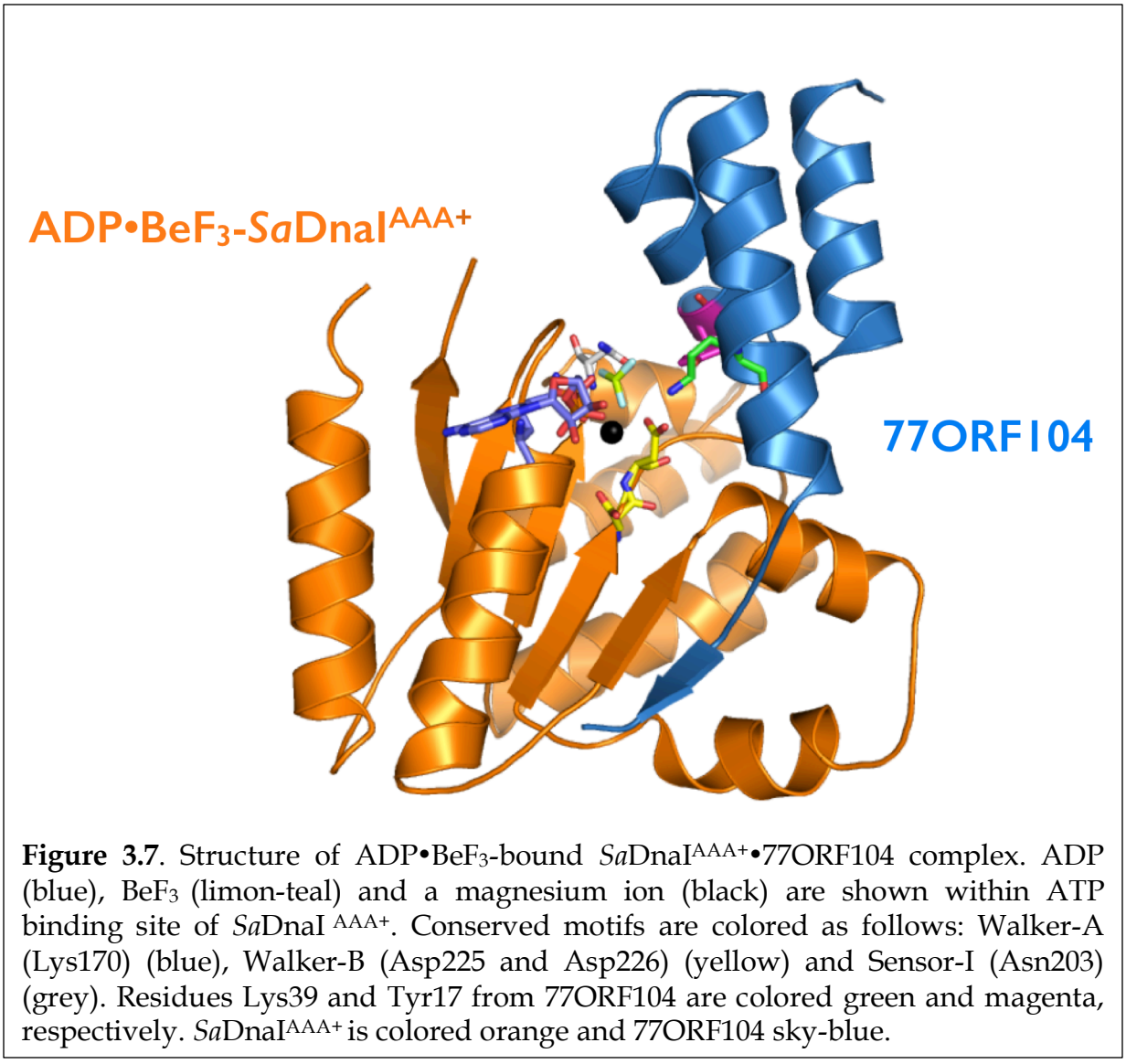

Figure 3.7. Structure of ADP•BeF_3-bound *Sa*DnaI^{AAA+}•77ORF104 complex. ADP (blue), BeF_3 (limon-teal) and a magnesium ion (black) are shown within ATP binding site of *Sa*DnaI $^{AAA+}$. Conserved motifs are colored as follows: Walker-A (Lys170) (blue), Walker-B (Asp225 and Asp226) (yellow) and Sensor-I (Asn203) (grey). Residues Lys39 and Tyr17 from 77ORF104 are colored green and magenta, respectively. *Sa*DnaI^{AAA+} is colored orange and 77ORF104 sky-blue.

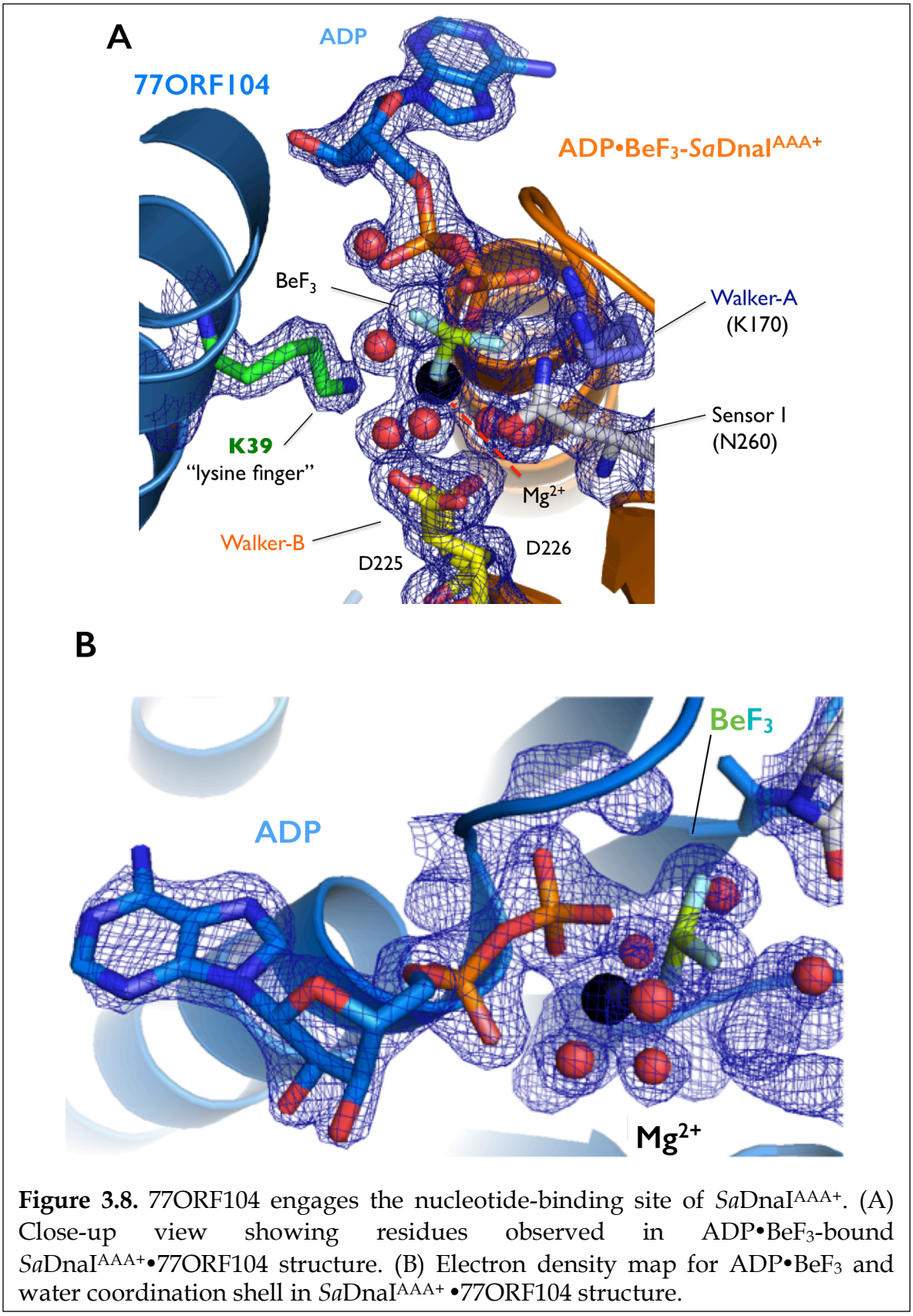

Figure 3.8. 77ORF104 engages the nucleotide-binding site of *Sa*DnaI^{AAA+}. (A) Close-up view showing residues observed in ADP•BeF_3-bound *Sa*DnaI^{AAA+}•77ORF104 structure. (B) Electron density map for ADP•BeF_3 and water coordination shell in *Sa*DnaI^{AAA+} •77ORF104 structure.

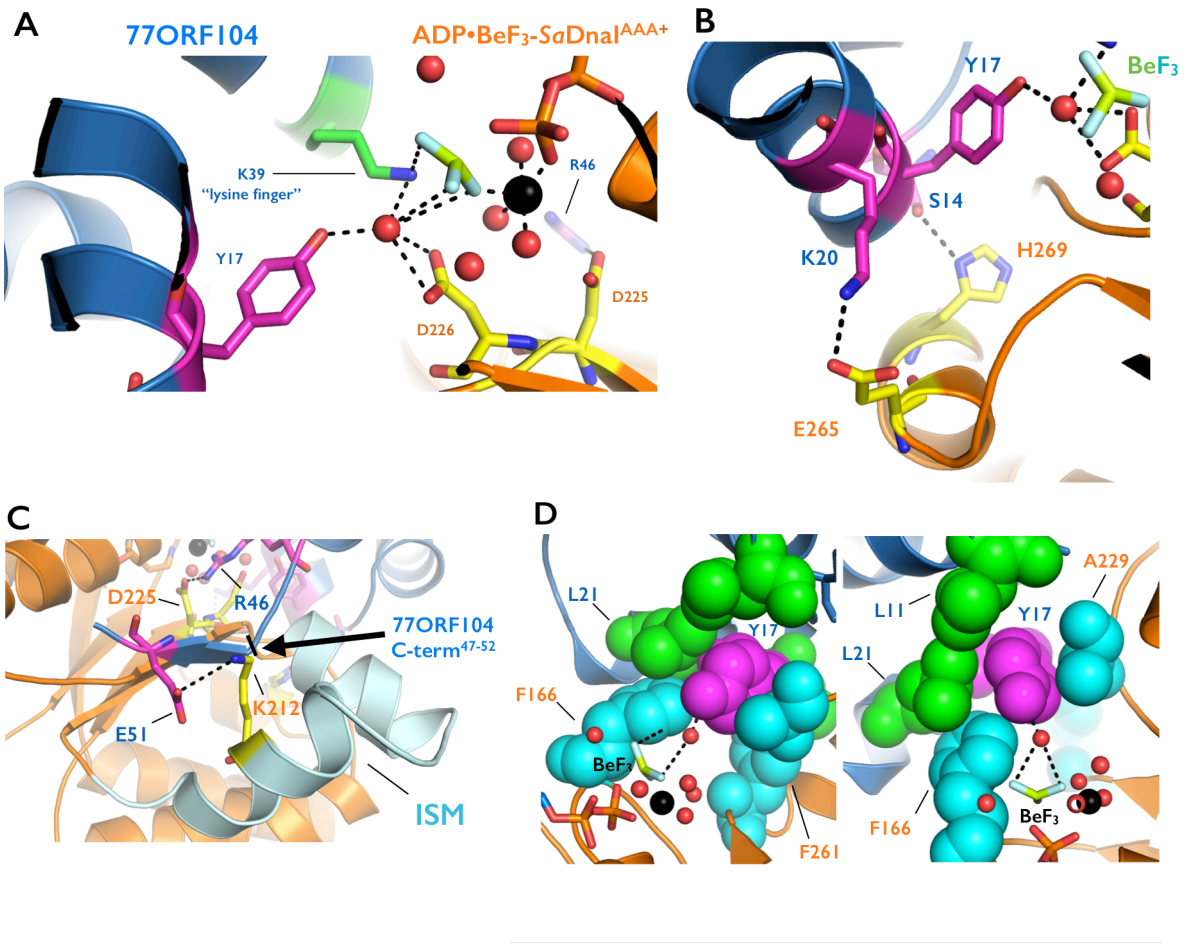

Figure 3.9. *Sa*DnaI^{AAA+}•77ORF104 contacts. The peptide engages bound nucleotide using residues: Y17 (magenta) and K39 (green). (A-C) Several electrostatic and polar contacts are observed within the binding interface between 77ORF104 and *Sa*DnaI^{AAA+}, respectively: lys20 with E265, R46 and D225, S14 and H265, and E21 and K212. (D) Tyr17 in 77ORF104 makes several hydrophobic contacts with *Sa*DnaI^{AAA+} residues (F166, F261, A229) and packs against two leucines within 77ORF104 (L21 and L11). Several views of the binding interface are shown for perspective. Residues belonging to *Sa*DnaI^{AAA+} and 77ORF104 are colored orange and sky-blue, respectively.

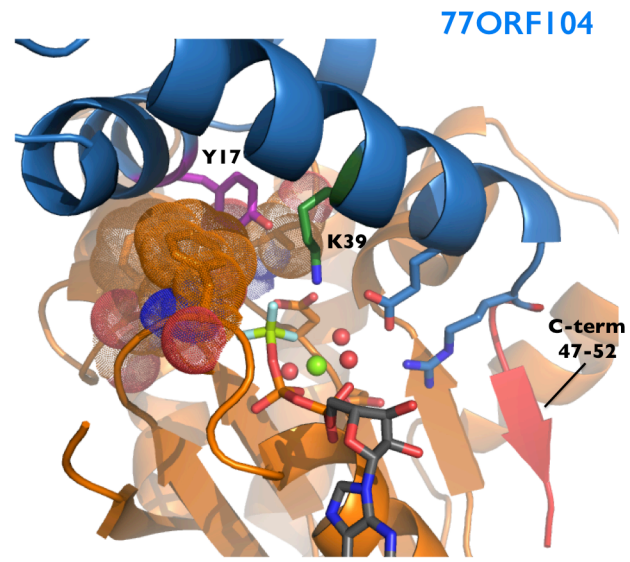

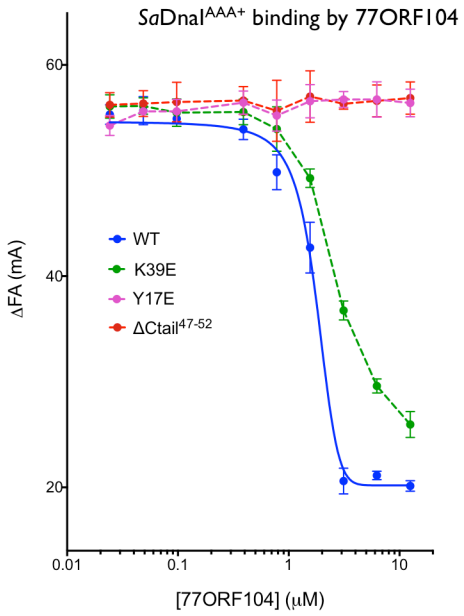

Figure 3.10. Analysis of 77ORF104 residues required for binding to *Sa*DnaI. (A) Close-up view showing prospective binding hotspot residues observed in ADP•BeF_3-*Sa*DnaI^{AAA+}•77ORF104 structure. (B) Binding assay showing the ability of different 77ORF104 mutants to compete away wild-type N-terminally labeled 77ORF104 peptide from interacting with *Sa*DnaI^{AAA+}. Competition is evident by a decrease in fluorescence anisotropy (ΔFA, milli-anisotropy units) as labeled protein is displaced by the unlabeled 77ORF104 competitor.

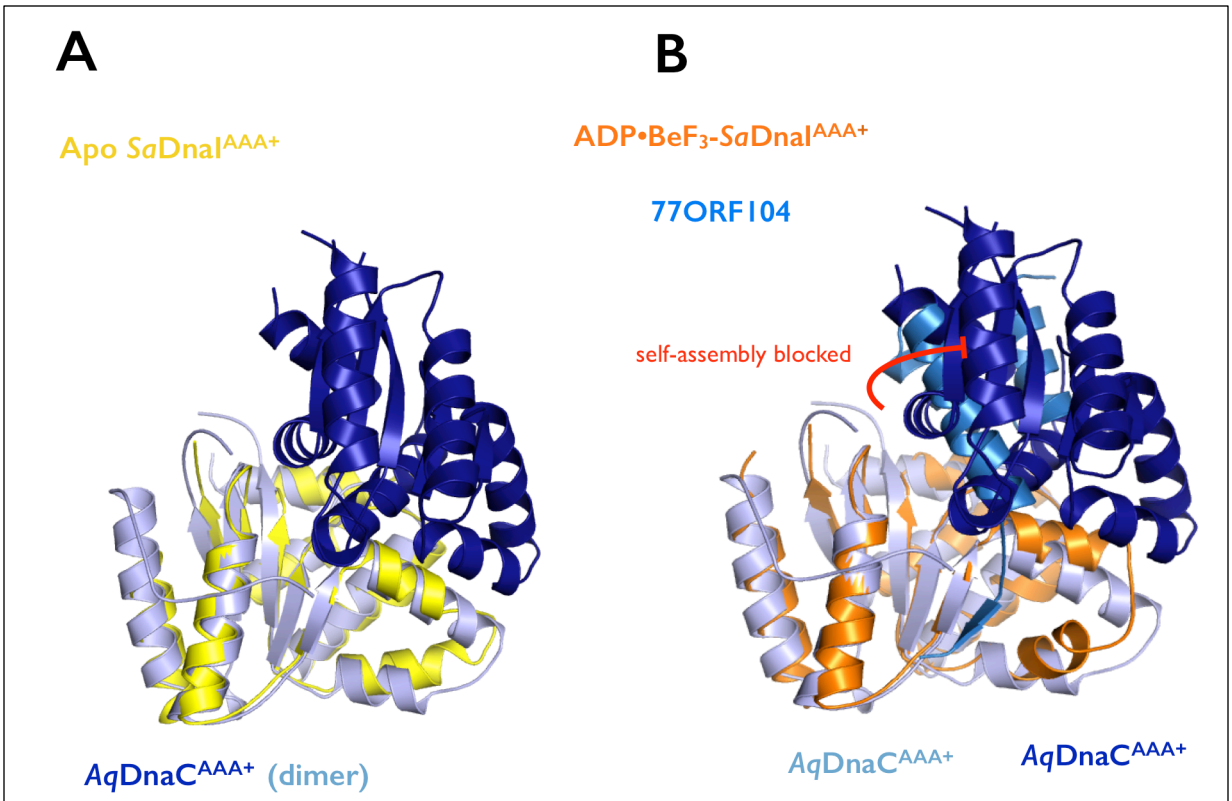

Figure 3.11. Physical consequences of 77ORF104 binding to *Sa*DnaI. *Aquifex aeolicus* DnaC^{AAA+} (*Aq*DnaC^{AAA+}) dimer aligned onto AAA+ domain from structures: (A) apo *Sa*DnaI^{AAA+} and (B) *Sa*DnaI^{AAA+}•77ORF104. A steric clash is observed in the *Sa*DnaI^{AAA+}• 77ORF104 structure between 77ORF104 and the modeled neighboring protomer of the *Aq*DnaC^{AAA+} dimer.

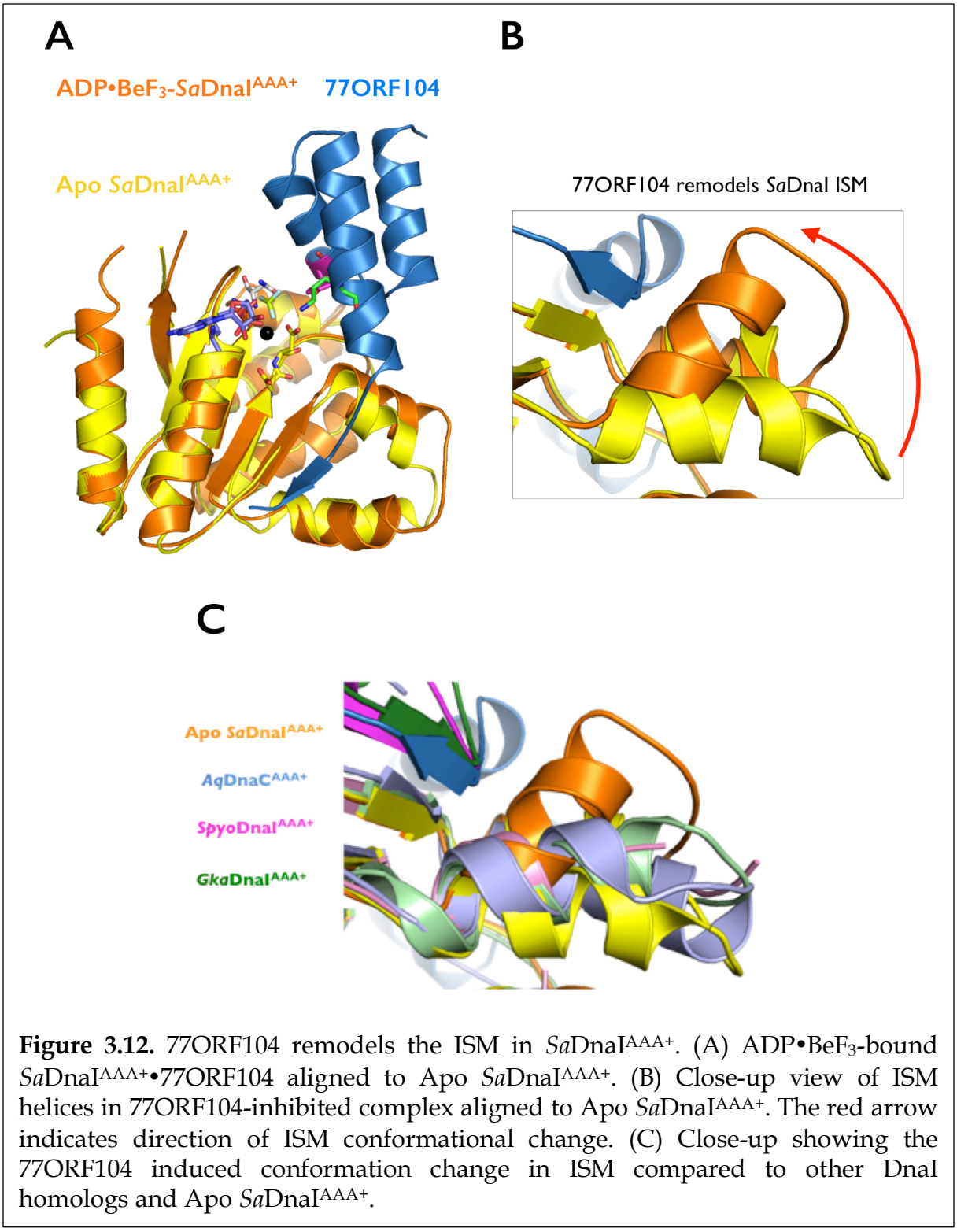

Figure 3.12. 77ORF104 remodels the ISM in *Sa*DnaI^{AAA+}. (A) ADP•BeF_3-bound *Sa*DnaI^{AAA+}•77ORF104 aligned to Apo *Sa*DnaI^{AAA+}. (B) Close-up view of ISM helices in 77ORF104-inhibited complex aligned to Apo *Sa*DnaI^{AAA+}. The red arrow indicates direction of ISM conformational change. (C) Close-up showing the 77ORF104 induced conformation change in ISM compared to other DnaI homologs and Apo *Sa*DnaI^{AAA+}.

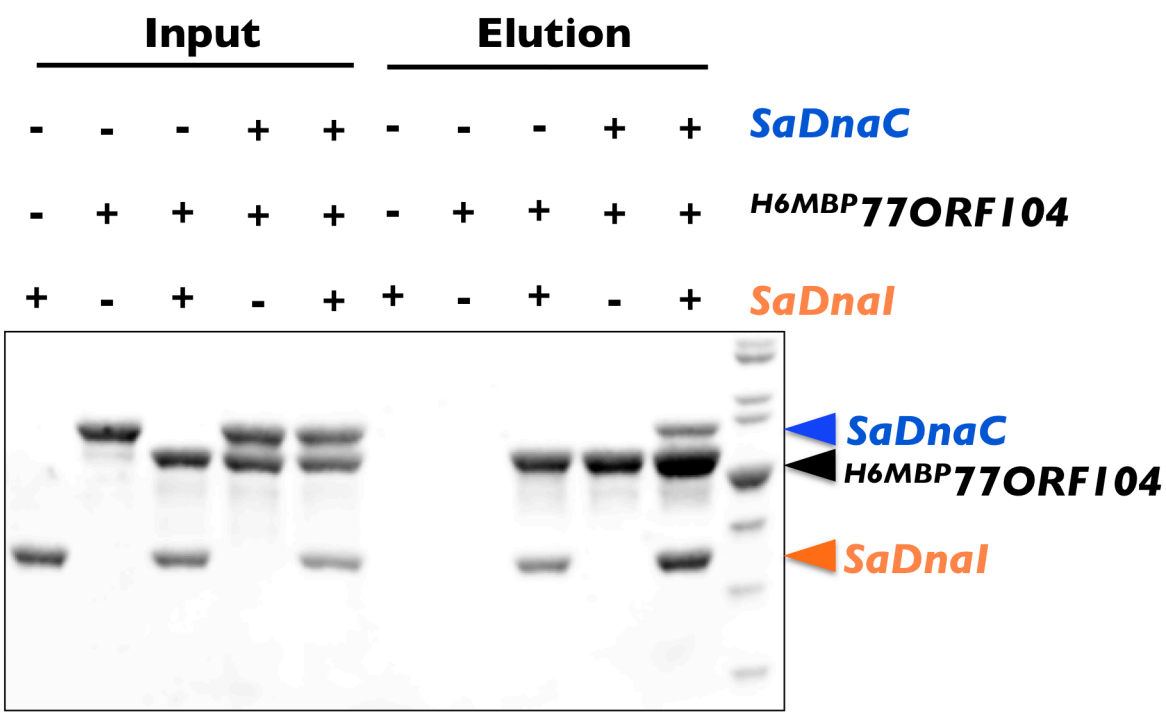

Figure 3.13. 77ORF104 associates with *Sa*DnaI when the helicase loader is bound to the host *Sa*DnaC helicase. SDS-PAGE gel of amylose pull-down experiments using purified His_6MBP-tagged 77ORF104, *Sa*DnaI, and the *Sa*DnaC replicative helicase. The positions of each protein are indicated on the right. Inputs are shown on the left. His_6MBP-tagged 77ORF104 co-precipitates with *Sa*DnaI alone and *Sa*DnaI bound to *Sa*DnaC replicative helicase, but not the *Sa*DnaC helicase alone. Pull-down experiments were performed in the absence of nucleotide. Performing the experiment in the presence of nucleotide generated the same result (not shown), indicating nucleotide is not required for association between the proteins *Sa*DnaI and *Sa*DnaC.

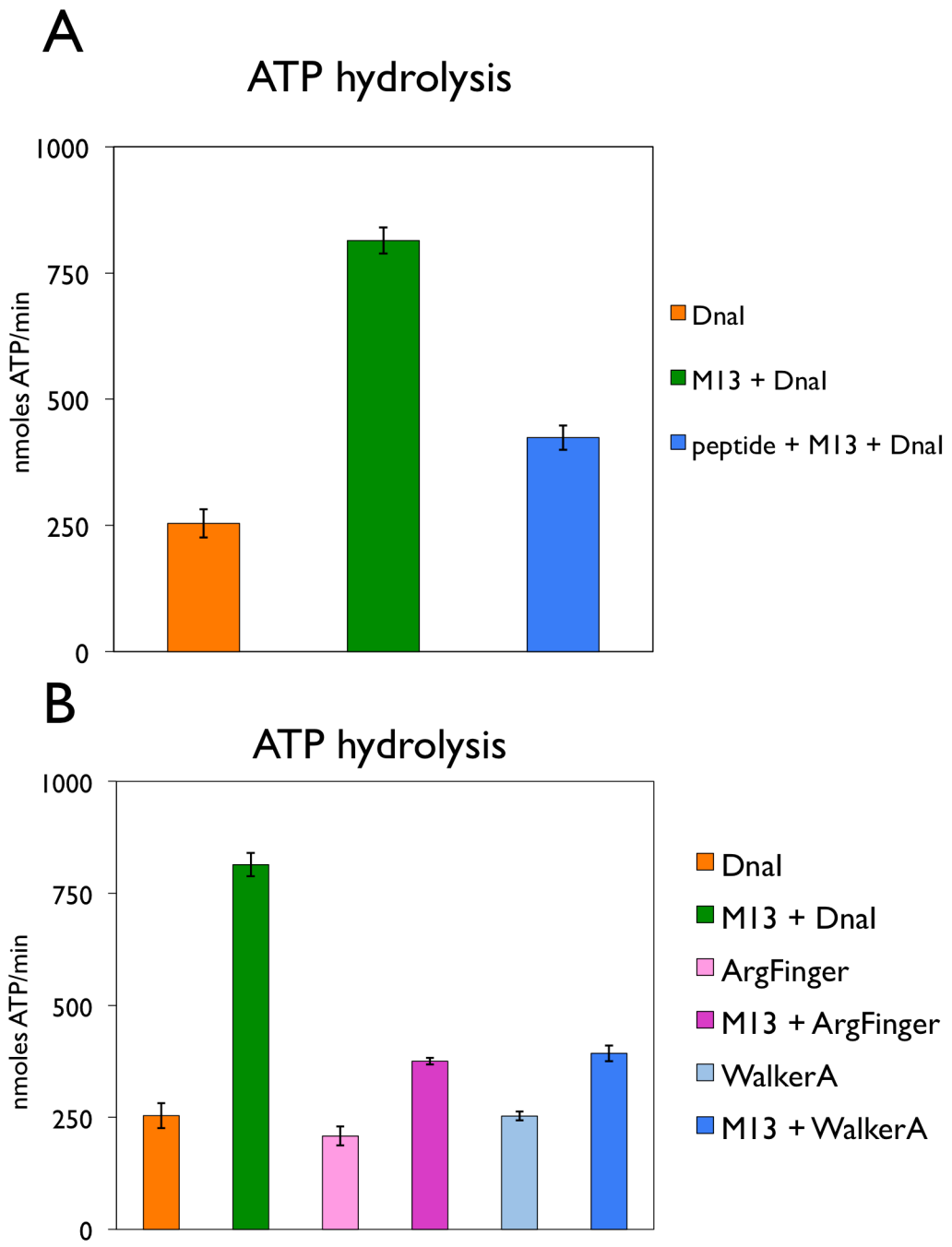

Figure 3.14. 77ORF104 inhibits M13-ssDNA stimulated ATP hydrolysis by *Sa*DnaI. (A) M13ssDNA stimulation of *Sa*DnaI ATP hydrolysis. 77ORF104 (peptide) inhibits this effect. (B) Effects of ATPase mutations on observed hydrolysis activity. Walker-A (K170A) and arginine finger (R288A) mutants show reduced stimulation of activity, comparable to that seen with 77ORF104.

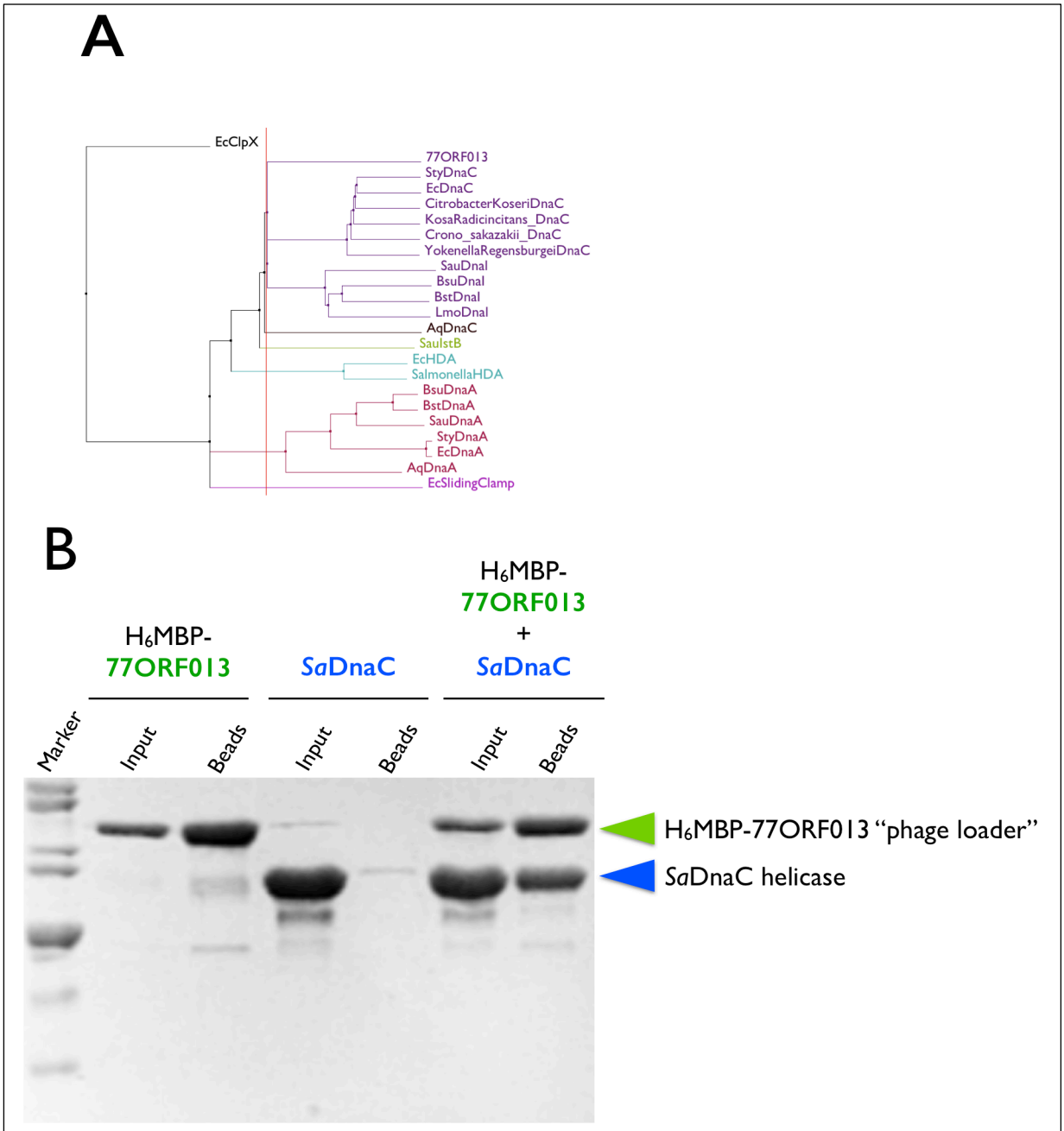

Figure 3.15. A helicase loader homolog encoded by phage 77 (ORF013) binds to the *Sa*DnaC replicative helicase. (A) Multiple sequence alignment of phage encoded gene ORF013 with various AAA+ ATPases from different clades. 77ORF013 clusters with DnaC/DnaI family helicase loaders indicating that it may serve as a replicative helicase loader for phage 77. (B) SDS-PAGE of amylose pull-down down experiments using His_6MBP-tagged phage loader 77ORF013 and the *S. aureus* DnaC replicative helicase. The 77ORF013 helicase loader binds to the host *Sa*DnaC helicase.

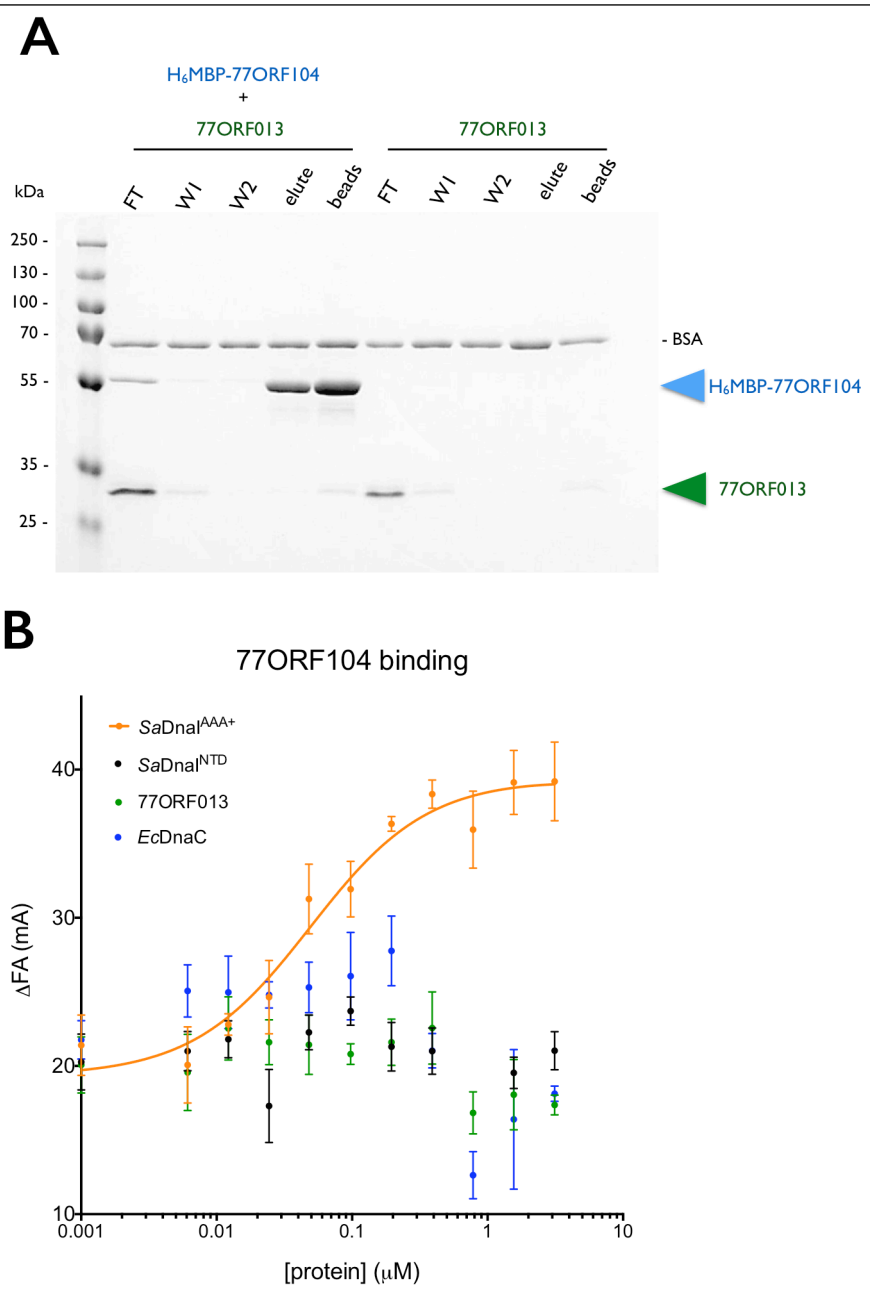

Figure 3.16. 77ORF104 does not bind to phage 77 helicase loader or *E. coli* DnaC helicase loader. (A) Amylose pulldown with His_6MBP-tagged 77ORF104 and phage loader 77ORF013. 77ORF104 does not bind phage loader helicase loader. (B) Binding to phage 77 ORF104 peptide to *Sa*DnaI^{AAA+}, *Sa*DnaI^{NTD}, 77ORF013, and *E. coli* DnaC as measured by a change in fluorescence anisotropy (ΔFA, milli-anisotropy units). The X-axis represents the concentration of each protein. Data points and error bars derive from three-independent experiments. No measurable binding was observed for the phage loader 77ORF013, *E. coli* DnaC. *Sa*DnaI^{AAA+} and *Sa*DnaI^{NTD} are included as positive and negative controls, respectively.

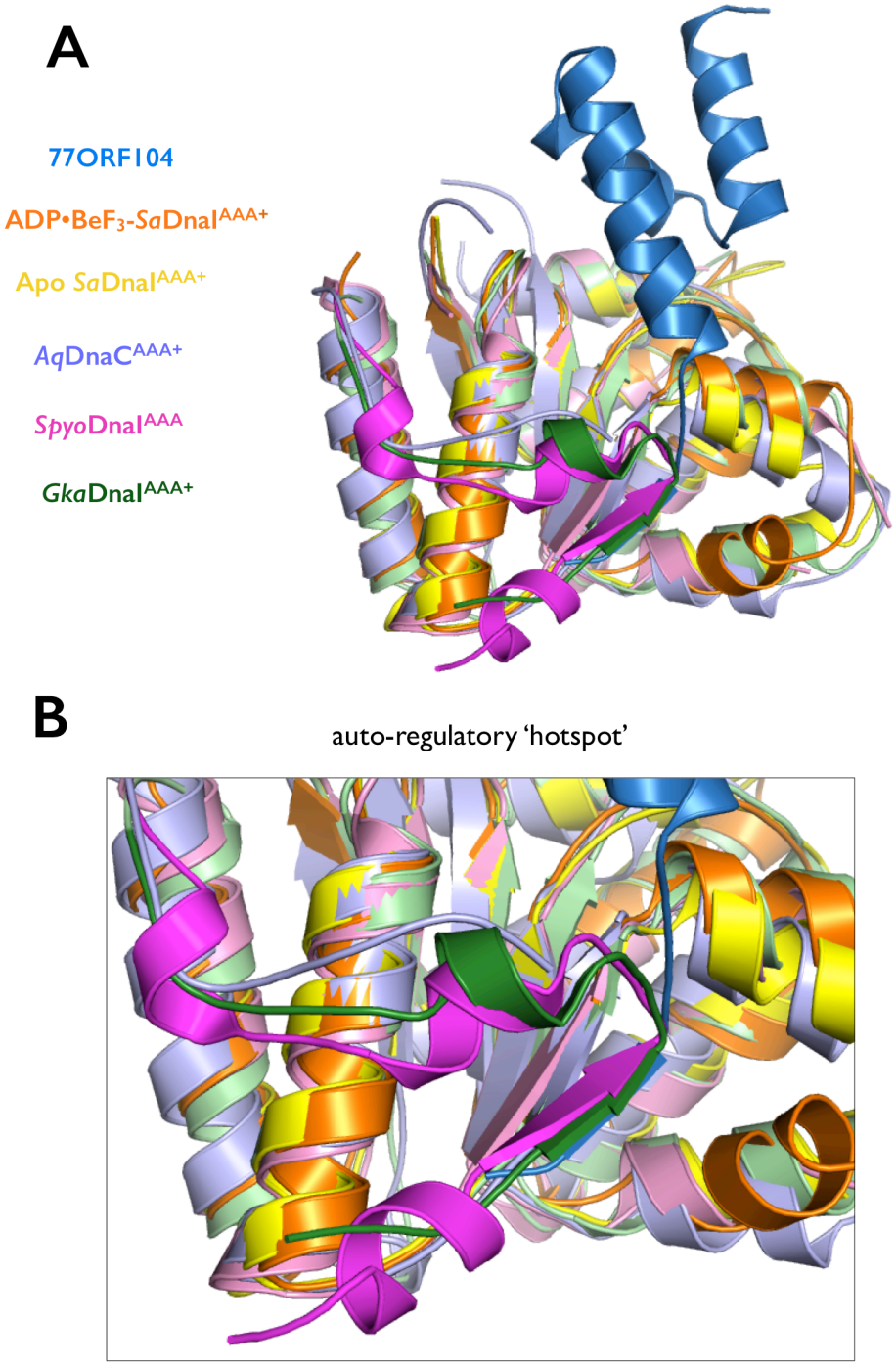

Figure 3.17. Auto-regulatory "hotspot" for controlling bacterial helicase loader self-assembly. (A) *Spyo*DnaI^{AAA+} and *Gka*DnaI $^{AAA+}$ were aligned onto the *Sa*DnaI^{AAA+} domain within *77ORF104*-bound SaDnaI^{AAA+} complex. 77ORF104 C-terminus forms a beta strand that occupies the same location as the linker regions of the DnaI homologs: *Spyo*DnaI^{AAA+} (linker shown in magenta) and *Gka*DnaI^{AAA+} (linker shown in green). (B) Close-up view of linker regions.

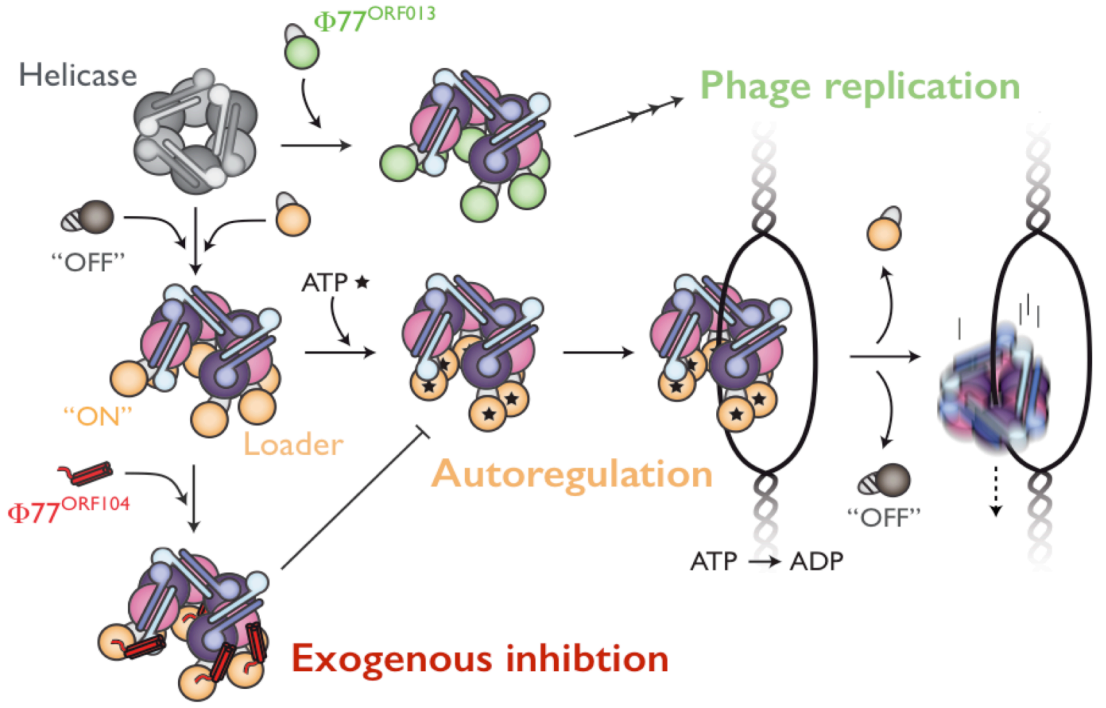

Figure 3.18. Model for auto-regulation of *Sa*DnaI helicase loader and inhibition mechanism by phage 77 to hijack host's replication machinery. Auto-regulatory element within loader's N-terminal linker region forms intra-molecular interaction with DnaI's AAA+ domain keeping the loader in an inactive or "OFF" auto-repressed state. Upon binding to the replicative helicase, the loader is activated to an "ON" state, which favors loader self-assembly and subsequent loading of the replicative helicase onto origin ssDNA. *S. aureus* phage 77 ORF104 inhibitor protein binds *Sa*DnaI blocking loader self-association and ability to properly function in the helicase loading reaction. *S. aureus* phage 77's helicase loader, encoded by ORF013, directly binds and hijacks the host replicative helicase re-directing the host's replication machinery to viral genome replication.

Chapter 4 – Conclusions and Future Directions

Conclusions

Throughout the three domains of life, dedicated ATP-dependent initiators and helicase loading factors serve essential roles in coordinating the productive loading of replicative helicases onto replication origins. Over several decades, an abundance of studies has greatly advanced our understanding of the core architectures and essential proteins required to successfully execute helicase loading during the initiation of DNA replication (reviewed in Chapter 1). Despite these advances, a detailed understanding of how initiation factors precisely chaperone the replicative helicase onto DNA has remained poorly understood at the molecular level.

In conducting structural and biochemical studies of the initiator, DnaA, and the helicase loader, DnaC, from the Gram-negative bacterium *E. coli*, along with efforts focused on the helicase loader, DnaI, from a Gram-positive bacterium *Staphylococcus aureus*, I have examined the individual roles the bacterial initiator and helicase loader contribute during DNA replication initiation. In my first set of experiments (Chapter 2), I developed several fluorescence-based helicase assays and demonstrated an important role for the N-terminal helicase-binding domain (NTD) of DnaA – in contrast to previous studies suggesting that DnaA exhibits a strand-specific preference for loading the helicase to just one strand of a melted origin, I found that the NTD of the initiator is required for helicase recruitment to both strands. Studies of the *E. coli* DnaC helicase loader revealed an unanticipated role for the protein in not only promoting helicase ring opening, but also in activating of double-stranded DNA unwinding activity. Interestingly, although the N-terminal helicase-binding domain of DnaC proved to be sufficient for activation of helicase activity, studies of DnaC ATP active site mutants demonstrate that the AAA+-family ATP binding and hydrolysis domain of DnaC also enhances the efficiency of helicase activation.

In my second set of studies (Chapter 3), I structurally and biochemically characterized the activity of the Gram-positive *S. aureus* DnaI helicase loader, and investigated how a viral peptide inhibitor from phage 77, termed "ORF104", interferes with host DNA replication by blocking *Sa*DnaI activity. Biochemical studies, combined with comparative structural analyses of the *Sa*DnaI loader both alone and in complex with ORF104, revealed the mechanism by which the viral inhibitor blocks loader function, namely, by acting both as a steric block for loader self-assembly and directly remodeling an element critical for oligomerization.

Future Directions

The present work provides new insights into how bacterial replication initiators and helicase loaders collaborate to achieve productive helicase loading in both Gram-positive and Gram-negative organisms. While the data presented in Chapter 2 for DnaA indicates that the initiator can recruit the helicase via its N-terminal domain to both strands of a model "pre-melted origin" (which contains a single DnaA binding site), it remains unclear whether DnaA carries out this function *in vivo*. Once DnaA is fully assembled at *oriC*, it is possible that, in the context of the DnaA-*oriC* initiation complex, DnaA may be positioned such that alternate protein-protein interactions would be required to achieve orientation-specific loading of the helicase to each strand of a melted origin (**Figure 2.2A**). Future work, using the DnaA mutants studied in Chapter 2 and an established helicase loading and replisome assembly assay that employs an intact *oriC*-containing plasmid (on which a more physiologically meaningful nucleoprotein initiation complex can form – see (Fang et al., 1999)) will be required to define how DnaA promotes helicase recruitment to one or both strands of a melted origin. In addition, studies are needed to determine whether the *E. coli* initiator associates with DnaC (as has been reported see (Mott et al., 2008)), and, if so, what role a DnaA-DnaC interaction might serve in facilitating orientation-specific helicase loading in a replisome assembly assay.

For the *E. coli* DnaC work, our results – combined with examination of the *E. coli* DnaBC EM structure – provide a more clear understanding of both how the bacterial helicase loader chaperones the replicative helicase onto DNA and how ATP binding and hydrolysis by the loader serves to modulate the efficiency of the helicase loading reaction. In our proposed model for replicative helicase loading in *E. coli*, the N-terminal domain of DnaC would first bind to the RecA fold of a closed DnaB ring. As successive loaders bind to the helicase, the interaction between the N-terminal domain of DnaC and DnaB would induce a conformational change that alleviates a restraining activity resident within the N-terminal DnaB collar, allowing the helicase ring to open (**Figure 2.15**) (Arias-Palomo et al., 2013; Strycharska et al., 2013). In the presence of ATP, we speculate that the AAA+ domains of neighboring DnaC subunits self-oligomerize, stabilizing the helicase in an open cracked ring conformation as visualized in an *Ec*DnaBC 3D-EM structure (Arias-Palomo et al., 2013) to permit DNA binding and loading of an activated helicase. Our DnaC ATPase motif mutant studies suggest that DnaC likely requires nucleotide hydrolysis to release from the activated DnaB hexamer. The idea that DnaB helicase activation requires DnaC release is supported by several studies, which have demonstrated that DnaB remains inactive when bound to DnaC (Allen Jr. and Kornberg, 1991; Davey et al., 2002; Makowska-Grzyska and Kaguni, 2010; Skarstad and Wold, 1995; Wahle et al., 1989b). Future studies and development of a helicase assay, capable of monitoring free versus bound DnaB-bound DnaC, will be needed to further explore the dynamics of DnaC release and helicase activation.

The recent upsurge in antibiotic resistance worldwide (Bush et al., 2011; Davies and Davies, 2010; Allen et al., 2014; Neu, 1992), combined with the current lack of diversity among antibiotic drugs currently on the market (Coates et al., 2011; Mann, 2005), and fiscally-based disincentives to fund antibiotic development (Nathan and Goldberg, 2005), underscores the perpetual need to discover novel antimicrobial targets. Although bacterial DNA replication components could be prime targets for antimicrobial drug discovery, currently no antibiotics inhibit core components of either the replisome or factors involved in DNA replication initiation (Robinson et al., 2012). In an effort to characterize the mode of action of a novel antibacterial protein and to better understand how bacterial helicase loaders function during the initiation of replication, we investigated a particular viral-host interaction between phage 77 and *S. aureus* DnaI helicase loader. Our studies of both the *S. aureus* DnaI helicase loader and the mechanism by which a phage protein inhibits the helicase loader has uncovered not only a novel viral mechanism for inhibition of DnaI, but also revealed an existing auto-regulatory element of the bacterial helicase loader, one that appears to be exploited by the virus as part of a strategy to inhibit host replication.

To date, although a limited number of DNA replication inhibitors have been identified, these studies highlight the promise of targeting DNA replication factors. Studies on phage-encoded DNA replication inhibitors have demonstrated their potency in inhibiting bacterial cell growth. One example has been found in *E. coli* phage N4, in which a protein called gp8 blocks cell growth through a direct association with the δ subunit of the *E. coli* DNA III clamp loader resulting in disruption of the clamp loading reaction (Yano and Rothman-Denes, 2011). Other phage-encoded replication inhibitors have been discovered in *S. aureus* phages, that target the *S. aureus* processivity clamp (*Staphylococcus* phages Twort gp168 and G1 gp240) and DnaG primase (*Staphylococcus* phage 96 gp078) (Belley et al., 2006; Liu et al., 2004). More recently, a study on an atypical toxin/anti-toxin system in *Caulobacter crescentus*, has identified a toxin, SocB, that inhibits replication through a direct interaction with the β sliding clamp. The SocB-β sliding clamp interaction results in termination of replication elongation by replication fork collapse and triggers the SOS response (Aakre et al., 2013). Although not discussed in the present dissertation, we performed a complimentary viral-host interaction study of the previously identified staph-specific DnaG primase inhibitor ("ORF078" from phage 71, a homolog of phage 96 gp078), which inhibits host DNA replication, revealing another promising anti-bacterial strategy; in particular, we have determined that 71ORF078 binds to DnaG through the C-terminal helicase-binding domain of the primase. Future structural and biochemical studies to characterize the primase-71ORF078 interaction and its mode of action will undoubtedly provide valuable insight into another phage DNA replication inhibition mechanism. Overall, the DNA replication inhibition mechanism described here, involving a phage protein inhibitor and an essential component of the DNA replication initiation machinery (described in Chapter 3) further highlights phage genomes as productive antimicrobial reserves for mining novel classes of antibiotic drugs.

REFERENCES

Aakre, C.D., Phung, T.N., Huang, D., and Laub, M.T. (2013). A bacterial toxin inhibits DNA replication elongation through a direct interaction with the β sliding clamp. Mol. Cell *52*, 617–628.

Abe, Y., Jo, T., Matsuda, Y., Matsunaga, C., Katayama, T., and Ueda, T. (2007). Structure and function of DnaA N-terminal domains: specific sites and mechanisms in inter-DnaA interaction and in DnaB helicase loading on oriC. J. Biol. Chem. *282*, 17816–17827.

Adams, P.D., Afonine, P. V., Bunkóczi, G., Chen, V.B., Davis, I.W., Echols, N., Headd, J.J., Hung, L.W., Kapral, G.J., Grosse-Kunstleve, R.W., et al. (2010). PHENIX: A comprehensive Python-based system for macromolecular structure solution. Acta Crystallogr. Sect. D Biol. Crystallogr. *66*, 213–221.

Adler, J., Lehman, I.R., Bessman, M.J., Simms, E.S., and Kornberg, A. (1958). Enzymatic Synthesis of Deoxyribonucleic Acid. Iv. Linkage of Single Deoxynucleotides to the Deoxynucleoside Ends of Deoxyribonucleic Acid. Proc Natl Acad Sci U S A *44*, 641–647.

Alfano, C., and Mcmacken, R. (1988). The role of template superhelicity in the initiation of bacteriophage λ DNA replication. Nucleic Acids Res. *16*, 9611–9630.

Alfano, C., and McMacken, R. (1989). Ordered assembly of nucleoprotein structures at the bacteriophage lambda replication origin during the initiation of DNA replication. J. Biol. Chem. *264*, 10699–10708.

Allen Jr., G.C., and Kornberg, A. (1991). Fine balance in the regulation of DnaB helicase by DnaC protein in replication in Escherichia coli. J. Biol. Chem. *266*, 22096–22101.

Allen, H.K., Trachsel, J., Looft, T., and Casey, T.A. (2014). Finding alternatives to antibiotics. Ann N Y Acad Sci. *1323*, 91-100.

Aravind, L., Leipe, D.D., and Koonin, E. V (1998). Toprim--a conserved catalytic domain in type IA and II topoisomerases, DnaG-type primases, OLD family nucleases and RecR proteins. Nucleic Acids Res *26*, 4205–4213.

Arias, E.E., and Walter, J.C. (2007). Strength in numbers: preventing rereplication via multiple mechanisms in eukaryotic cells. Genes Dev *21*, 497–518.

Arias-Palomo, E., O'Shea, V.L., Hood, I. V., and Berger, J.M. (2013). The bacterial DnaC helicase loader is a DnaB ring breaker. Cell *153*, 438–448.

Arthur, A.K., Höss, A., and Fanning, E. (1988). Expression of simian virus 40 T antigen in Escherichia coli: localization of T-antigen origin DNA-binding domain to within 129 amino acids. J. Virol. *62*, 1999–2006.

Atlung, T., Clausen, E.S., and Hansen, F.G. (1985). Autoregulation of the dnaA gene of Escherichia coli K12. Mol Gen Genet *200*, 442–450.

Bailey, S., Eliason, W.K., and Steitz, T.A. (2007). Structure of hexameric DnaB helicase and its complex with a domain of DnaG primase. Science *318*, 459–463.

Barry, E.R., and Bell, S.D. (2006). DNA replication in the archaea. Microbiol Mol Biol Rev *70*, 876–887.

Bell, S.P., and Dutta, A. (2002). DNA replication in eukaryotic cells. Annu Rev Biochem *71*, 333–374.

Bell, S.P., and Stillman, B. (1992). ATP-dependent recognition of eukaryotic origins of DNA replication by a multiprotein complex. Nature *357*, 128–134.

Belley, A., Callejo, M., Arhin, F., Dehbi, M., Fadhil, I., Liu, J., McKay, G., Srikumar, R., Bauda, P., Ha, N., et al. (2006). Competition of bacteriophage polypeptides with native replicase proteins for binding to the DNA sliding clamp reveals a novel mechanism for DNA replication arrest in Staphylococcus aureus. Mol. Microbiol. *62*, 1132–1143.

Benkovic, S.J., Valentine, A.M., and Salinas, F. (2001). Replisome-mediated DNA replication. Annu. Rev. Biochem. *70*, 181–208.

Bessman, M.J., Kornberg, A., and Lehman, I.R. (1956). Enzymatic synthesis of deoxyribonucleic acid. Biochim Biophys Acta *21*(1), 197-198.

Bird, L.E., Pan, H., Soultanas, P., and Wigley, D.B. (2000). Mapping protein-protein interactions within a stable complex of DNA primase and DnaB helicase from Bacillus stearothermophilus. Biochemistry *39*, 171–182.

Biswas, S.B., Flowers, S., and Biswas-Fiss, E.E. (2004). Quantitative analysis of nucleotide modulation of DNA binding by DnaC protein of Escherichia coli. Biochem J *379*, 553–562.

Bowers, J.L., Randell, J.C., Chen, S., and Bell, S.P. (2004). ATP hydrolysis by ORC catalyzes reiterative Mcm2-7 assembly at a defined origin of replication. Mol Cell *16*, 967–978.

Bowman, G.D., Goedken, E.R., Kazmirski, S.L., O'Donnell, M., and Kuriyan, J. (2005). DNA polymerase clamp loaders and DNA recognition. FEBS Lett *579*, 863–867.

Bramhill, D., and Kornberg, A. (1988a). Duplex opening by dnaA protein at novel sequences in initiation of replication at the origin of the E. coli chromosome. Cell *52*, 743–755.

Bramhill, D., and Kornberg, A. (1988b). A model for initiation at origins of DNA replication. Cell *54*, 915–918.

Brendler, T., Sawitzke, J., Sergueev, K., and Austin, S. (2000). A case for sliding SeqA tracts at anchored replication forks during Escherichia coli chromosome replication and segregation. EMBO J. *19*, 6249–6258.

Bruand, C., and Ehrlich, S.D. (1995). The Bacillus subtilis dnaI gene is part of the dnaB operon. Microbiol. *141*, 1199-1200.

Bryant, J.A., and Aves, S.J. (2011). Initiation of DNA replication: functional and evolutionary aspects. Ann Bot *107*, 1119-1126.

Bush, K., Courvalin, P., Dantas, G., Davies, J., Eisenstein, B., Huovinen, P., Jacoby, G.A., Kishony, R., Kreiswirth, B.N., Kutter, E., et al. (2011). Tackling antibiotic resistance. Nat. Rev. Microbiol. *9*, 894–896.

Chakraborty, T., Yoshinaga, K., Lother, H., and Messer, W. (1982). Purification of the E. coli dnaA gene product. EMBO J *1*, 1545–1549.

Chang, P., and Marians, K.J. (2000). Identification of a region of Escherichia coli DnaB required for functional interaction with DnaG at the replication fork. J Biol Chem *275*, 26187–26195.

Chen, V.B., Arendall, W.B., Headd, J.J., Keedy, D.A., Immormino, R.M., Kapral, G.J., Murray, L.W., Richardson, J.S., and Richardson, D.C. (2010). MolProbity: All-atom structure validation for macromolecular crystallography. Acta Crystallogr. Sect. D Biol. Crystallogr. *66*, 12–21.

Chiaramello, A.E., and Zyskind, J.W. (1989). Expression of Escherichia coli dnaA and mioC genes as a function of growth rate. J. Bacteriol. *171*, 4272–4280.

Christie, G.E., Matthews, A.M., King, D.G., Lane, K.D., Olivarez, N.P., Tallent, S.M., Gill, S.R., and Novick, R.P. (2010). The complete genomes of Staphylococcus aureus bacteriophages 80 and 80α-Implications for the specificity of SaPI mobilization. Virology *407*, 381–390.

Coates, A.R., Halls, G., and Hu, Y. (2011). Novel classes of antibiotics or more of the same? Br. J. Pharmacol. *163*, 184–194.

Costa, A., Hood, I. V., and Berger, J.M. (2013). Mechanisms for initiating cellular DNA replication. Annu. Rev. Biochem. *82*, 25–54.

Crooke, E., Thresher, R., Hwang, D.S., Griffith, J., and Kornberg, A. (1993). Replicatively active complexes of DnaA protein and the Escherichia coli chromosomal origin observed in the electron microscope. J Mol Biol *233*, 16–24.

Cunningham, E.L., and Berger, J.M. (2005). Unraveling the early steps of prokaryotic replication. Curr Opin Struct Biol *15*, 68–76.

Davey, M.J., and O'Donnell, M. (2003). Replicative helicase loaders: ring breakers and ring makers. Curr Biol *13*, R594–R596.

Davey, M.J., Fang, L., McInerney, P., Georgescu, R.E., and O'Donnell, M. (2002). The DnaC helicase loader is a dual ATP/ADP switch protein. Embo J *21*, 3148–3159.

Davies, J., and Davies, D. (2010). Origins and evolution of antibiotic resistance. Microbiol. Mol. Biol. Rev. *74*, 417–433.

Davis, I.W., Murray, L.W., Richardson, J.S., and Richardson, D.C. (2004). MolProbity: Structure validation and all-atom contact analysis for nucleic acids and their complexes. Nucleic Acids Res. *32*.

Dehbi, M., Moeck, G., Arhin, F.F., Bauda, P., Bergeron, D., Kwan, T., Liu, J., McCarty, J., DuBow, M., and Pelletier, J. (2009). Inhibition of transcription in Staphylococcus aureus by a primary sigma factor-binding polypeptide from phage G1. J. Bacteriol. *191*, 3763–3771.

Denniston-Thompson, K., Moore, D.D., Kruger, K.E., Furth, M.E., and Blattner, F.R. (1977). Physical structure of the replication origin of bacteriophage lambda. Science *198*, 1051–1056.

Diffley, J.F., and Stillman, B. (1990). The initiation of chromosomal DNA replication in eukaryotes. Trends Genet *6*, 427–432.

Diffley, J.F., Cocker, J.H., Dowell, S.J., and Rowley, A. (1994). Two steps in the assembly of complexes at yeast replication origins in vivo. Cell *78*, 303–316.

Ding, Q., and MacAlpine, D.M. (2011). Defining the replication program through the chromatin landscape. Crit Rev Biochem Mol Biol *46*, 165–179.

Dodson, M., Roberts, J., McMacken, R., and Echols, H. (1985). Specialized nucleoprotein structures at the origin of replication of bacteriophage lambda: complexes with lambda

O protein and with lambda O, lambda P, and Escherichia coli DnaB proteins. Proc. Natl. Acad. Sci. U. S. A. *82*, 4678–4682.

Dodson, M., Echols, H., Wickner, S., Alfano, C., Mensa-Wilmot, K., Gomes, B., LeBowitz, J., Roberts, J.D., and McMacken, R. (1986). Specialized nucleoprotein structures at the origin of replication of bacteriophage lambda: localized unwinding of duplex DNA by a six-protein reaction. Proc. Natl. Acad. Sci. U. S. A. *83*, 7638–7642.

Duderstadt, K.E., and Berger, J.M. (2008). AAA+ ATPases in the initiation of DNA replication. Crit Rev Biochem Mol Biol *43*, 163–187.

Duderstadt, K.E., and Berger, J.M. (2013). A structural framework for replication origin opening by AAA+ initiation factors. Curr. Opin. Struct. Biol. *23*, 144–153.

Duderstadt, K.E., Mott, M.L., Crisona, N.J., Chuang, K., Yang, H., and Berger, J.M. (2010). Origin remodeling and opening in bacteria rely on distinct assembly states of the DnaA initiator. J Biol Chem *285*, 28229–28239.

Duderstadt, K.E., Chuang, K., and Berger, J.M. (2011). DNA stretching by bacterial initiators promotes replication origin opening. Nature *478*, 209–213.

Duderstadt, K.E., Reyes-Lamothe, R., van Oijen, A.M., and Sherratt, D.J. (2014). Replication-fork dynamics. Cold Spring Harb. Perspect. Biol. *6*.

Dueber, E.L.C., Corn, J.E., Bell, S.D., and Berger, J.M. (2007). Replication origin recognition and deformation by a heterodimeric archaeal Orc1 complex. Science *317*, 1210–1213.

Duncker, B.P., Chesnokov, I.N., and McConkey, B.J. (2009). The origin recognition complex protein family. Genome Biol *10*, 214.

Dutta, A., and Bell, S.P. (1997). Initiation of DNA replication in eukaryotic cells. Annu Rev Cell Dev Biol *13*, 293–332.

Ellison, V., and Stillman, B. (2001). Opening of the clamp: An intimate view of an ATP-driven biological machine. Cell *106*, 655–660.

Enemark, E.J., Stenlund, A., and Joshua-Tor, L. (2002). Crystal structures of two intermediates in the assembly of the papillomavirus replication initiation complex. EMBO J. *21*, 1487–1496.

Erzberger, J.P., and Berger, J.M. (2006). Evolutionary relationships and structural mechanisms of AAA+ proteins. Annu Rev Biophys Biomol Struct *35*, 93–114.

Erzberger, J.P., Pirruccello, M.M., and Berger, J.M. (2002). The structure of bacterial DnaA: implications for general mechanisms underlying DNA replication initiation. Embo J *21*, 4763–4773.

Erzberger, J.P., Mott, M.L., and Berger, J.M. (2006). Structural basis for ATP-dependent DnaA assembly and replication-origin remodeling. Nat Struct Mol Biol *13*, 676–683.

Evrin, C., Clarke, P., Zech, J., Lurz, R., Sun, J., Uhle, S., Li, H., Stillman, B., and Speck, C. (2009). A double-hexameric MCM2-7 complex is loaded onto origin DNA during licensing of eukaryotic DNA replication. Proc Natl Acad Sci U S A *106*, 20240–20245.

Fang, L., Davey, M.J., and O'Donnell, M. (1999). Replisome assembly at oriC, the replication origin of E. coli, reveals an explanation for initiation sites outside an origin. Mol Cell *4*, 541–553.

Finkel, S.E., and Johnson, R.C. (1992). The Fis protein: it's not just for DNA inversion anymore. Mol. Microbiol. *6*, 3257–3265.

Von Freiesleben, U., Rasmussen, K. V., and Schaechter, M. (1994). SeqA limits DnaA activity in replication from oriC in escherichia coli. Mol. Microbiol. *14*, 763–772.

Friedman, D.I. (1988). Integration host factor: a protein for all reasons. Cell *55*, 545–554.

Friedman, D.I. (1992). Interaction between bacteriophage lambda and its Escherichia coli host. Curr. Opin. Genet. Dev. *2*, 727–738.

Fujikawa, N., Kurumizaka, H., Nureki, O., Terada, T., Shirouzu, M., Katayama, T., and Yokoyama, S. (2003). Structural basis of replication origin recognition by the DnaA protein. Nucleic Acids Res *31*, 2077–2086.

Fujimitsu, K., and Katayama, T. (2004). Reactivation of DnaA by DNA sequence-specific nucleotide exchange in vitro. Biochem. Biophys. Res. Commun. *322*, 411–419.

Fujimitsu, K., Senriuchi, T., and Katayama, T. (2009). Specific genomic sequences of E. coli promote replicational initiation by directly reactivating ADP-DnaA. Genes Dev. *23*, 1221–1233.

Fuller, C.W., Beauchamp, B.B., Engler, M.J., Lechner, R.L., Matson, S.W., Tabor, S., White, J.H., and Richardson, C.C. (1983). Mechanisms for the initiation of bacteriophage T7 DNA replication. Cold Spring Harb Symp Quant Biol *47 Pt 2*, 669–679.

Fuller, R.S., Funnell, B.E., and Kornberg, A. (1984). The dnaA protein complex with the E. coli chromosomal replication origin (oriC) and other DNA sites. Cell *38*, 889–900.

Funnell, B.E., Baker, T.A., and Kornberg, A. (1987). In vitro assembly of a prepriming complex at the origin of the Escherichia coli chromosome. J Biol Chem *262*, 10327–10334.

Furth, M.E., and Yates, J.L. (1978). Specificity determinants for bacteriophage lambda DNA replication. J. Mol. Biol. *126*, 227–240.

Furth, M.E., & W. (1983). in Lambda II (Cold Spring Harbor, NY: Cold Spring Harbor Laboratory).

Galletto, R., Jezewska, M.J., and Bujalowski, W. (2003). Interactions of the Escherichia coli DnaB helicase hexamer with the replication factor the DnaC protein. Effect of nucleotide cofactors and the ssDNA on protein-protein interactions and the topology of the complex. J Mol Biol *329*, 441–465.

Galletto, R., Jezewska, M.J., and Bujalowski, W. (2004a). Unzipping mechanism of the double-stranded DNA unwinding by a hexameric helicase: the effect of the 3′ arm and the stability of the dsDNA on the unwinding activity of the Escherichia coli DnaB helicase. J Mol Biol *343*, 101–114.

Galletto, R., Jezewska, M.J., and Bujalowski, W. (2004b). Unzipping mechanism of the double-stranded DNA unwinding by a hexameric helicase: quantitative analysis of the rate of the dsDNA unwinding, processivity and kinetic step-size of the Escherichia coli DnaB helicase using rapid quench-flow method. J Mol Biol *343*, 83–99.

Gao, D. (2000). tau Binds and Organizes Escherichia coli Replication Proteins through Distinct Domains. DOMAIN III, SHARED BY gamma AND tau , BINDS delta delta ′ AND chi psi. J. Biol. Chem. *276*, 4447–4453.

Georgescu, R.E., Kurth, I., and O'Donnell, M.E. (2011). Single-molecule studies reveal the function of a third polymerase in the replisome. Nat. Struct. Mol. Biol. *19*, 113–116.

Gille, H., and Messer, W. (1991). Localized DNA melting and structural pertubations in the origin of replication, oriC, of Escherichia coli in vitro and in vivo. Embo J *10*, 1579–1584.

Grainge, I., Scaife, S., and Wigley, D.B. (2003). Biochemical analysis of components of the pre-replication complex of Archaeoglobus fulgidus. Nucleic Acids Res *31*, 4888–4898.

Grosse-Kunstleve, R.W., and Adams, P.D. (2003). Substructure search procedures for macromolecular structures. In Acta Crystallographica - Section D Biological Crystallography, pp. 1966–1973.

Hamdan, S.M., Loparo, J.J., Takahashi, M., Richardson, C.C., and van Oijen, A.M. (2009). Dynamics of DNA replication loops reveal temporal control of lagging-strand synthesis. Nature *457*, 336–339.

Hansen, F.G., Atlung, T., Braun, R.E., Wright, A., Hughes, P., and Kohiyama, M. (1991). Initiator (DnaA) protein concentration as a function of growth rate in Escherichia coli and Salmonella typhimurium. J Bacteriol. *173*, 5194-5199.

Hardy, C.D., Crisona, N.J., Stone, M.D., and Cozzarelli, N.R. (2004). Disentangling DNA during replication: a tale of two strands. Philos Trans R Soc L. B Biol Sci *359*, 39–47.

Heller, R.C., and Marians, K.J. (2005a). The disposition of nascent strands at stalled replication forks dictates the pathway of replisome loading during restart. Mol Cell *17*, 733-743.

Heller, R.C., and Marians, K.J. (2005b). Unwinding of the nascent lagging strand by Rep and PriA enables the direct restart of stalled replication forks. J Biol Chem *280*, 34143-34151.

Heller, R.C., and Marians, K.J. (2006). Replisome assembly and the direct restart of stalled replication forks. Nat Rev Mol Cell Biol *7*, 932–943.

Hiasa, H., and Marians, K.J. (1994). Topoisomerase IV can support oriC DNA replication in vitro. J. Biol. Chem. *269*, 16371–16375.

Hiasa, H., and Marians, K.J. (1996). Two distinct modes of strand unlinking during theta-type DNA replication. J. Biol. Chem. *271*, 21529–21535.

Hobom, G., Grosschedl, R., Lusky, M., Scherer, G., Schwarz, E., and Kössel, H. (1979). Functional analysis of the replicator structure of lambdoid bacteriophage DNAs. Cold Spring Harb. Symp. Quant. Biol. *43*, 165–178.

Hsu, J., Bramhill, D., and Thompson, C.M. (1994). Open complex formation by DnaA initiation protein at the Escherichia coli chromosomal origin requires the 13-mers precisely spaced relative to the 9-mers. Mol Microbiol *11*, 903–911.

Hwang, D.S., Kornberg, A., Deog Su Hwang, and Kornberg, A. (1992). Opening of the replication origin of Escherichia coli by DnaA protein with protein HU or IHF. J Biol Chem *267*, 23083–23086.

Ioannou, C., Schaeffer, P.M., Dixon, N.E., and Soultanas, P. (2006). Helicase binding to DnaI exposes a cryptic DNA-binding site during helicase loading in Bacillus subtilis. Nucleic Acids Res *34*, 5247–5258.

Itsathitphaisarn, O., Wing, R.A., Eliason, W.K., Wang, J., and Steitz, T.A. (2012). The Hexameric Helicase DnaB Adopts a Nonplanar Conformation during Translocation. Cell *151*, 267-277.

Iyer, L.M., Leipe, D.D., Koonin, E. V, and Aravind, L. (2004). Evolutionary history and higher order classification of AAA+ ATPases. J Struct Biol *146*, 11–31.

Jacob, F., Brenner, S., and Cuzin, F. (1963). On the regulation of DNA replication in bacteria. Cold Spring Harb. Symp. Quant. Biol. *28*, 329–348.

Jeruzalmi, D., O'Donnell, M., and Kuriyan, J. (2002). Clamp loaders and sliding clamps. Curr. Opin. Struct. Biol. *12*, 217–224.

Jezewska, M.J., Rajendran, S., Bujalowska, D., and Bujalowski, W. (1998). Does single-stranded DNA pass through the inner channel of the protein hexamer in the complex with the Escherichia coli DnaB Helicase? Fluorescence energy transfer studies. J Biol Chem *273*, 10515–10529.

Johansson, E., and Dixon, N. (2013). Replicative DNA polymerases. Cold Spring Harb. Perspect. Biol. *5*.

Johnson, A., and O'Donnell, M. (2005). Cellular DNA replicases: components and dynamics at the replication fork. Annu Rev Biochem *74*, 283–315.

Kabsch, W. (1988). Evaluation of single-crystal X-ray diffraction data from a position-sensitive detector. J. Appl. Cryst. *21*, 916–924.

Kabsch, W. (2010). XDS. Acta Crystallogr. Sect. D Biol. Crystallogr. *66*, 125–132.

Kaguni, J.M. (2006). DnaA: controlling the initiation of bacterial DNA replication and more. Annu Rev Microbiol. *60*, 351-375.

Kaguni, J.M. (2011). Replication initiation at the *Escherichia coli* chromosomal origin. Curr. Opin. Chem. Biol. *15*, 606–613.

Kaguni, J.M., and Kornberg, A. (1984). Topoisomerase I confers specificity in enzymatic replication of the Escherichia coli chromosomal origin. J. Biol. Chem. *259*, 8578–8583.

Kaplan, D.L. (2000). The 3'-tail of a forked-duplex sterically determines whether one or two DNA strands pass through the central channel of a replication-fork helicase. J Mol Biol *301*, 285–299.

Kaplan, D.L., and Steitz, T.A. (1999). DnaB from Thermus aquaticus unwinds forked duplex DNA with an asymmetric tail length dependence. J Biol Chem. *274*, 6889-6897.

Katayama, T., Ozaki, S., Keyamura, K., and Fujimitsu, K. (2010). Regulation of the replication cycle: conserved and diverse regulatory systems for DnaA and oriC. Nat. Rev. Microbiol. *8*, 163–170.

Katoh, K., and Standley, D.M. (2013). MAFFT multiple sequence alignment software version 7: Improvements in performance and usability. Mol. Biol. Evol. *30*, 772–780.

Kawaguchi, A., and Nagata, K. (2007). De novo replication of the influenza virus RNA genome is regulated by DNA replicative helicase, MCM. EMBO J. *26*, 4566–4575.

Kawakami, H., and Katayama, T. (2010). DnaA, ORC, and Cdc6: similarity beyond the domains of life and diversity. Biochem Cell Biol *88*, 49–62.

Kelch, B.A., Makino, D.L., O'Donnell, M., and Kuriyan, J. (2011). How a DNA polymerase clamp loader opens a sliding clamp. Science *334*, 1675–1680.

Kelman, L.M., and Kelman, Z. (2003). Archaea: an archetype for replication initiation studies? Mol Microbiol *48*, 605–615.

Kelman, Z., and O'Donnell, M. (1995). DNA polymerase III holoenzyme: structure and function of a chromosomal replicating machine. Annu Rev Biochem *64*, 171–200.

Keyamura, K., and Katayama, T. (2011). DnaA Protein DNA-binding Domain Binds to Hda Protein to Promote Inter-AAA+ Domain Interaction Involved in Regulatory Inactivation of DnaA. J Biol Chem *286*, 29336–29346.

Keyamura, K., Abe, Y., Higashi, M., Ueda, T., and Katayama, T. (2009). DiaA dynamics are coupled with changes in initial origin complexes leading to helicase loading. J Biol Chem *284*, 25038–25050.

Khodursky, A.B., Peter, B.J., Schmid, M.B., DeRisi, J., Botstein, D., Brown, P.O., and Cozzarelli, N.R. (2000). Analysis of topoisomerase function in bacterial replication fork movement: use of DNA microarrays. Proc. Natl. Acad. Sci. U. S. A. *97*, 9419–9424.

Kimura, M., Miki, T., Hiraga, S., Nagata, T., and Yura, T. (1979). Conditionally lethal amber mutations in the dnaA region of the Escherichia coli chromosome that affect chromosome replication. J. Bacteriol. *140*, 825–834.

Klein, E., Smith, D.L., and Laxminarayan, R. (2007). Hospitalizations and deaths caused by methicillin-resistant Staphylococcus aureus, United States, 1999-2005. Emerg. Infect. Dis. *13*, 1840–1846.

Klein, E.Y., Sun, L., Smith, D.L., and Laxminarayan, R. (2013). The changing epidemiology of methicillin-resistant Staphylococcus aureus in the United States: A national observational study. Am. J. Epidemiol. *177*, 666–674.

Klinkert, J., and Klein, A. (1978). Roles of bacteriophage lambda gene products O and P during early and late phases of infection cycle. J. Virol. *25*, 730–737.

Kobori, J.A., and Kornberg, A. (1982a). The Escherichia coli dnaC gene product. II. Purification, physical properties, and role in replication. J Biol Chem *257*, 13763–13769.

Kobori, J.A., and Kornberg, A. (1982b). The Escherichia coli dnaC gene product. I. Overlapping of the dnaC proteins of Escherichia coli and Salmonella typhimurium by cloning into a high copy number plasmid. J Biol Chem *257*, 13757–13762.

Kobori, J.A., and Kornberg, A. (1982c). The Escherichia colidnaC gene product. III. Properties of the dnaB-dnaC protein complex. J Biol Chem *257*, 13770–13775.

Kohiyama, M. (1968). DNA synthesis in temperature sensitive mutants of Escherichia coli. Cold Spring Harb Symp Quant Biol *33*, 317–324.

Kohiyama, M. et al., Cousin, D., Ryter, A., and Jacob, F. (1966). [Thermosensitive mutants of Escherichia coli K 12. I. Isolation and rapid characterization]. Ann Inst Pasteur *110*, 465–486.

Koonin, E. V (1992). DnaC protein contains a modified ATP-binding motif and belongs to a novel family of ATPases including also DnaA. Nucleic Acids Res *20*, 1997.

Kornberg, A. (1960). Biologic synthesis of deoxyribonucleic acid. Stanford Med Bull *18*, 1503–1508.

Kornberg, A. (1968). The synthesis of DNA. Sci Am *219*, 64–78.

Kornberg and Baker, T. A., A. (1992). DNA Replication. W.H. Freeman and Company, New York.

Kowalski, D., and Eddy, M.J. (1989). The DNA unwinding element: a novel, cis-acting component that facilitates opening of the Escherichia coli replication origin. Embo J *8*, 4335–4344.

Krause, M., Rückert, B., Lurz, R., Messer, W., Ruckert, B., Lurz, R., and Messer, W. (1997). Complexes at the replication origin of Bacillus subtilis with homologous and heterologous DnaA protein. J Mol Biol *274*, 365–380.

Kwan, T., Liu, J., DuBow, M., Gros, P., and Pelletier, J. (2005). The complete genomes and proteomes of 27 Staphylococcus aureus bacteriophages. Proc. Natl. Acad. Sci. U. S. A. *102*, 5174–5179.

Learn, B.A., Um, S.J., Huang, L., and McMacken, R. (1997). Cryptic single-stranded-DNA binding activities of the phage lambda P and Escherichia coli DnaC replication initiation proteins facilitate the transfer of E. coli DnaB helicase onto DNA. Proc. Natl. Acad. Sci. U. S. A. *94*, 1154–1159.

LeBowitz, J.H., and McMacken, R. (1984a). Initiation of DNA synthesis on single-stranded DNA templates in vitro promoted by the bacteriophage lambda O and P replication proteins. Adv. Exp. Med. Biol. *179*, 77–89.

LeBowitz, J.H., and McMacken, R. (1984b). The bacteriophage lambda O and P protein initiators promote the replication of single-stranded DNA. Nucleic Acids Res *12*, 3069–3088.

Lebowitz, J.H., and Mcmacken, R. (1984). The bacteriophage λ O and P protein initiators promote the replication of single-stranded DNA. Nucleic Acids Res. *12*, 3069–3088.

LeBowitz, J.H., and McMacken, R. (1986). The Escherichia colidnaB replication protein is a DNA helicase. J Biol Chem *261*, 4738–4748.

Lee, P.S., and Grossman, A.D. (2006). The chromosome partitioning proteins Soj (ParA) and Spo0J (ParB) contribute to accurate chromosome partitioning, separation of replicated sister origins, and regulation of replication initiation in Bacillus subtilis. Mol Microbiol *60*, 853–869.

Leipe, D.D., Aravind, L., Grishin, N. V, and Koonin, E. V (2000). The bacterial replicative helicase DnaB evolved from a RecA duplication. Genome Res *10*, 5–16.

Leonard, A.C., and Grimwade, J.E. (2005). Building a bacterial orisome: emergence of new regulatory features for replication origin unwinding. Mol Microbiol *55*, 978–985.

Leonard, A.C., and Grimwade, J.E. (2010). Initiation of DNA replication. In EcoSal—Escherichia coli and Salmonella: Cellular and Molecular Biology (Washington, DC).

Li, Z., and Crooke, E. (1999). Functional analysis of affinity-purified polyhistidine-tagged DnaA protein. Protein Expr. Purif. *17*, 41–48.

Liberek, K., Osipiuk, J., Zylicz, M., Ang, D., Skorko, J., and Georgopoulos, C. (1990). Physical interactions between bacteriophage and Escherichia coli proteins required for initiation of lambda DNA replication. J. Biol. Chem. *265*, 3022–3029.

Liu, J., Dehbi, M., Moeck, G., Arhin, F., Bauda, P., Bergeron, D., Callejo, M., Ferretti, V., Ha, N., Kwan, T., et al. (2004). Antimicrobial drug discovery through bacteriophage genomics. Nat. Biotechnol. *22*, 185–191.

Lo, Y.H., Tsai, K.L., Sun, Y.J., Chen, W.T., Huang, C.Y., and Hsiao, C.D. (2009). The crystal structure of a replicative hexameric helicase DnaC and its complex with single-stranded DNA. Nucleic Acids Res *37*, 804–814.

Loscha, K. V, Jaudzems, K., Ioannou, C., Su, X.C., Hill, F.R., Otting, G., Dixon, N.E., and Liepinsh, E. (2009). A novel zinc-binding fold in the helicase interaction domain of the Bacillus subtilis DnaI helicase loader. Nucleic Acids Res *37*, 2395–2404.

Lu, M., Campbell, J.L., Boye, E., and Kleckner, N. (1994). SeqA: A negative modulator of replication initiation in E. coli. Cell *77*, 413–426.

Ludlam, A. V, McNatt, M.W., Carr, K.M., and Kaguni, J.M. (2001). Essential amino acids of Escherichia coli DnaC protein in an N-terminal domain interact with DnaB helicase. J Biol Chem *276*, 27345–27353.

MacNeill, S.A. (2001). DNA replication: Partners in the Okazaki two-step. Curr. Biol. *11*, R842-R844.

Makowska-Grzyska, M., and Kaguni, J.M. (2010). Primase Directs the Release of DnaC from DnaB. Mol Cell *37*, 90–101.

Mallory, J.B., Alfano, C., and McMacken, R. (1990). Host virus interactions in the initiation of bacteriophage λ DNA replication: Recruitment of Escherichia coli DnaB helicase by λ P replication protein. J. Biol. Chem. *265*, 13297–13307.

Mann, J. (2005). Antibiotics: Actions, Origins, Resistance. Nat. Prod. Rep. *22*, 304.

Marszalek, J., and Kaguni, J.M. (1994). DnaA protein directs the binding of DnaB protein in initiation of DNA replication in Escherichia coli. J Biol Chem *269*, 4883–4890.

Marszalek, J., Zhang, W., Hupp, T.R., Margulies, C., Carr, K.M., Cherry, S., and Kaguni, J.M. (1996). Domains of DnaA protein involved in interaction with DnaB protein, and in unwinding the Escherichia coli chromosomal origin. J Biol Chem *271*, 18535–18542.

Masai, H., and Arai, K.I. (1995). DnaA-dependent assembly of the ABC primosome at the A site, a single- stranded DNA hairpin containing a dnaA box. Eur. J. Biochem. *230*, 384–395.

McCoy, A.J., Grosse-Kunstleve, R.W., Adams, P.D., Winn, M.D., Storoni, L.C., and Read, R.J. (2007). Phaser crystallographic software. J. Appl. Crystallogr. *40*, 658–674.

McGlynn, P. (2011). Helicases that underpin replication of protein-bound DNA in Escherichia coli. Biochem Soc Trans. *39*, 606-610.

McHenry, C.S., and Crow, W. (1979). DNA polymerase III of Escherichia coli. Purification and identification of subunits. J. Biol. Chem. *254*, 1748–1753.

McInerney, P., Johnson, A., Katz, F., and O'Donnell, M. (2007). Characterization of a triple DNA polymerase replisome. Mol Cell *27*, 527–538.

Meinke, G., Phelan, P., Moine, S., Bochkareva, E., Bochkarev, A., Bullock, P.A., and Bohm, A. (2007). The crystal structure of the SV40 T-antigen origin binding domain in complex with DNA. PLoS Biol. *5*, 0144–0156.

Mensa-Wilmot, K., Seaby, R., Alfano, C., Wold, M.S., Gomes, B., and McMacken, R. (1989). Reconstitution of a nine-protein system that initiates bacteriophage λ DNA replication. J. Biol. Chem. *264*, 2853–2861.

Miroux, B., and Walker, J.E. (1996). Over-production of proteins in Escherichia coli: mutant hosts that allow synthesis of some membrane proteins and globular proteins at high levels. J. Mol. Biol. *260*, 289–298.

Mott, M.L., and Berger, J.M. (2007). DNA replication initiation: mechanisms and regulation in bacteria. Nat. Rev. Microbiol. *5*, 343–354.

Mott, M.L., Erzberger, J.P., Coons, M.M., and Berger, J.M. (2008). Structural synergy and molecular crosstalk between bacterial helicase loaders and replication initiators. Cell *135*, 623–634.

Murray, H., and Errington, J. (2008). Dynamic control of the DNA replication initiation protein DnaA by Soj/ParA. Cell *135*, 74–84.

Naktinis, V., Onrust, R., Fang, L., and O'Donnell, M. (1995). Assembly of a chromosomal replication machine: two DNA polymerases, a clamp loader, and sliding clamps in one holoenzyme particle. II. Intermediate complex between the clamp loader and its clamp. J Biol Chem *270*, 13358–13365.

Nathan, C., and Goldberg, F.M. (2005). Outlook: the profit problem in antibiotic R&D. Nat. Rev. Drug Discov. *4*, 887–891.

Neu, H.C. (1992). The crisis in antibiotic resistance. Science *257*, 1064–1073.

Neuwald, A.F., Aravind, L., Spouge, J.L., and Koonin, E. V (1999). AAA+: A class of chaperone-like ATPases associated with the assembly, operation, and disassembly of protein complexes. Genome Res *9*, 27–43.

O'Donnell, M. (2006). Replisome architecture and dynamics in Escherichia coli. J. Biol. Chem. *281*, 10653–10656.

O'Donnell, M., Langston, L., and Stillman, B. (2013). Principles and concepts of DNA replication in bacteria, archaea, and eukarya. Cold Spring Harb. Perspect. Biol. *5*.

O'Shea, V.L., and Berger, J.M. (2014). Loading strategies of ring-shaped nucleic acid translocases and helicases. Curr. Opin. Struct. Biol. *25*, 16–24.

Odegrip, R., Schoen, S., Haggård-Ljungquist, E., Park, K., and Chattoraj, D.K. (2000). The interaction of bacteriophage P2 B protein with Escherichia coli DnaB helicase. J. Virol. *74*, 4057–4063.

Ogura, T., and Wilkinson, A.J. (2001). AAA+ superfamily ATPases: common structure--diverse function. Genes Cells *6*, 575–597.

Ogura, Y., Ogasawara, N., Harry, E.J., and Moriya, S. (2003). Increasing the ratio of Soj to Spo0J promotes replication initiation in Bacillus subtilis. J Bacteriol *185*, 6316–6324.

Van Oijen, A.M., and Loparo, J.J. (2010). Single-molecule studies of the replisome. Annu. Rev. Biophys. *39*, 429–448.

Okazaki, R., Okazaki, T., Sakabe, K., Sugimoto, K., and Sugino, A. (1968). Mechanism of DNA chain growth. I. Possible discontinuity and unusual secondary structure of newly synthesized chains. Proc Natl Acad Sci U S A *59*, 598–605.

Ozaki, S., and Katayama, T. (2009). DnaA structure, function, and dynamics in the initiation at the chromosomal origin. Plasmid *62*, 71–82.

Ozaki, S., and Katayama, T. (2012). Highly organized DnaA-oriC complexes recruit the single-stranded DNA for replication initiation. Nucleic Acids Res *40*, 1648–1665.

Rahn-Lee, L., Gorbatyuk, B., Skovgaard, O., and Losick, R. (2009). The conserved sporulation protein YneE inhibits DNA replication in Bacillus subtilis. J Bacteriol *191*, 3736–3739.

Randell, J.C., Bowers, J.L., Rodriguez, H.K., and Bell, S.P. (2006). Sequential ATP hydrolysis by Cdc6 and ORC directs loading of the Mcm2-7 helicase. Mol Cell *21*, 29–39.

Remus, D., Beuron, F., Tolun, G., Griffith, J.D., Morris, E.P., and Diffley, J.F. (2009). Concerted loading of Mcm2-7 double hexamers around DNA during DNA replication origin licensing. Cell *139*, 719–730.

Reyes-Lamothe, R., Sherratt, D.J., and Leake, M.C. (2010). Stoichiometry and architecture of active DNA replication machinery in Escherichia coli. Science (80-.). *328*, 498–501.

Robinson, A., J. Causer, R., and E. Dixon, N. (2012). Architecture and Conservation of the Bacterial DNA Replication Machinery, an Underexploited Drug Target. Curr. Drug Targets *13*, 352–372.

Romano, L.J., Tamanoi, F., and Richardson, C.C. (1981). Initiation of DNA replication at the primary origin of bacteriophage T7 by purified proteins: requirement for T7 RNA polymerase. Proc Natl Acad Sci U S A *78*, 4107–4111.

Roth, A., and Messer, W. (1995). The DNA binding domain of the initiator protein DnaA. EMBO J. *14*, 2106–2111.

Ryan, V.T., Grimwade, J.E., Nievera, C.J., and Leonard, A.C. (2002). IHF and HU stimulate assembly of pre-replication complexes at Escherichia coli oriC by two different mechanisms. Mol. Microbiol. *46*, 113–124.

Ryan, V.T., Grimwade, J.E., Camara, J.E., Crooke, E., and Leonard, A.C. (2004). Escherichia coli prereplication complex assembly is regulated by dynamic interplay among Fis, IHF and DnaA. Mol. Microbiol. *51*, 1347–1359.

S, T. (1975). Roles of genes O and P in the replication of bacteriophage lambda DNA. J Mol Biol *94*, 385–396.

Sakamoto, Y., Nakai, S., Moriya, S., Yoshikawa, H., and Ogasawara, N. (1995). The Bacillus subtilis dnaC gene encodes a protein homologous to the DnaB helicase of Escherichia coli. Microbiology *141*, 641–644.

Salgado, C.D., Farr, B.M., and Calfee, D.P. (2003). Community-acquired methicillin-resistant Staphylococcus aureus: a meta-analysis of prevalence and risk factors. Clin. Infect. Dis. *36*, 131–139.

Sambrook, J., Fritsch, E.F., and Maniatis, T. (1989). Molecular Cloning.

San Martin, C., Radermacher, M., Wolpensinger, B., Engel, A., Miles, C.S., Dixon, N.E., and Carazo, J.M. (1998). Three-dimensional reconstructions from cryoelectron microscopy images reveal an intimate complex between helicase DnaB and its loading partner DnaC. Structure *6*, 501–509.

San Martin, M.C., Stamford, N.P., Dammerova, N., Dixon, N.E., and Carazo, J.M. (1995). A structural model for the Escherichia coli DnaB helicase based on electron microscopy data. J Struct Biol *114*, 167–176.

Sanders, C.M., and Stenlund, A. (1998). Recruitment and loading of the E1 initiator protein: an ATP-dependent process catalysed by a transcription factor. EMBO J *17*, 7044–7055.

Schaeffer, P.M., Headlam, M.J., and Dixon, N.E. (2005). Protein-protein interactions in the eubacterial replisome. IUBMB Life *57*, 5-12.

Schaper, S., and Messer, W. (1995). Interaction of the initiator protein DnaA of Escherichia coli with its DNA target. J. Biol. Chem. *270*, 17622–17626.

Schmid, M.B. (1990). More than just "histone-like" proteins. Cell *63*, 451–453.

Schneider, C.A., Rasband, W.S., and Eliceiri, K.W. (2012). NIH Image to ImageJ: 25 years of image analysis. Nat. Methods *9*, 671–675.

Schnos, M., and Inman, R.B. (1991). Daughter origins can be held together by O protein in phage lambda replicative intermediates. Virology *183*, 753–756.

Schnos, M., Zahn, K., Inman, R.B., and Blattner, F.R. (1988). Initiation protein induced helix destabilization at the lambda origin: a prepriming step in DNA replication. Cell *52*, 385–395.

Scholefield, G., Whiting, R., Errington, J., and Murray, H. (2011). Spo0J regulates the oligomeric state of Soj to trigger its switch from an activator to an inhibitor of DNA replication initiation. Mol Microbiol *79*, 1089–1100.

Schuck, S., and Stenlund, A. (2005). Assembly of a double hexameric helicase. Mol Cell *20*, 377–389.

Sedman, J., and Stenlund, A. (1998). The papillomavirus E1 protein forms a DNA-dependent hexameric complex with ATPase and DNA helicase activities. J Virol *72*, 6893–6897.

Seitz, H., Weigel, C., and Messer, W. (2000). The interaction domains of the DnaA and DnaB replication proteins of Escherichia coli. Mol. Microbiol. *37*, 1270–1279.

Sekimizu, K., Bramhill, D., and Kornberg, A. (1987). ATP activates dnaA protein in initiating replication of plasmids bearing the origin of the E. coli chromosome. Cell *50*, 259–265.

Sekimizu, K., Bramhill, D., and Kornberg, A. (1988a). Sequential early stages in the in vitro initiation of replication at the origin of the Escherichia coli chromosome. J Biol Chem *263*, 7124–7130.

Sekimizu, K., Yat-ming Yung, B., and Kornberg, A. (1988b). The dnaA protein of Escherichia coli. Abundance, improved purification, and membrane binding. J. Biol. Chem. *263*, 7136–7140.

Sélo, I., Négroni, L., Créminon, C., Grassi, J., and Wal, J.M. (1996). Preferential labeling of α-amino N-terminal groups in peptides by biotin: Application to the detection of specific anti-peptide antibodies by enzyme immunoassays. J. Immunol. Methods *199*, 127–138.

Sherratt, D.J. (2003). Bacterial chromosome dynamics. Science *301*, 780–785.

Simmons, L.A., Breier, A.M., Cozzarelli, N.R., and Kaguni, J.M. (2004). Hyperinitiation of DNA replication in Escherichia coli leads to replication fork collapse and inviability. Mol. Microbiol. *51*, 349–358.

Skarstad, K., and Wold, S. (1995). The speed of the Escherichia coli fork in vivo depends on the DnaB:DnaC ratio. Mol. Microbiol. *17*, 825–831.

Skarstad, K., Thony, B., Hwang, D.S., Kornberg, A., Thöny, B., Hwang, D.S., and Kornberg, A. (1993). A novel binding protein of the origin of the Escherichia coli chromosome. J Biol Chem *268*, 5365–5370.

Slater, S., Wold, S., Lu, M., Boye, E., Skarstad, K., and Kleckner, N. (1995). E. coli SeqA protein binds oriC in two different methyl-modulated reactions appropriate to its roles in DNA replication initiation and origin sequestration. Cell *82*, 927–936.

Smits, W.K., Goranov, A.I., and Grossman, A.D. (2010). Ordered association of helicase loader proteins with the Bacillus subtilis origin of replication in vivo. Mol Microbiol *75*, 452–461.

Smits, W.K., Merrikh, H., Bonilla, C.Y., and Grossman, A.D. (2011). Primosomal proteins DnaD and DnaB are recruited to chromosomal regions bound by DnaA in Bacillus subtilis. J Bacteriol *193*, 640–648.

Soultanas, P. (2002). A functional interaction between the putative primosomal protein DnaI and the main replicative DNA helicase DnaB in Bacillus. Nucleic Acids Res. *41*, 5303-5320.

Soultanas, P. (2012). Loading mechanisms of ring helicases at replication origins. Mol Microbiol *84*, 6–16.

Speck, C., and Messer, W. (2001). Mechanism of origin unwinding: Sequential binding of DnaA to double- and single-stranded DNA. EMBO J. *20*, 1469-1476.

Speck, C., and Stillman, B. (2007). Cdc6 ATPase activity regulates ORC x Cdc6 stability and the selection of specific DNA sequences as origins of DNA replication. J Biol Chem *282*, 11705–11714.

Speck, C., Weigel, C., and Messer, W. (1999). ATP- and ADP-DnaA protein, a molecular switch in gene regulation. EMBO J. *18*, 6169–6176.

Speck, C., Chen, Z., Li, H., and Stillman, B. (2005). ATPase-dependent cooperative binding of ORC and Cdc6 to origin DNA. Nat Struct Mol Biol *12*, 965–971.

Stein, R.A., Wilkinson, J.C., Guyer, C.A., and Staros, J. V. (2001). An analytical approach to the measurement of equilibrium binding constants: Application to EGF binding to EGF receptors in intact cells measured by flow cytometry. Biochemistry *40*, 6142–6154.

Stevens, W.F., Adhya, W., Szybalski, W. (1971). The Bacteriophage Lambda (Cold Spring Harbor, NY: Cold Spring Harbor Laboratory).

Stillman, B. (2005). Origin recognition and the chromosome cycle. FEBS Lett *579*, 877–884.

Struble, E.B., Gittis, A.G., Bianchet, M.A., and McMacken, R. (2007). Crystallization and preliminary crystallographic characterization of the origin-binding domain of the bacteriophage λ O replication initiator. Acta Crystallogr. Sect. F Struct. Biol. Cryst. Commun. *63*, 542–545.

Strycharska, M.S., Arias-Palomo, E., Lyubimov, A.Y., Erzberger, J.P., O'Shea, V.L., Bustamante, C.J., and Berger, J.M. (2013). Nucleotide and partner-protein control of bacterial replicative helicase structure and function. Mol Cell *52*, 844–854.

Studier, F.W. (2005). Protein production by auto-induction in high-density shaking cultures. Protein Expr. Purif. *41*, 207–234.

Su'etsugu, M., Shimuta, T.R., Ishida, T., Kawakami, H., and Katayama, T. (2005). Protein associations in DnaA-ATP hydrolysis mediated by the Hda-replicase clamp complex. J. Biol. Chem. *280*, 6528–6536.

Su'etsugu, M., Fujimitsu, K., and Katayama, T. (2006). Reconstitution of in vitro inactivation and reactivation systems of DnaA protein for the control of chromosomal replication initiation in Escherichia coli. 2006 IEEE Int. Symp. Micro-Nano Mech. Hum. Sci. MHS.

Su'etsugu, M., Nakamura, K., Keyamura, K., Kudo, Y., and Katayama, T. (2008). Hda monomerization by ADP binding promotes replicase clamp-mediated DnaA-ATP hydrolysis. J. Biol. Chem. *283*, 36118–36131.

Su'etsugu, M., Harada, Y., Keyamura, K., Matsunaga, C., Kasho, K., Abe, Y., Ueda, T., and Katayama, T. (2013). The DnaA N-terminal domain interacts with Hda to facilitate replicase clamp-mediated inactivation of DnaA. Environ. Microbiol. *15*, 3183–3195.

Sutera Jr., V.A., and Lovett, S.T. (2006). The role of replication initiation control in promoting survival of replication fork damage. Mol Microbiol *60*, 229–239.

Taylor, K., and Wegrzyn, G. (1995). Replication of coliphage lambda DNA. FEMS Microbiol. Rev. *17*, 109–119.

Terwilliger, T.C., Adams, P.D., Read, R.J., McCoy, A.J., Moriarty, N.W., Grosse-Kunstleve, R.W., Afonine, P. V., Zwart, P.H., and Hung, L.W. (2009). Decision-making in structure solution using Bayesian estimates of map quality: The PHENIX AutoSol wizard. Acta Crystallogr. Sect. D Biol. Crystallogr. *65*, 582–601.

Ticau S., Friedman L.J., Ivica N.A., Gelles J., B.S.P. (2015). Single-molecule studies of origin licensing reveal mechanisms ensuring bidirectional helicase loading. Cell *161*, 513–525.

Tormo-Más, M.A., Mir, I., Shrestha, A., Tallent, S.M., Campoy, S., Lasa, I., Barbé, J., Novick, R.P., Christie, G.E., and Penadés, J.R. (2010). Moonlighting bacteriophage proteins derepress staphylococcal pathogenicity islands. Nature *465*, 779–782.

Tsai, K.L., Lo, Y.H., Sun, Y.J., and Hsiao, C.D. (2009). Molecular interplay between the replicative helicase DnaC and its loader protein DnaI from Geobacillus kaustophilus. J Mol Biol. *393*, 1056-1069.

Tsodikov, O. V., and Biswas, T. (2011). Structural and thermodynamic signatures of DNA recognition by mycobacterium tuberculosis DnaA. J. Mol. Biol. *410*, 461–476.

Tsurimoto, T., and Matsubara, K. (1981). Purified bacteriophage lambda O protein binds to four repeating sequences at the lambda replication origin. Nucleic Acids Res. *9*, 1789–1799.

Úbeda, C., Maiques, E., Barry, P., Matthews, A., Tormo, M.Á., Lasa, Í., Novick, R.P., and Penadés, J.R. (2008). SaPI mutations affecting replication and transfer and enabling autonomous replication in the absence of helper phage. Mol. Microbiol. *67*, 493–503.

Ullsperger, C., and Cozzarelli, N.R. (1996). Contrasting enzymatic activities of topoisomerase IV and DNA gyrase from Escherichia coli. J. Biol. Chem. *271*, 31549–31555.

Velten, M., McGovern, S., Marsin, S., Ehrlich, S.D., Noirot, P., and Polard, P. (2003). A two-protein strategy for the functional loading of a cellular replicative DNA helicase. Mol Cell *11*, 1009–1020.

Wagner, J.K., Marquis, K.A., and Rudner, D.Z. (2009). SirA enforces diploidy by inhibiting the replication initiator DnaA during spore formation in Bacillus subtilis. Mol Microbiol *73*, 963–974.

Wahle, E., Lasken, R.S., and Kornberg, A. (1989a). The dnaB-dnaC replication protein complex of Escherichia coli. I. Formation and properties. J Biol Chem *264*, 2463-2468.

Wahle, E., Lasken, R.S., and Kornberg, A. (1989b). The dnaB-dnaC replication protein complex of Escherichia coli. II. Role of the complex in mobilizing dnaB functions. J Biol Chem *264*, 2469–2475.

Walker, J.E., Saraste, M., Runswick, M.J., and Gay, N.J. (1982). Distantly related sequences in the alpha- and beta-subunits of ATP synthase, myosin, kinases and other ATP-requiring enzymes and a common nucleotide binding fold. Embo J *1*, 945–951.

Wang, J.C. (1971). Interaction between DNA and an Escherichia coli protein omega. J. Mol. Biol. *55*, 523–533.

Wang, J.C. (2002). Cellular roles of DNA topoisomerases: a molecular perspective. Nat. Rev. Mol. Cell Biol. *3*, 430–440.

Wang, Z.X. (1995). An exact mathematical expression for describing competitive binding of two different ligands to a protein molecule. FEBS Lett. *360*, 111–114.

Wang, G., Klein, M.G., Tokonzaba, E., Zhang, Y., Holden, L.G., and Chen, X.S. (2008). The structure of a DnaB-family replicative helicase and its interactions with primase. Nat Struct Mol Biol *15*, 94–100.

Wang, X., Lesterlin, C., Reyes-Lamothe, R., Ball, G., and Sherratt, D.J. (2011). Replication and segregation of an Escherichia coli chromosome with two replication origins. Proc. Natl. Acad. Sci. U. S. A. *108*, E243–E250.

Wang, JC., and Liu LF. (1979). In Molecular Genetics (New York).

Weigel, C., and Seitz, H. (2002). Strand-specific loading of DnaB helicase by DnaA to a substrate mimicking unwound oriC. Mol Microbiol *46*, 1149–1156.

Weigel, C., and Seitz, H. (2006). Bacteriophage replication modules. FEMS Microbiol. Rev. *30*, 321–381.

Weigel, C., Schmidt, A., Rückert, B., Lurz, R., and Messer, W. (1997). DnaA protein binding to individual DnaA boxes in the Escherichia coli replication origin, oriC. EMBO J. *16*, 6574–6583.

Wickner, S.H. (1978). DNA replication proteins of Escherichia coli and phage lambda. Cold Spring Harb. Symp. Quant. Biol. *43*, 303–310.

Wickner, S., and Hurwitz, J. (1975). Interaction of Escherichia colidnaB and dnaC(D) gene products in vitro. Proc Natl Acad Sci U S A *72*, 921–925.

Wickner, S.H., and Zahn, K. (1986). Characterization of the DNA binding domain of bacteriophage lambda O protein. J. Biol. Chem. *261*, 7537–7543.

Wilson, V.G., and Ludes-Meyers, J. (1991). A bovine papillomavirus E1-related protein binds specifically to bovine papillomavirus DNA. J. Virol. *65*, 5314–5322.

Wold, M.S., Mallory, J.B., Roberts, J.D., LeBowitz, J.H., and McMacken, R. (1982). Initiation of bacteriophage lambda DNA replication in vitro with purified lambda replication proteins. Proc. Natl. Acad. Sci. U. S. A. *79*, 6176–6180.

Wold, S., Crooke, E., and Skarstad, K. (1996). The Escherichia coli Fis protein prevents initiation of DNA replication from oriC in vitro. Nucleic Acids Res *24*, 3527–3532.

Xu, Q., McMullan, D., Abdubek, P., Astakhova, T., Carlton, D., Chen, C., Chiu, H.J., Clayton, T., Das, D., Deller, M.C., et al. (2009). A Structural Basis for the Regulatory Inactivation of DnaA. J. Mol. Biol. *385*, 368–380.

Yano, S.T., and Rothman-Denes, L.B. (2011). A phage-encoded inhibitor of Escherichia coli DNA replication targets the DNA polymerase clamp loader. Mol. Microbiol. *79*, 1325–1338.

Yao, N.Y., and O'Donnell, M. (2009). Replisome structure and conformational dynamics underlie fork progression past obstacles. Curr. Opin. Cell Biol. *21*, 336–343.

Yardimci, H., Loveland, A.B., Habuchi, S., Van Oijen, A.M., and Walter, J.C. (2010). Uncoupling of Sister Replisomes during Eukaryotic DNA Replication. Mol. Cell *40*, 834–840.

Yeeles, J.T.P., and Marians, K.J. (2013). Dynamics of leading-strand lesion skipping by the replisome. Mol. Cell *52*, 855–865.

Zahn, K., and Blattner, F.R. (1985). Binding and bending of the lambda replication origin by the phage O protein. EMBO J. *4*, 3605–3616.

Zechiedrich, E.L., and Cozzarelli, N.R. (1995). Roles of topoisomerase IV and DNA gyrase in DNA unlinking during replication in Escherichia coli. Genes Dev. *9*, 2859–2869.

Zylicz, M., Gorska, I., Taylor, K., and Georgopoulos, C. (1984). Bacteriophage λ replication proteins: Formation of a mixed oligomer and binding to the origin of λ DNA. MGG Mol. Gen. Genet. *196*, 401–406.

Appendix

Appendix A: Purification of *E. coli* DnaA, DnaC, DnaB

Materials

- Chemically competent *E. coli* C41 cells (Miroux and Walker, 1996)
- BL21(DE3) CodonPlus cells
- 1000X Kanamycin (30 mg/mL)
- 1000X Ampicillin (100 mg/mL)
- 1000X Chloramphenicol (34 mg/mL) in 100% ethanol
- 1000X Leupeptin (1 mg/mL)
- 1000X Pepstatin A (1 mg/mL) in 100% ethanol
- 100X PMSF (phenylmethanesulfonylfluoride) (100mM PMSF in 100% ethanol)
- 1 LB- Kanamycin agar plate with 0.05 % glucose added
- 1 LB-carbenicillin agar plate
- 1 L 2XYT Media autoclaved in a baffled glass flask
- 1 mM IPTG
- Sonicator
- Avanti J-20 centrifuge rotor
- JLA 8.1 centrifuge rotor
- Sorval RC5B centrifuge
- SS34 centrifuge rotor and tubes
- ÄTKA FPLC
- Parastaltic pump and XX pump lines
- 1 mL HiTrap Chelating HP (GE Healthcare)
- 5 mL HiTrap Chelating HP (GE Healthcare)
- HiPrep 16/60 Sephacryl S-200 HR column (GE Healthcare)
- HiPrep 16/60 Sephacryl S-300 HR column (GE Healthcare)
- SYPRO Orange Protein Gel Stain (5,000X in DMSO) (Life Technologies)
- Alexa Fluor 488 5-SDP Ester 1 mg (Sulfodichlorophenol Ester) (Life Technologies)

A.1 Media

2XYT Media (per 1L)

- Weigh 31 g 2XYT media mix (Sigma-Aldrich).
- Transfer to a baffled 2L flask and add 900 mL H_2O.
- Autoclave for 45 minutes.

A.2 Transformation of BL21 (DE3) cells

Transformation

- Chill 100 µl BL21 (DE3) cells on ice.
- Add 2 µg of vector (approximately 0.5-1µl of plasmid miniprep) to cells.
- Incubate on ice for 30 minutes.
- Heat shock for 45 seconds at 42°C.
- Add 850 µl 2XYT media to cells and incubate at 37°C for 45 minutes.
- Spin down cells at high speed for 5 minutes.
- Aspirate off supernatant.
- Add 50 µl of transformation to LB plate.

A.3 Expression of H_6MBP-*Ec*DnaC

- Transform C41 cells in protocol described above, plasmid is Amp^r.
- Grow a 50 mL 2XYT starter culture using a single colony.
- Inoculate 1L 2XYT media with 20 mL overnight culture.
- Grow at 37°C with shaking until an OD600 of 0.4 – 0.5.
- Induce with 1 mM IPTG for 2-2.5 hours at 37 ^oC.
- Resuspend pellet in 30 mL buffer and flash freeze, or flash freeze pellet and resuspend frozen cells, or resuspend and lyse right away.

A.4 Purification of H_6MBP-*Ec*DnaC wild-type and ATPase mutants

Buffers

Buffer A - Ni loading buffer/cell resuspension/lysis buffer - (high Salt/low imidazole)

50 mM HEPES-KOH pH 7.5

1 M KCl

10 % glycerol

30 mM imidazole

10 mM $MgCl_2$

0.010 mM ATP

1 mM BME

After cell lysis, add 5 µg/mL DNase I.

Buffer B Wash (low salt/low imidazole)

50 mM HEPES-KOH pH 7.5

500 mM KCl

10 % glycerol

30 mM imidazole

10 mM $MgCl_2$

0.010 mM ATP

1 mM BME

Buffer C (Ni Elution /Amylose Load/ Wash Buffer)

50 mM HEPES-KOH pH 7.5

500 mM KCl

10 % glycerol

500 mM imidazole

10 mM $MgCl_2$

0.010 mM ATP

1 mM BME

Amylose Elution Buffer

50 mM HEPES-KOH pH 7.5

500 mM KCl

10 % glycerol

10 mM Maltose

10 mM $MgCl_2$

0.010 mM ATP

1 mM BME

*Ec*DnaC s200 sizing buffer

50 mM HEPES-KOH pH 7.5

500 mM KCl

10 % glycerol

10 mM $MgCl_2$

0.010 mM ATP

1 mM BME

*Note: reducing agent and protease inhibitors were added fresh to all buffers

1 μM pepstatin-A

1 μM leupeptin

1 mM PMSF

Preparation of His6MBP-*Ec*DnaC cell extract

- Thaw cell pellets (3L) on ice.
- Resuspend in Ni Buffer A.
- Lyse cells by sonication at a setting of 4.5 for 30 seconds, repeat 3 times.
- Spin down sonicated cells at 14,000 in a Sorval RC5B centrifuge using SS34 centrifuge rotor and tubes at 4°C for 30 minutes.

Day 1: Ni Column, Amylose, TEV cleavage

- Run cell extract over 5 mL HiTrap Chelating HP column.
- Wash Ni column with Buffer A (high salt/low imidazole), checking for completion by Bradford test.
- Wash Ni column with ~10-15 mL of Buffer B (low salt/low imidazole)
- Elute sample from Ni with Buffer C (low salt/high imidazole), checking for completion with Bradford test.
- Pour a 30 mL amylose column.
- Run Ni elution over amylose column in the cold room by gravity or on the FPLC
- Wash amylose column 3X with 30 mLs.
- Elute protein with Amylose Elution Buffer.
- Add ATP to 0.1 mM to amylose elution and concentrate (note: concentrating without raising the ATP will lead to aggregation.).
- Incubate TEV cleavage reaction overnight for ~20 hours at 4°C (cold room).

Day 2: Ortho-Ni, s200 sizing

- Remove His6-MBP tag and TEV protease from *Ec*DnaC protein by re-passage over a second 5 ml HiTrap Chelating HP column in Buffer A, collect flow-through, checking for completion by Bradford test.
- Wash Ni column with ~25ml of Buffer A (high salt/low imidazole)
- Wash Ni column with ~25ml of Buffer B (low salt/low imidazole)
- Elute TEV and His6-MBP tag with Buffer C, checking for completion with Bradford test.
- Raise [ATP] to [0.1 mM] before concentrating Ortho-Ni flow-through containing *Ec*DnaC to < 1 mL
- Run over s200 sizing column.

*Note: reducing agent and protease inhibitors were added fresh to all buffers

1 μM pepstatin-A

1 μM leupeptin

1 mM PMSF

A.5 Expression and Purification of hexameric *E. coli* DnaB helicase

*Ec*DnaB Expression

- Transform *Ec*DnaB plasmid into C41 cells in protocol described above.
- Grow a 50 mL 2XYT starter culture at 37°C using a single colony.
- Inoculate 1L 2XYT media with 20 mL overnight culture.
- Grow 1L cultures at 37°C with shaking to an OD600 of 0.4-0.5.
- Induce with IPTG and express at 37°C for 2 hours
- Spin down sonicated cells at 4,000 RPM in Avanti J-20 centrifuge using JLA 8.1 centrifuge rotor at 4°C for 20 minutes.
- Flash-freeze cell pellets in liquid nitrogen before storage at -80°C.

*Ec*DnaB Purification

- Thaw cell pellet on ice and resuspend in DnaB resuspension buffer.
- Lyse cells by sonication for 20 seconds at 4.5 setting, 3X.
- Pre-cut lysed cells with 10 % ammonium sulfate.
- Spin 10% ammonium sulfate cut at 14,000 RPM (Sorval RC5B centrifuge using SS34 centrifuge rotor) for 20 minutes at 4°C.
- Add ammonium sulfate to lysate to final concentration 30%.
- Invert several times and wait for a cloudy precipitate to form.
- Spin down sonicated cells at 14,000 RPM (Sorval RC5B centrifuge using SS34 centrifuge rotor and tubes) at 4°C for 20 minutes.
- Pour off supernatant and re-suspend pellet in 100mM NaCl Q Buffer.
- Flow resuspension over Q column equilibrated in 100mM NaCl Q Buffer.
- Wash with 100mM NaCl Q Buffer, check for completion by Bradford.

*Ec*DnaB Buffers

DnaB Resuspension Buffer (same as 100 mM NaCl Q column equilibration buffer)

100mM NaCl

20mM HEPES-KOH pH 7.5

10% glycerol

10mM $MgCl_2$

0.01mM ATP

1mM BME

100mM NaCl Q Buffer

100mM NaCl

20mM HEPES-KOH pH 7.5

10% glycerol

10mM $MgCl_2$

0.01mM ATP

1mM BME

Wash Buffer (400mM NaCl Q Buffer)

400mM NaCl

20mM HEPES-KOH pH 7.5

10% glycerol

10mM $MgCl_2$

0.01mM ATP

1mM BME

Elute Buffer (500mM NaCl Q Buffer)

500mM NaCl

20mM HEPES-KOH pH 7.5

10% glycerol

10mM $MgCl_2$

0.01mM ATP

1mM BME

*Ec*DnaB s300 Sizing Buffer

20mM Tris pH 8.5

800mM NaCl

10% glycerol

5mM $MgCl_2$

1mM BME

add to s300 buffer before run:

0.01 mM ATP
protease inhibitors

*Note: reducing agent and protease inhibitors were added fresh to all buffers

1 μM pepstatin-A

1 μM leupeptin

1 mM PMSF

A.6 Expression and Purification of *E. coli* DnaA His6-tagged constructs

(based on protocols from Duderstadt et al., 2010; Li and Crooke, 1999)

Expression of His6–*Ec*DnaA

- Transform His6-*Ec*DnaA plasmid into C41 competent cells
- Grow a 50 mL 2XYT starter culture at 37°C using a single colony.
- Inoculate 1L 2XYT media with 15 mL overnight culture.
- Grow 1L cultures at 37°C with shaking to an OD600 of 0.6
- Grow for 1.5 hours exactly.
- Spin down sonicated cells at 4,000 RPM in Avanti J-20 centrifuge using JLA 8.1 centrifuge rotor at 4°C for 30 minutes.
- Resuspend cell pellets in *Ec*DnaA binding buffer.
- Flash freeze cell resuspension in liquid nitrogen before storage at -80°C.

(Note: do not let expression go over 1.5 hours, be very careful of the time. Going over 1.5 hours will result in lower yield and more aggregated protein.)

Purification of His6-*Ec*DnaA proteins

Buffers

Binding Buffer

20 mM sodium phosphate pH 7.8

500 mM sodium chloride

20% Sucrose

20 mM imidazole

Wash Buffer

20 mM sodium phosphate pH 7.8

500 mM sodium chloride

30 mM imidazole

20% Sucrose

Unfolding Buffer (7M Urea)

20 mM sodium phosphate pH 7.8

500 mM sodium chloride

20% Sucrose

20 mM imidazole

7 M urea

*Ec*DnaA HD Refolding Buffer

50 mM Pipes-KOH pH 6.8

10 mM magnesium acetate

200 mM ammonium sulfate

20% sucrose

Elution Buffer (700 mM Imidazole)

50 mM Pipes-KOH pH 6.8

10 mM magnesium acetate

200 mM ammonium sulfate

20% sucrose

700 mM imidazole

s200 *Ec*DnaA sizing buffer

50 mM Pipes-KOH pH 6.8

10 mM magnesium acetate

200 mM ammonium sulfate

20% sucrose

0.1 mM EDTA

2 mM DTT

*Note: reducing agent and protease inhibitors were added fresh to all buffers

1 μM pepstatin-A

1 μM leupeptin

1 mM PMSF

*Ec*DnaA Purification

- Cells were thawed on ice until no chunks remained in luke warm water.
- Cells where then sonicated at ~4.5 for ~40 seconds two times.
- DNase I was added to 5ug/mL and 10 mM MgCl2 was added and lysate was left for 5 mins. (25 ul of 5mg/ml DNaseI to 25 mLs cells, 200 ul 1M MgCl2)
- Cell lysate was then spun down at 15,000 rpm for 20 mins.
- Supernatant was then run over 1 mL Chelating HiTrap HP column pre-equilibrated in Binding Buffer after stripping/regenerating.
- Wash buffer was run over equivalent to 25 mLs.
- Binding Buffer + 7 M urea was ran over column to remove nucleotide and contaminants. (note: do not add ATP to ANY buffers! unfolding and refolding step releases the tightly bound nucleotide from DnaA generating the apo DnaA)
- Protein was refolded in *Ec*DnaA HD Refolding Buffer.
- Refolded *Ec*DnaA was eluted in elution buffer and concentrated to ~2 mL.
- Sample was then ran over s200 sizing buffer. Monomer fractions were concentrated to greater than 30 uM and flash frozen in liquid nitrogen for long-term storage at -80°C.

Appendix B: Purification of *S. aureus* and phage 77 proteins

B.1 Expression of H6MBP-tagged 77ORF104, *Sa*DnaI(full-length or AAA+), SaDnaI(NTD or CTD)

- Transform phage77 or *S. aureus* DnaI plasmids into BL21 (DE3) CodonPlus (RILS) cells.
- Inoculate 50 mL 2XYT starter cultures with entire transformation and grow overnight with shaking at 37°C in 2XYT media. (Note: remember to add chloramphenicol to cultures).
- Inoculate 1L 2XYT cultures with 25 mLs starter overnight culture.
- Grow cells to an OD600 of 0.5-0.6.
- Induced with 1 mM IPTG and express for 3-4 hours at 37°C.
- Spin cells down at 4,000 RPM in Avanti for 20 minutes.
- Flash freeze cell pellets in liquid nitrogen before storage at -80°C.

B.2 Purification of H6MBP-77ORF104 & H6MBP-*Sa*DnaI(AAA+/ NTD/CTD)

Buffers

Staph Buffer A Ni Loading Buffer/Lysis Buffer (high salt/low imidazole)

50 mM HEPES-NaOH pH 7.5

1 mM KCl

10% (v/v) glycerol

10 mM MgCl2

20 mM imidazole

Staph Buffer B Wash buffer (low salt/low imidazole)

50 mM HEPES-NaOH pH 7.5

150 mM KCl

10% (v/v) glycerol

10 mM MgCl2

20 mM imidazole

Staph Buffer C Elution buffer (low salt/high imidazole)

50 mM HEPES-NaOH pH 7.5

150 mM KCl

10% (v/v) glycerol

10 mM MgCl2

300 mM imidazole

Staph Dilution Buffer

50 mM HEPES-NaOH pH 7.5

500 mM KCl

10% (v/v) glycerol

10 mM MgCl2

Staph s200 Buffer

50 mM HEPES-NaOH pH 7.5

500 mM KCl

10% (v/v) glycerol

10 mM MgCl2

*Note: reducing agent and protease inhibitors were added fresh to all buffers

1 μM pepstatin-A

1 μM leupeptin

1 mM PMSF

Preparation of cell extract

- Thaw cell pellets (3L) on ice.
- Resuspend in Buffer A.
- Lyse cells by sonication at a setting of 4.5 for 30 seconds, repeat 3 times.
- Spin down sonicated cells at 14,000 RPM at 4°C for 30 minutes.

Day 1: Ni Column, TEV cleavage

- Run cell extract over 5 mL HiTrap Chelating HP column.
- Wash Ni column with Buffer A (high salt/low imidazole), checking for completion by Bradford test.
- Wash Ni column with ~10-15 mL of Buffer B (low salt/low imidazole).
- Elute sample from Ni with Buffer C (low salt/high imidazole), checking for completion with Bradford test.
- Concentrate elution and buffer exchange into Dilution Buffer to dilute imidazole.
- Concentrate to approximately 5 mLs before adding His-tagged tobacco etch virus protease (TEV).
- Incubate TEV cleavage reaction overnight for ~20 hours at 4°C (cold room).

Day 2: Ortho-Ni, sizing

- Remove His6-MBP tag and TEV protease from *Sa*DnaI or 77ORF104 protein by re-passage over a second 5 ml HiTrap Chelating HP column in Buffer A, checking for completion by Bradford test.
- Wash Ni column with ~25 mL of Buffer A (high salt/low imidazole).
- Wash Ni column with ~25 mL of Buffer B (low salt/low imidazole).
- Elute TEV and His6-MBP tag with Buffer C, checking for completion with Bradford test.
- Concentrate Ortho-Ni *Sa*DnaI or 77ORF104 protein to 2 mL before running on s200 sizing column.

B.3 Purification of H_6MBP-*Sa*DnaI full-length

(*Note: purification differs from truncated *Sa*DnaI protein preps. Full-length *Sa*DnaI behaves differently and crystallizes while concentrating or at low temperatures (on ice or in cold room). To avoid unwanted protein aggregation, do not add nucleotide to full-length prep.)

Buffers

*Sa*DnaI^{FL} Buffer A Ni Loading Buffer/Lysis Buffer (high salt/low imidazole)

50 mM HEPES-NaOH pH 7.5

1 mM NaCl

10% (v/v) glycerol

10 mM MgCl2

20 mM imidazole

*Sa*DnaI^{FL} Buffer B Wash buffer (low salt/low imidazole)

50 mM HEPES-NaOH pH 7.5

150 mM NaCl

10% (v/v) glycerol

10 mM MgCl2

20 mM imidazole

*Sa*DnaI^{FL} Buffer C Elution buffer (low salt/high imidazole)

50 mM HEPES-NaOH pH 7.5

150 mM NaCl

10% (v/v) glycerol

10 mM MgCl2

300 mM imidazole

*Sa*DnaI^{FL} Dilution Buffer

50 mM HEPES-NaOH pH 7.5

1 M NaCl

10% (v/v) glycerol

10 mM MgCl2

*Sa*DnaI^{FL} s200 Buffer

50 mM HEPES-NaOH pH 7.5

500 mM NaCl

10% (v/v) glycerol

10 mM MgCl2

*Note: reducing agent and protease inhibitors were added fresh to all buffers

1 μM pepstatin-A

1 μM leupeptin

1 mM PMSF

Preparation of *Sa*DnaI^{FL}cell extract

- Thaw cell pellets (3L) on ice
- Resuspend in *Sa*DnaI^{FL} Buffer A
- Lyse cells by sonication at a setting of 4.5 for 30 seconds, Repeat 3 times
- Spin down sonicated cells at 14,000 at 4^{o}C for 30 minutes

*Sa*DnaI^{FL} Day 1: Ni Column, TEV cleavage

- Run cell extract over 5 mL HiTrap Chelating HP column
- Wash Ni column with *Sa*DnaI^{FL} Buffer A (high salt/low imidazole), checking for completion by Bradford test
- Wash Ni column with ~10-15 mL of *Sa*DnaI^{FL} Buffer B (low salt/low imidazole)
- Elute sample from Ni with *Sa*DnaI^{FL} Buffer C (low salt/high imidazole), checking for completion with Bradford test.
- Concentrate elution and buffer exchange into *Sa*DnaI^{FL} Dilution Buffer to dilute imidazole
- Concentrate to approximately 5 mLs before adding His-tagged tobacco etch virus protease (TEV)
- Incubate TEV cleavage reaction overnight for ~20 hours at 4°C (cold room)
- The next morning before running the ortho-nickel column you must incubate the TEV + *Sa*DnaI^{FL} reaction at room temperature for ~20-30 minutes to re-solubilize the protein. *Sa*DnaI^{FL} crystallizes at lower temps (on ice or 4°C).

*Sa*DnaI^{FL} Day 2: Ortho-Ni, sizing

- Once *Sa*DnaI^{FL} has went back into solution at room temperature re-passage over 5 mL HiTrap Chelating HP column in Buffer A to remove His6-MBP tag and TEV protease, checking for completion by Bradford test.
- Wash Ni column with ~30 mL of *Sa*DnaI^{FL} Buffer A (high salt/low imidazole).
- Wash Ni column with ~25 mL of *Sa*DnaI^{FL} Buffer B (low salt/low imidazole).
- Elute TEV and His6-MBP tag with Buffer C, checking for completion with Bradford test.
- Concentrate Ortho-Ni *Sa*DnaI^{FL} protein to 2 mL.
- After concentrating *Sa*DnaI^{FL} will have crystallized in solution.
- Warm pre-s200 sample at room temperature for 20-30 minutes or until *Sa*DnaI^{FL} has completely went back into solution.
- Load solubilized *Sa*DnaI^{FL} and run s200 sizing column.
- Collect monomeric *Sa*DnaI^{FL} fractions and concentrate.
- Warm final s200 pure *Sa*DnaI^{FL} sample at room temperature for 20-30 minutes. Flash freeze aliquots in liquid nitrogen and store at -80°C.

B.4 Purification of H_6MBP-SeMet-*Sa*DnaI^{AAA+}

Minimal Media for SeMet Expression of *Sa*DnaI^{AAA+} and 77ORF104 peptide

(*Note: media and protocol based on SeMet expression in (Studier, 2005))

20X Amino Acids Stock (17 amino acids for Se-Met)

- heat ~700 mL water in microwave 3 minutes before adding amino acids
- add 4 grams each amino acid (0.2 g/L) to 1L (NOT Cys, Tyr)
- pH to 7.5
- add 0.2 g native methionine (addition of a small amount of native methionine helps cells grow better and increases protein yield.)
- final concentrations are 0.01 g/L Met, 0.1 g/L Se-Met

(*Note: 2 g Seleno-Methionine is added fresh to each 1L culture on the day of SeMet protein expression)

SeMet Minimal Media Stocks

20X PO4 (autoclave)

1 M Na2HPO4 (dibasic)

1 M KH2PO4

0.5 M (NH4)2SO4

1000X MgSO4

2M MgSO4

1000X FeCl3

20 mM FeCl3 in 200X Diluted 37% HCl:

50 mL stock:

add 250 ul Concentrated HCl to 49.75 mL sH20 (200X Dilution)

add 162.2 mg FeCl3 (MW: 162.2 g/mol)

100X Glycerol

50% Glycerol

For 1 liter of SeMet minimal medium add fresh 100 mg SeMet per 1L

20X PO_4	50 mL
20X 18AAs	50 mL (including the methionine or seleno-methionine)
100X glycerol	10 mL
1000X $FeCl_3$	1 mL
1000X MgSO4	1 ml
1000X antibiotic	1 mL
glucose	0.5 g
H_2O	887 mL (autoclaved in 1L baffled flask)

Se-Met protein expression

- Transform BL21 (DE3) CodonPlus (RILS) cells.
- Grow (25 mLs per 1L expression) Overnight culture in 2YT (regular media).
- Spin down Overnight Culture: 25 mL cells @ 4000.
- Resuspend 25 mL cells into Se-MET Minimal Media.
- Inoculate 1 L Se-Met minimal media with 25 mL resuspended Cells.
- Grow @ 37C to an OD600 of 0.6.
- Induce with 1 mM IPTG.
- Express for 3 hours, spin down 1 L cultures, flash freeze pellets in Liquid Nitrogen.

*Note: make sure you add reducing agent to all purification buffers (0.5 mM TCEP)

Se-Met protein purification

- Se-Met protein purifications were performed as described above for native protein prep with one change: 0.5 mM TCEP was added to all purification buffers.

B.5 Expression and Purification of H_6MBP-77ORF013

Expression of His6-MBP-77ORF013 phage helicase loader (DnaC/DnaI homolog)

- Transform 77ORF013 plasmid into BL21 (DE3) CodonPlus (RILS) cells.
- Inoculate 50 mL 2XYT starter cultures with entire transformation and grow overnight with shaking at 37°C in 2XYT media.
- Add chloramphenicol to cultures to overnight starter cultures.
- Inoculate 1L 2XYT cultures with 25 mLs starter overnight culture.
- Grow cells to an OD600 of 0.5-0.6
- Induced with 1 mM IPTG and express for 3-4 hours at 37°C
- Spin cells down at 4,000 RPM in Avanti for 20 minutes.
- Flash freeze cell pellets in liquid nitrogen before storage at -80°C.

Purification of His6-MBP-77ORF013 phage helicase loader

- Purify as described for *Sa*DnaI^{AAA+} above.

B.6 Expression and Purification of *Sa*DnaC helicase hexamer (*Sa*DnaC)6

Expression of His6-MBP-*Sa*DnaC replicative helicase (*Sa*DnaC)6

- Transform His6-MBP-tagged *Sa*DnaC plasmid into BL21 (DE3) CodonPlus (RILS) cells.
- Inoculate 50 mL 2XYT starter cultures with entire transformation and grow overnight with shaking at 37°C in 2XYT media.
- Add chloramphenicol to starter cultures.
- Inoculate 1L 2XYT cultures with 20 mLs starter overnight culture.
- Grow cells to an OD600 of 0.4-0.5
- Induced with 1 mM IPTG and express for 3 hours at 37°C
- Spin cells down at 4,000 RPM in Avanti for 20 minutes.
- Flash freeze cell pellets in liquid nitrogen before storage at -80°C.

H6MBP-*Sa*DnaC Helicase Purification

Preparation of cell extract

- Thaw cell pellets (3L) on ice.
- Resuspend in *Sa*DnaC Lysis Buffer.
- Lyse cells by sonication at a setting of 4.5 for 30 seconds, repeat 3 times.
- Spin down sonicated cells at 14K at 4°C for 30 minutes.
- Add 0.2 grams ammonium sulfate per 1 mL lysate to precipitate the helicase in the lysis supernatant.
- Spin at 14,000 at 4°C, 20 minutes.
- Resuspend precipitate pellet in *Sa*DnaC Buffer A.

Buffers

*Sa*DnaC Lysis Buffer

50 mM Tris-HCl pH 7.5

500 mM NaCl

10% (v/v) glycerol

20 mM imidazole

0.5 mM BME

0.01 mM ATP

*Sa*DnaC Buffer A (high Salt/low imidazole)

50 mM Tris-HCl pH 7.5

1 M NaCl

10% (v/v) glycerol

20 mM imidazole

1 mM BME

0.01 mM ATP

*Sa*DnaC Buffer B (low Salt/low imidazole)

50 mM Tris-HCl pH 7.5

200 mM NaCl

10% (v/v) glycerol

20 mM imidazole

1 mM BME

0.01 mM ATP

*Sa*DnaC Buffer C (low Salt/high imidazole)

50 mM Tris-HCl pH 7.5

200 mM NaCl

10% (v/v) glycerol

200 mM Imidazole

1 mM BME

0.01 mM ATP

Day 1: Ni Column, TEV cleavage (*Sa*DnaC Prep)

- Run cell extract over 5 mL HiTrap Chelating HP column.
- Wash Ni column with *Sa*DnaC Buffer A (high salt/low imidazole), checking for completion by Bradford test.
- Wash Ni column with ~25 mL of *Sa*DnaC Buffer B (low salt/low imidazole).
- Elute sample from Ni with *Sa*DnaC Buffer C (low salt/high imidazole), checking for completion with Bradford test.
- Concentrate Ni elution before adding His-tagged tobacco etch virus protease (TEV).
- Incubate TEV cleavage reaction overnight for ~20 hours at 4°C (cold room).

Day 2: Ortho-Ni, s300 sizing (*Sa*DnaC Prep)

- Re-passage TEV cleavage reaction over 5 ml HiTrap Chelating HP column in *Sa*DnaC Buffer A, checking for completion by Bradford test.
- Wash Ni column with ~30 mL of *Sa*DnaC Buffer A (high salt/low imidazole).
- Wash Ni column with ~30 mL of *Sa*DnaC Buffer B (low salt/low imidazole).
- Elute TEV and His6-MBP tag with Buffer C, checking for completion with Bradford test.
- Concentrate Ortho-Ni *Sa*DnaC protein to 2 mL.
- Load *Sa*DnaC and run s300 sizing column.
- Collect hexameric (*Sa*DnaC)6 fractions and concentrate.
- Flash freeze aliquots in liquid nitrogen and store at -80°C.

*Sa*DnaC helicase s300 Buffer

50mM Tris pH 7.5

800mM NaCl

10% glycerol

1 mM EDTA

2 mM BME

0.1 mM ATP

Appendix C: Synthetic Melted Origin *oriC* Fork Helicase Assay

Materials

- Victor V3 plate reader (Perkin Elmer)
- HE MICROPLATE, 384 WELL, BLACK - Molecular Devices 0200-5202

DnaA-dependent *oriC* Fork Helicase Assay Protocol

(note: for 80 µl reaction volume)

- Incubate *oriC* fork with DnaA for 5 minutes on ice.
- Add DnaB helicase and DnaC helicase loader and incubate reaction for 5 minutes on ice.
- Add capture strands to reactions.
- Thoroughly mix reactions with multi-channel pipette.
- Transfer 18 µl of each reaction (in triplicate) into a 384-well plate for plate reader measurements. (note: pre-chill 384-well plate on ice.)
- Transfer 384-well plate into plate reader pre set to 37°C and begin Cy3 and Cy5 raw fluorescence reads using appropriate method.
- Collect measurements for 30 minutes.

1X *oriC* Fork Helicase Assay Buffer

20 mM HEPES-NaOH pH 7.5

5 mM Mg acetate

5 % glycerol

Add fresh:

1 mM ATP

0.2 mg/mL BSA

2 mM DTT

Appendix D: Pull-down Assays

(note: this protocol was developed for use of an MBP-tagged protein as the "bait" and an untagged protein as "prey")

Materials

SDS loading buffer

Amylose agarose beads (NEB)

SYPRO Orange Stain (5000X) (Life Technologies)

Glacial Acetic Acid

Buffers

2X Pull-Down Binding Buffer

- 40 mM HEPES 7.5
- 200 mM NaCl
- 10 mM MgCl2
- 20% Glycerol
- 2 mM DTT

1X Protein Dilution Buffer

- 20 mM HEPES 7.5
- 100 mM NaCl
- 10 mM MgCl2
- 10% Glycerol

SYPRO Orange Protein Stain

- 10% Acetic Acid
- 1X SYPRO Orange

Amylose Pull-down Protocol

- Incubate MBP-tagged-proteins with protein with untagged "prey" protein in a 1.5 mL microfuge tube at room temperature for 20 minutes in 200 µL.
- Equilibrate amylose beads with 1X Pull-down Binding Buffer (wash with water 3X, then 3X with 1X Pull-down Binding Buffer).
- Add 50 µL Amylose beads.
- Incubate with Amylose beads for 15 minutes at room temperature.
- Spin down beads at low speed (1000 RPM)
- Aspirate nearly all of supernatant and save supernatant as flow-through. (Note: do not let the beads go dry. It is not important at this point to aspirate the entire supernatant).
- Resuspend beads gently with 100 µL wash Buffer
- Spin down beads at 1000 RPM, save as wash 1 (W1), repeat again and save wash 2 (W2).
- Now aspirate all of the liquid carefully. (Note: using a gauge needle will help aspirate the liquid without aspirating the beads).
- Add 30 µL 2X SDS loading dye to amylose beads.
- Boil the beads in a 95°C water bath for 5 minutes.
- Run bead samples on a 12% SDS-PAGE gel at 150V until the dye front reaches the bottom.
- Wash the gel three times with milliqH_2O. (Note: it is important to use fresh gloves when wash the gel prior to adding the stain. To obtain a highly quality gel stain avoiding touching the gel.)
- Incubate washed gel with 25 mL SYPRO Orange Protein Stain in 10% glacial acetic acid for 30 minutes in a (NO Coomassie) gel case covered in aluminum foil.

Appendix E: Anisotropy-based Competition and Binding Assays

Materials

- CLARIOStar microplate reader (BMG LAB TECH).
- GraphPad Prism Version 6 software.
- 96-well tray type - Round Bottom Polypropylene - costar 3790.
- Greiner Bio-One Microplate, 384 Well, PS, Flat-Bottom, Small Volume, HiBase, Non-Binding, Black.

Procedure

- Make a master mix containing all of the components of the reaction condition except the protein.
- Using a 4X Protein Stock make 8-16 dilutions (each a 2-fold dilution of the previous one) in a 96 well tray using the 1X Dilution Buffer include a no protein condition. (96-well tray type - Round Bottom Polypropylene - costar 3790).
- Dispense 15 ul aliquots of the Master Mix into a 96-well tray and use a multichannel to mix 5 ul of each protein dilution with it.
- Transfer 20 ul of this mix into 384-well tray (Greiner small volume Bio-One Microplate).
- Transfer 384-well plate into CLARIOStar plate reader.
- Set gain aiming for values between 1500-1800.
- Measure plate at 25°C.

Appendix F: Radioactive ATPase assays

Materials

- [γ^{32}P]ATP, 4500 Ci/mmol (MP Biomedicals)
- TLC Plates (PEI-cellulose, matrix, Sigma-Aldrich)
- 200μM cold ATP
- Typhoon FLA 9500 Laser Scanner (GE Healthcare Life Sciences) PhosphorImager
- ImageJ software
- M13mp18 ssDNA (New England Biolabs, Inc.)

Buffers

1X ATPase Assay Reaction Buffer

50 mM HEPES-NaOH pH 7.5

100 mM KCl

10 mM MgCl2

10 % glycerol

Assay Protocol

(note: reactions were prepared at a final volume of 30 μL)

- Prepare fresh 1 mM cold ATP.
- Dilute stock of [γ^{32}P]ATP to 50 nM [4500 Ci/mmol (MP Biomedicals)].
- Prepare ATP hydrolysis reaction on ice. Add everything but the [γ^{32}P]ATP + cold ATP. For M13mp18 ssDNA reactions, add ssDNA at a final concentration of 750 ng/μL.
- Place reactions in thermocycler pre-incubated at 37°C.
- Add Hot + Cold ATP to start reaction. Add Hot [γ^{32}P]ATP and Cold ATP at final concentrations of 5 nM and 200 μM, respectively.
- Collect 3 μL for each time point and immediately quench with 3 μL 10X Stop Mix (1% SDS, 250 mM EDTA pH 8.0)
- Run 1 μL of each reaction time point on TLC for 30 minutes. (note: make sure each spot is spaced 8 mm apart.)
- Air dry TLC and expose overnight for at least 12 hours using phosphor screen.
- Scan screen using Typhoon FLA 9500 Laser Scanner PhosphorImager. (note: be careful to check the PMT setting. Usually, a PMT of 600 is sufficient.)